AD-A049 138 NAVAL OCEAN SYSTEMS CENTER SAN DIEGO CALIF F/G 17/2.1
HIGH-FREQUENCY INTERFERENCE SUPPRESSION. INTERFERENCE IS IDENTI--ETC(U)
AUG 77 G J BROWN
UNCLASSIFIED NOSC/TR-155 NL

1 OF 2
ADA049138

(12) Sc

NOSC

NOSC / TR 155

NOSC / TR 155

Technical Report 155

HIGH-FREQUENCY INTERFERENCE SUPPRESSION

Interference is identified and then eliminated

Gary J Brown

8 August 1977

Research and Development, August 1976 to August 1977

Prepared for
NAVAL ELECTRONIC SYSTEMS COMMAND

NAVAL OCEAN SYSTEMS CENTER
SAN DIEGO, CALIFORNIA 92152

NAVAL OCEAN SYSTEMS CENTER, SAN DIEGO, CA 92152

AN ACTIVITY OF THE NAVAL MATERIAL COMMAND

RR GAVAZZI, CAPT USN
Commander

HL BLOOD
Technical Director

ADMINISTRATIVE INFORMATION

Work reported upon herein was performed by members of the Intra-task Force/Ship-to-Ship Communications Branch, Surface/Shore Systems Division under Program Element 62721N, Project F21222, Task Area XF21222091, and Work Unit B194 between August 1976 and August 1977. This report was approved for publication 8 August 1977.

Released by
CA Nelson, Head
Surface/Shore Systems Division

Under authority of
RO Eastman, Head
Communications System and
Technology Department

UNCLASSIFIED

SECURITY CLASSIFICATION OF THIS PAGE *(When Data Entered)*

REPORT DOCUMENTATION PAGE

READ INSTRUCTIONS BEFORE COMPLETING FORM

1. REPORT NUMBER: NOSC Technical Report 155 (TR 155)
2. GOVT ACCESSION NO.
3. RECIPIENT'S CATALOG NUMBER

4. TITLE *(and Subtitle)*: HIGH-FREQUENCY INTERFERENCE SUPPRESSION • Interference is identified and then eliminated •

5. TYPE OF REPORT & PERIOD COVERED: Research and Development Technical Rept. August 1976 to August 1977

6. PERFORMING ORG. REPORT NUMBER

7. AUTHOR(s): Gary J. Brown

8. CONTRACT OR GRANT NUMBER(s): NOSC/TR-155

9. PERFORMING ORGANIZATION NAME AND ADDRESS: Naval Ocean Systems Center, San Diego, California 92152

10. PROGRAM ELEMENT, PROJECT, TASK AREA & WORK UNIT NUMBERS: 62721N; F21222; XF21222091 (B194)

11. CONTROLLING OFFICE NAME AND ADDRESS: Naval Electronic Systems Command, Washington, DC 20360

12. REPORT DATE: 8 August 1977

13. NUMBER OF PAGES: 104

14. MONITORING AGENCY NAME & ADDRESS *(if different from Controlling Office)*: 106p.

15. SECURITY CLASS. *(of this report)*: Unclassified

15a. DECLASSIFICATION/DOWNGRADING SCHEDULE

16. DISTRIBUTION STATEMENT *(of this Report)*: F21222

Approved for public release; distribution is unlimited

17. DISTRIBUTION STATEMENT *(of the abstract entered in Block 20, if different from Report)*: XF21222091

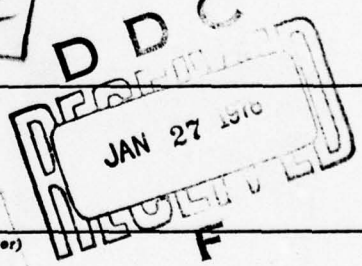

18. SUPPLEMENTARY NOTES

19. KEY WORDS *(Continue on reverse side if necessary and identify by block number)*

High-frequency radio communications
Excision processing
Narrowband and broadband suppression techniques

20. ABSTRACT *(Continue on reverse side if necessary and identify by block number)*

This report investigates techniques for suppressing interferences that occur on a communication channel, specifically the high-frequency radio channel. The interferences are divided into 2 categories, those that occupy a narrow bandwidth with respect to the communicator's signal and those that occupy a bandwidth approximately equal to or greater than the communicator's bandwidth. The processing techniques which are examined are based upon using large time-bandwidth product (TW) signals, where TW is much larger than the symbol alphabet size, whereby large portions of the symbol TW space can be altered or totally eliminated while still maintaining quality communication due to the symbol coding redundancy.

DD FORM 1 JAN 73 1473 EDITION OF 1 NOV 65 IS OBSOLETE S/N 0102-LF-014-6601

UNCLASSIFIED

SECURITY CLASSIFICATION OF THIS PAGE *(When Data Entered)*

393159

The suppression problem is divided into two areas; first, the identification of the interference and, second, its elimination. A simple threshold algorithm (called the quantile algorithm) is used for identification where a level is set based on one point of the exceedance function over the ensemble of the time-envelope samples (for broadband interference in the time domain) or the magnitude of frequency samples (for narrowband interference in the frequency domain). The suppression techniques investigated include excising (setting to zero) samples that exceed the threshold level, clipping at the threshold level, and a logarithmic weighting of samples.

Simulations were used to evaluate various techniques and it was found that with only one type of interference present, the simple quantile algorithm and excision processing worked well for either narrowband or broadband interference. However, with both types of interference present at the same time, two problems occurred; the quantile algorithm set the threshold too high and an undesirable interaction took place between the broadband and narrowband suppression techniques. Slightly more complicated algorithms improved performance on the channel but satisfactory operation required large (>128) time-bandwidth products.

Another approach using a hybrid technique that divided the TW space into a time-frequency grid showed good results and a simpler processing implementation for large TW products.

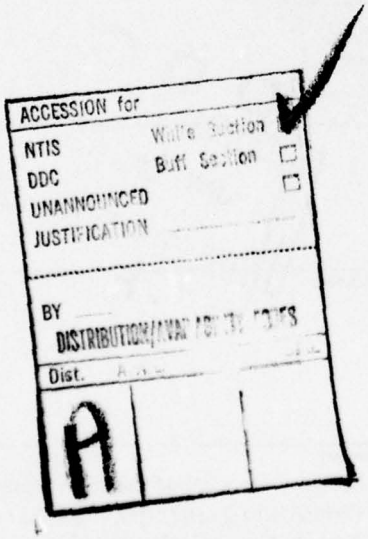

CONTENTS

ILLUSTRATIONS

ILLUSTRATIONS (Continued)

TABLES

INTRODUCTION

This report documents the adaptive-communications signal-processing development performed under the Survivable High-Frequency Communications (SHFC) project. Some of the results from an earlier project[1] are included in this report together with results of new work.

The basic objective of the new work was to develop and evaluate new techniques for suppression of noise and interference particularly as applied to signals with large bandwidths and time-bandwidth products capable of being used in the high-frequency (3 to 30 MHz) region. To this end, certain conclusions from earlier work were used in this new effort. These were:

1. If digital processing is used, a sample word size of 12 bits is required;
2. A fast Fourier transform (FFT) using 16-bit block floating-point arithmetic is sufficient for a time-bandwidth (TW) product of 1024 or less;
3. An algorithm which eliminates all frequency-domain samples above a certain threshold is effective in suppressing narrowband interference;
4. The threshold may be estimated simply based upon the noise-envelope exceedance function; and
5. Broadband noise may be suppressed effectively by a nonlinear weighting of the time-domain samples based upon the noise characteristics and the instantaneous sample envelope.

In performing the previous work, a system for evaluating different signal-processing approaches was fabricated. This system, called the Simulation Test Facility (STF), used signal and noise generators to produce representative types of interference which could then be added to sampled signal-waveform representations. This technique was used to generate receiver operating curves for various processing schemes with different signal and noise parameters. A description of the STF capabilities is given in the appendix. The STF was used to:

1. Perform a trade-off between threshold excision and threshold whitening against narrowband interference;
2. Perform a trade-off between clipping, blanking, and logarithmic processing on the time domain input in burst interference;
3. Determine effectiveness of the noise suppression algorithms for small TW signals;
4. Investigate integration of the time domain and frequency domain interference suppression algorithms; and

---

[1] NELC TN 3210, Signal Processing Algorithm Developments for the Simulation Test Facility, by GJ Brown, 17 August 1976.
(NELC (now NOSC) TNs are informal documents intended chiefly for internal use.)

5. Evaluate signal processing simplifications and alternatives.

Unless otherwise stated, the STF was used with the following parameter values:

1. Processed Time-Bandwidth Product = 2.56 ms x 100 kHz;
2. Signal Time-Bandwidth Product = 1.28 ms x 100 kHz (centered in processing time interval);
3. Signal Modulation = 2 symbols with random phase coding; and
4. Time Smoothing Function = Kaiser Bessel window.

SIGNAL PROCESSING IN THE TIME DOMAIN

Interference in the high-frequency spectrum can be characterized roughly as broadband or narrowband. Broadband interference is that arising from lightning discharges, ignition systems, and machinery which has a burst-type characteristic when examined in the time domain. Narrowband interference is that caused by other high-frequency users and appears fairly constant when examined in the time domain.

Many techniques have been suggested for suppressing broadband burst interference; all of these depend upon identifying the burst as extraordinarily large and eliminating or weighting the burst to minimize its effect. This method of suppression requires that the signal structure contain sufficient redundancy so that the desired information is not totally suppressed along with the noise burst.

Three techniques for suppression will be included in this portion of the report. These include threshold clipping, threshold excision, and the Hall-receiver technique. The first two techniques depend upon the setting of a threshold amplitude while their phase is retained. waveform; samples above the threshold are then considered to be a noise burst. If clipping is used, these samples are then set to the threshold amplitude while their phase is retained. If excision is used, the samples which exceed the threshold are set to zero. The Hall-receiver technique[2] is optimum for a particular noise environment which is characteristic of atmospheric noise conditions. This receiver does not use a threshold but does require knowledge of noise statistics.

BROADBAND NOISE SUPPRESSION USING THRESHOLD EXCISION

Simplified diagrams of a burst-interference model and threshold-excision receiver are given in figure 1. All parameters have been normalized by the signal power, P_S. In this simple model, the noise into the receiver is either due to the hf background (with probability $1-\rho$) or to burst Gaussian noise interference (with probability ρ). The noise is chosen independently of the received signal, which is a biphase modulated sequence.

---

[2]SEL Report 66-052, A New Model for "Impulsive" Phenomena: Application to Atmospheric Noise Communication Channels, by HM Hall, 1966.

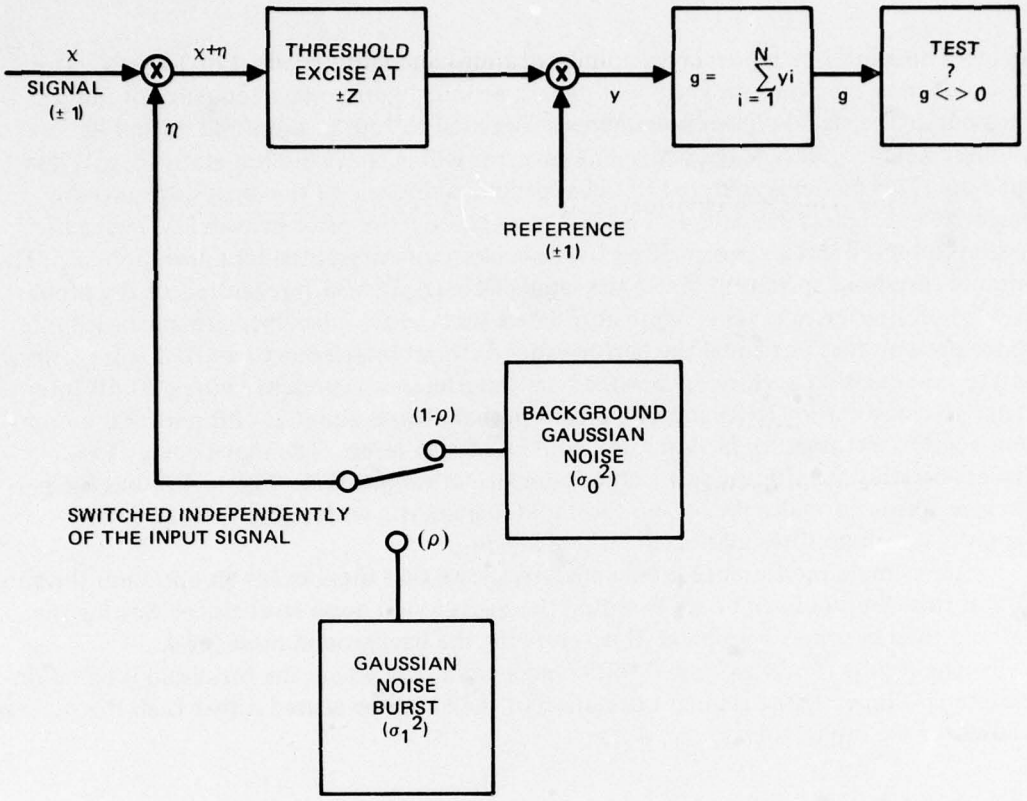

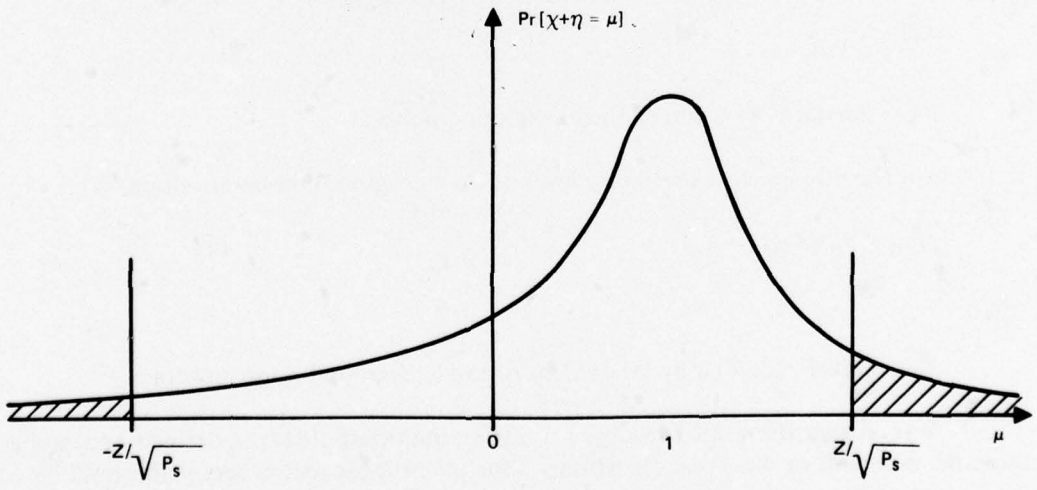

Figure 1. Simplified receiver and noise models.

A symbol decision is made on an accumulated time-bandwidth product of TW = N. The simple coherent receiver uses antipodal signals, assumed here to be a sequence of plus or minus ones. The signal-plus-noise samples are excised to zero at threshold +z and –z. Assuming a symbol of N plus-ones is sent, an error will occur if the test statistic, g, is less than zero. This model is analyzed in the appendix, and some of the analysis results are summarized in figures 2, 3 and 4. Figure 2 plots the symbol-error probability versus the excision threshold level, z, normalized to the background-noise standard deviation, σ_o. The optimum threshold appears at about the same place, ($z_{opt} = 3\sigma_o$) regardless of the probability (ρ) of interference. This figure also shows that even the best performance with interference present does not equal the performance without interference (ρ=o). Figure 3 shows that the best excision performance when burst interference is present, with a 20 dB Interference-to-Noise Ratio (INR) and 20 percent probability, is about 2.5 dB poorer than optimum receiver performance in stationary white Gaussian noise. The signal energy loss accounts for only 0.5 dB; the rest is due to imperfect suppression. Figure 4 shows the performance versus normalized-excision threshold, parametric with signal-to-noise ratio. Again, the optimum threshold occurs where $z = 3\sigma_o$.

This simple interference-model analysis shows that there exists an optimum threshold, and that this threshold can be set based on the background noise level alone. Setting the threshold then becomes a problem of determining the background noise level.

The results can be extended to the incoherent case where the threshold is based on the noise envelope. If the standard deviation of the envelope is used rather than the standard deviation of the input, then,

$$z_{opt} = 4.5\ \sigma,$$

where

σ = standard deviation of the background noise envelope

$= 1.53\ \sigma_o$

σ_o = standard deviation of the background noise.

In terms of the 90-percent exceedence level of the background noise envelope,

$$z_{opt} = 9.8\ X_{90}, \qquad (1)$$

where

X_{90} = level exceeded by 90 percent of the background noise envelope

Several algorithms are available for setting the threshold level, defined basically as quantile, moment, or multipass algorithms. The quantile algorithm sets a threshold based on 1 point of the envelope exceedence function. For example, using the 90 percent point and assuming a zero mean Gaussian noise input, the noise envelope is Rayleigh distributed as:

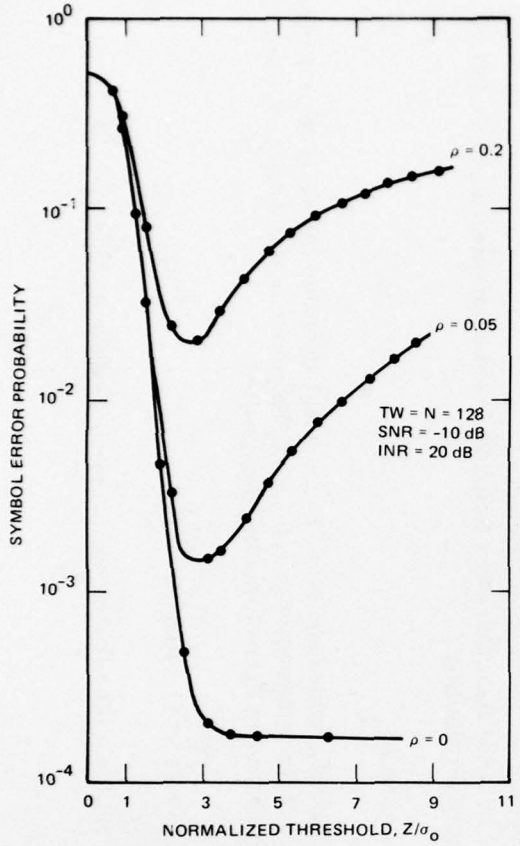

Figure 2. Excision threshold optimization.

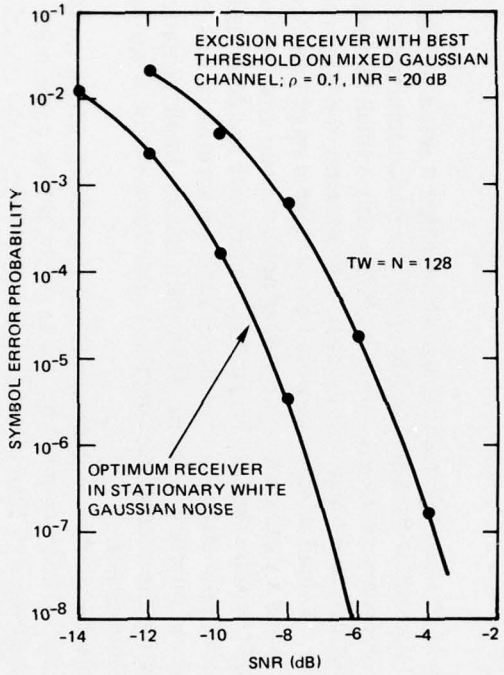

Figure 3. Best excision performance.

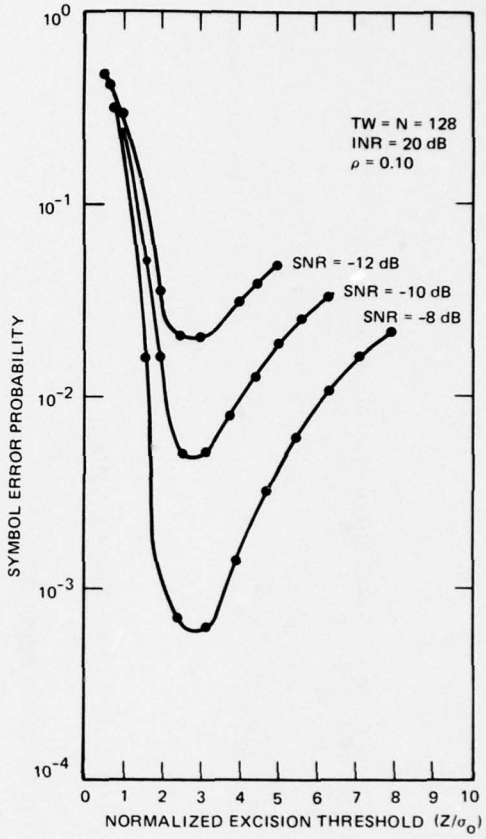

Figure 4. Excision threshold optimization (SNR-12, -10, and -8 dB).

$$\Pr\left\{n = x\right\} = \frac{x}{\sigma_o^2} \quad e^{-x^2/2\sigma_o^2} \quad U(x)$$

$$\Pr\left\{n \geq x\right\} = e^{-x^2/2\sigma_o^2}$$

and

$$e^{-X^2_{90}/2\sigma_o^2} = .90 \rightarrow X_{90} = 0.459\sigma_o$$

Therefore the optimum threshold is

$$z_{opt} = 9.8 \; X_{90} \qquad (1)$$

The advantage of using the quantile algorithm is that it sets a threshold based upon the smallest 10 percent of the samples, hopefully the background noise. The algorithm does have some secondary problems, however. When only a small number of samples are available, it is difficult to estimate consistently with accuracy the 90-percent point of the background noise. A small sample size would occur when a small time-bandwidth product is processed. When a significant number of samples contain interference, the threshold will be biased high because the true background sample size has decreased. So two estimation problems exist; estimating the exceedence function accurately, and differentiating between background and interference noises in the estimation. Implementation is also a problem since generating the exceedence function requires some kind of sorting process, which is difficult to implement.

There are alternative implementation possibilities which could be used to estimate the 90 percent exceedence point by, for example, setting a preliminary threshold, calculating the exceedence, and then calculating an adjustment to the threshold. Other alternatives exist, but the work documented in this report will use the exceedence function based on all the available samples, including interference.

The moment algorithm sets a threshold based upon the first and second moments of the sampled distribution

$$z = \mu_1 + \alpha \mu_2, \qquad (2)$$

where α is a predetermined constant. The moment algorithm threshold value depends upon the statistics of the interference as well as the background noise. Therefore, using the simple model shown before in figure 1, the threshold will be

$$z = \alpha \left(\rho \, \sigma_1^2 + (1 - \rho) \, \sigma_0^2\right)^{1/2}, \qquad (3)$$

and will be optimum for a fixed α only at specific values of ρ and σ_1^2.

The multipass algorithm combines some features from the moment algorithm and the quantile algorithm. It measures the first (μ_1) and second (μ_2) moments of the noise envelope and uses the statistic

$$V_d = (\mu_2/\mu_1{}^2), \qquad (4)$$

to determine the presence or absence of burst noise. For Gaussian noise, V_d is 1.27 and should be larger for impulsive noise. If V_d is large, a threshold is set and large samples are excised. V_d is then recalculated with the remaining unexcised samples. The procedure is repeated until V_d is close to 1.27. This algorithm suffers from the problems of both the moment and quantile algorithms. It is complex in that multiple passes are required. In addition, V_d does not always supply a reliable indication of the noise impulsiveness, and as more samples are eliminated, the estimates of μ_1 and μ_2 become less reliable.

Based upon the preceding, the following strategy was chosen: the quantile excision algorithm was used for TW products of 128 or larger; for smaller TW products, the moment algorithm was used.

The threshold excision algorithm is illustrated in figure 5. The algorithm was modified to excise additional samples adjacent to those exceeding the threshold. This increased the sensitivity of the algorithm without undue over-excision. A technique similar to this was found to improve algorithm performance when applied to the narrowband interference problem.[3]

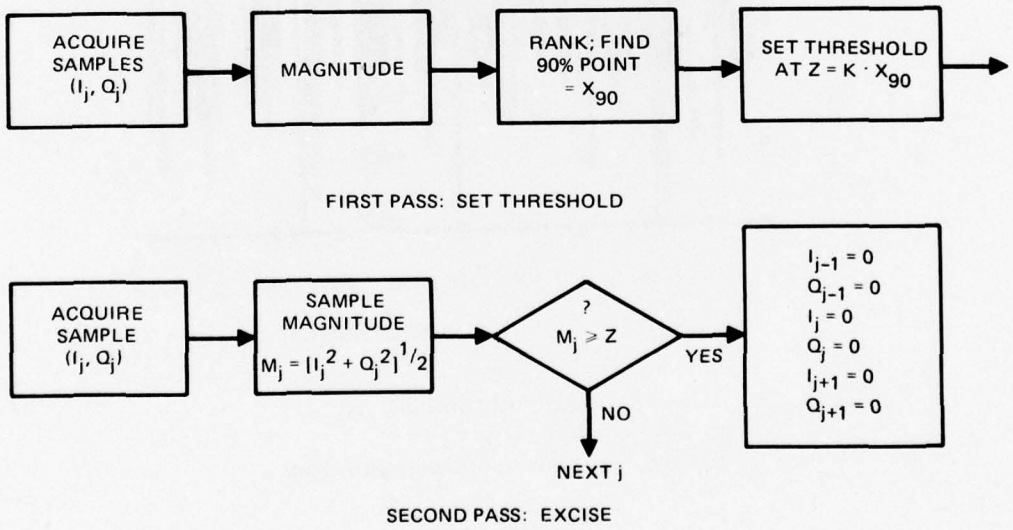

Figure 5. Time-domain excision algorithm.

[3]University of Missouri-Rolla Technical Report CSR-76-1, Analysis and Simulation of a Large WT Product Signalling Technique in Typical HF Environments, by RE Ziemer and R Kister, January 1976

Figure 6 shows 3 "snapshots" taken from the STF showing the input interference-plus-noise-plus-signal time-domain envelope (a), the envelope after burst noise excision (b), and the correlation function (c). This sample represented a time duration of 2.04 ms, and a bandwidth of 100 kHz, in which the signal occupied the center 1.024 ms. The interference pulses occurred at a 4-kHz rate and 10-μs duration, and consisted of pulsed Gaussian noise. The background noise was also stationary, white and Gaussian. The STF used a symbol alphabet consisting of two random-phase coded signals with TW of 128.

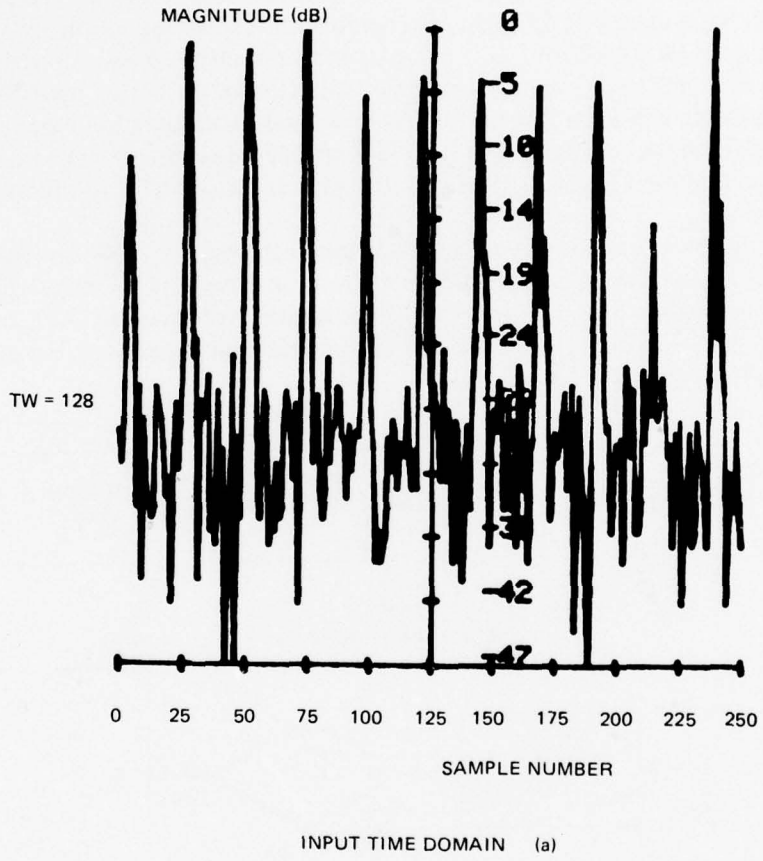

Figure 6. Time envelope for burst interference.

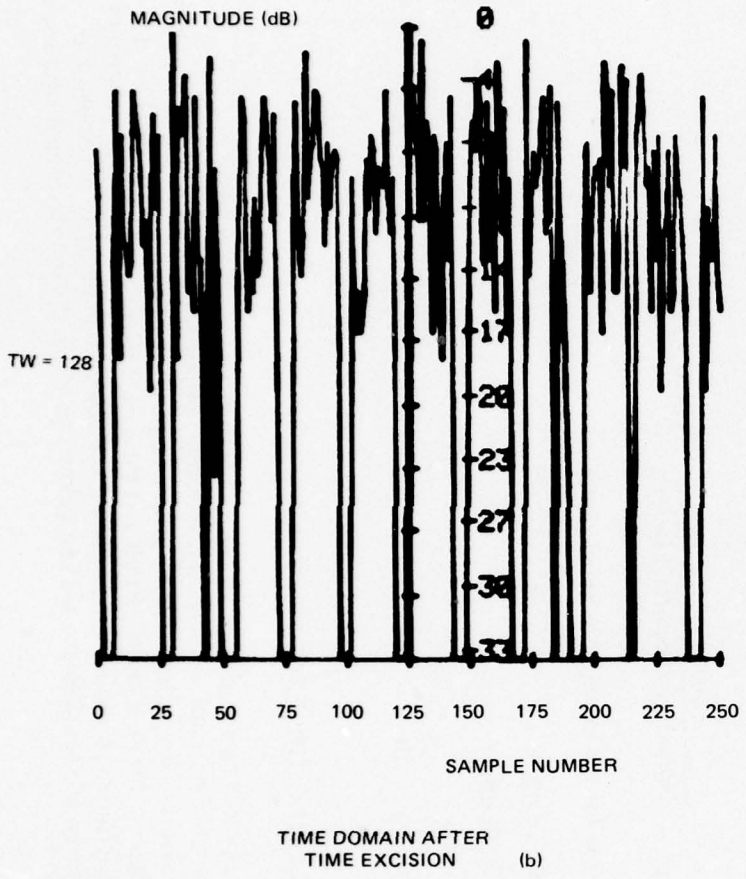

TIME DOMAIN AFTER
TIME EXCISION (b)

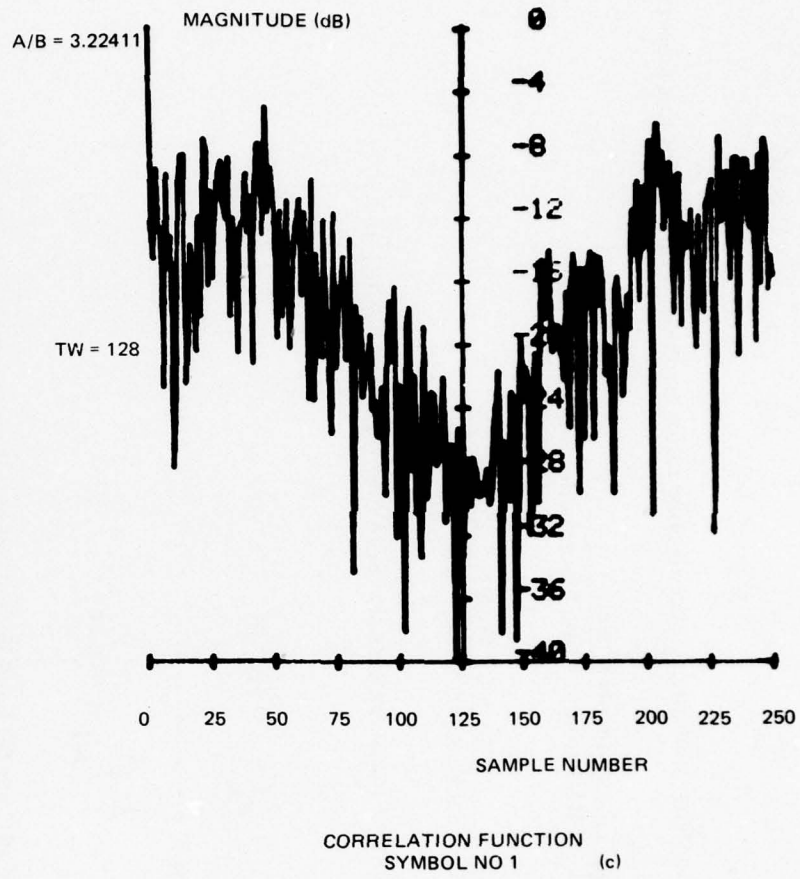

CORRELATION FUNCTION
SYMBOL NO 1 (c)

Figure 6. Continued.

The signal- and interference-to-noise ratios are defined throughout this report as

$$SNR = \frac{\text{Signal Power}}{\text{Background Noise Power}} = \frac{P_S}{P_N}$$

$$INR = \frac{\text{Interference Power}}{\text{Background Noise Power}} = \frac{P_I}{P_N}$$

where the power measurements are taken over the signal bandwidth

$$SNR = \frac{\frac{1}{T}\int_{t-T}^{t} S^2(t)\ dt}{\frac{1}{T}\int_{t-T}^{t} n^2(t)\ dt}$$

and S(t) and n(t) are the band limited signal and noise waveforms. The SNR is related to signal energy-to-noise power spectral density by the signal time-bandwidth (TW) product

$$\frac{E_S}{N_{0\,1}} = \frac{\text{Signal Energy}}{\text{Noise Power Spectral Density}} = SNR \cdot (TW)$$

The parameters for the example in figure 6 were

SNR = -4 dB

INR = 16 dB

TW = 128

E_S/N_{01} = 17 dB

SELECTING THE EXCISION THRESHOLD

In the preceding paragraphs, it was shown that, under certain interference conditions, an excision threshold $z = 9.8\ X_{90}$ is nearly optimum over a broad range of interference parameters. This threshold was verified empirically using the STF. An example is shown in figure 7 for an SNR of -10 dB and the same interference condition shown in figure 6. An optimum threshold appears at a normalized value of about 9. Above this value, the interference is under-excised and below this value, the interference is over-excised.

This agrees approximately with equation (1) and the threshold value of 9 is used in all the simulation results presented in a later section of this report.

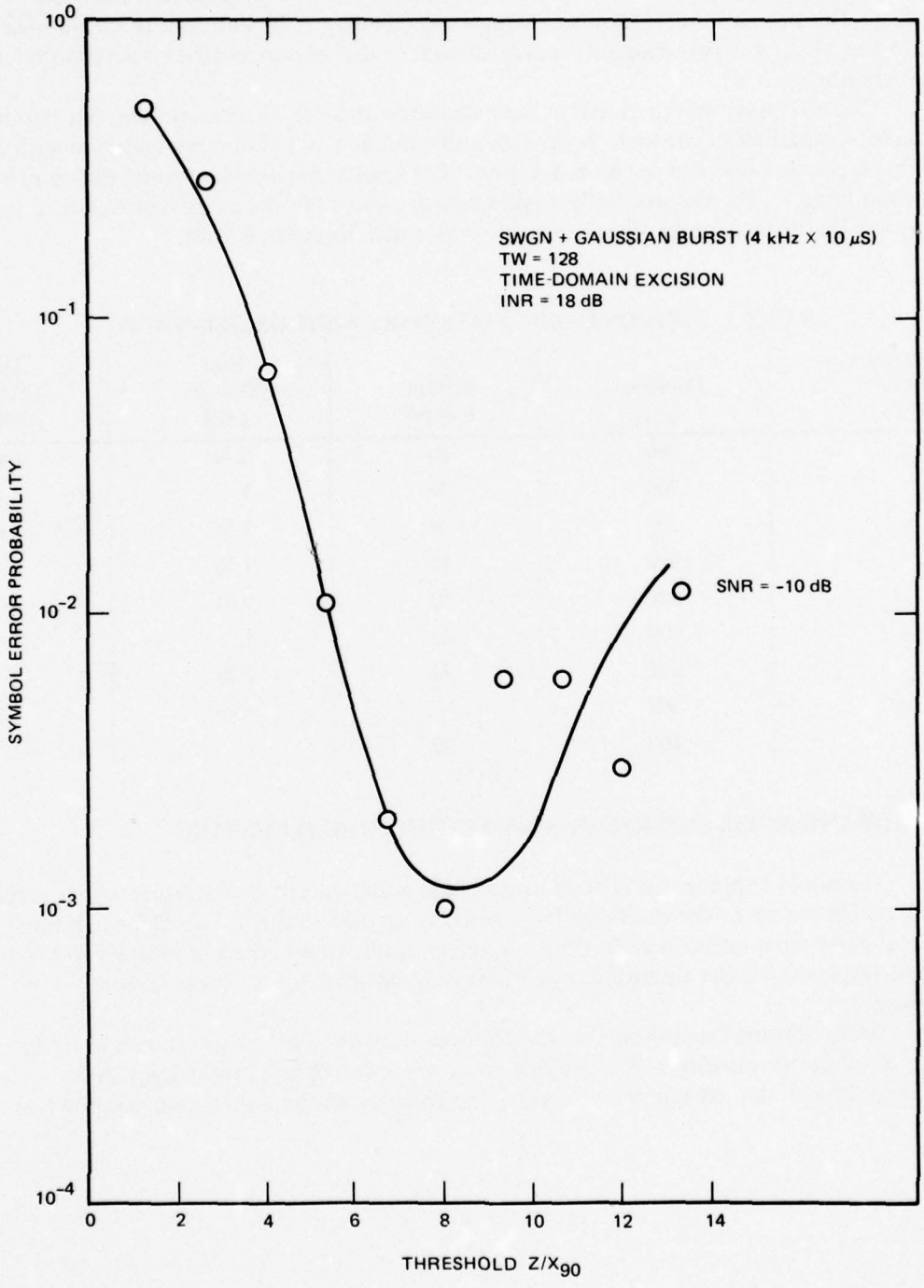

Figure 7. Excision threshold optimization for burst noise.

PROCESSING LOSSES DUE TO EXCISION

Excision will cause processing losses due to the reduced signal time-bandwidth product. The primary loss is from the reduced signal energy. In addition, there are losses due to loss of symbol orthogonality and mismatch to the references (the correlation references are not excised).

The STF was used to ascertain the magnitude of these losses under varying amounts of excision on a SWGN channel. A periodic, time-domain, excision mask was used with a variable repetition rate and excision duration. The results, as compared to no excision, are shown in table 1. The theoretical loss takes into account only the excised energy loss, so it appears that losses due to other causes are very small, less than 0.2 dB.

TABLE 1. EXCISION LOSS IN STATIONARY WHITE GAUSSIAN NOISE.

Repetition Rate (kHz)	Duration (μs)	Percent Excised	Loss (Theory) (dB)	Loss (Actual) (dB)
2	100	10	0.46	0.6
	200	20	1	1.2
	300	30	1.55	1.6
	400	40	2.22	2.4
	500	50	3.01	3
4	100	20	1	1.4
	200	40	2.22	2
	300	60	3.98	4.2
	400	80	7	~7

BROADBAND NOISE SUPPRESSION USING THRESHOLD CLIPPING

Threshold clipping is similar to threshold excision except that samples which exceed the threshold are set to the threshold level itself rather than to zero. This algorithm also differs slightly from excision in that it is no longer simple to set adjacent samples to the clipping level, so that the algorithm tested here does not perform adjacent-sample processing.

Some clipping "snapshots" similar to those shown in figure 6 are shown in figure 8. To speed up the algorithm, the clipping process is approximated using right shifts (divide by 2) and may set samples at slightly less than the clipping threshold, as shown in figure 8b.

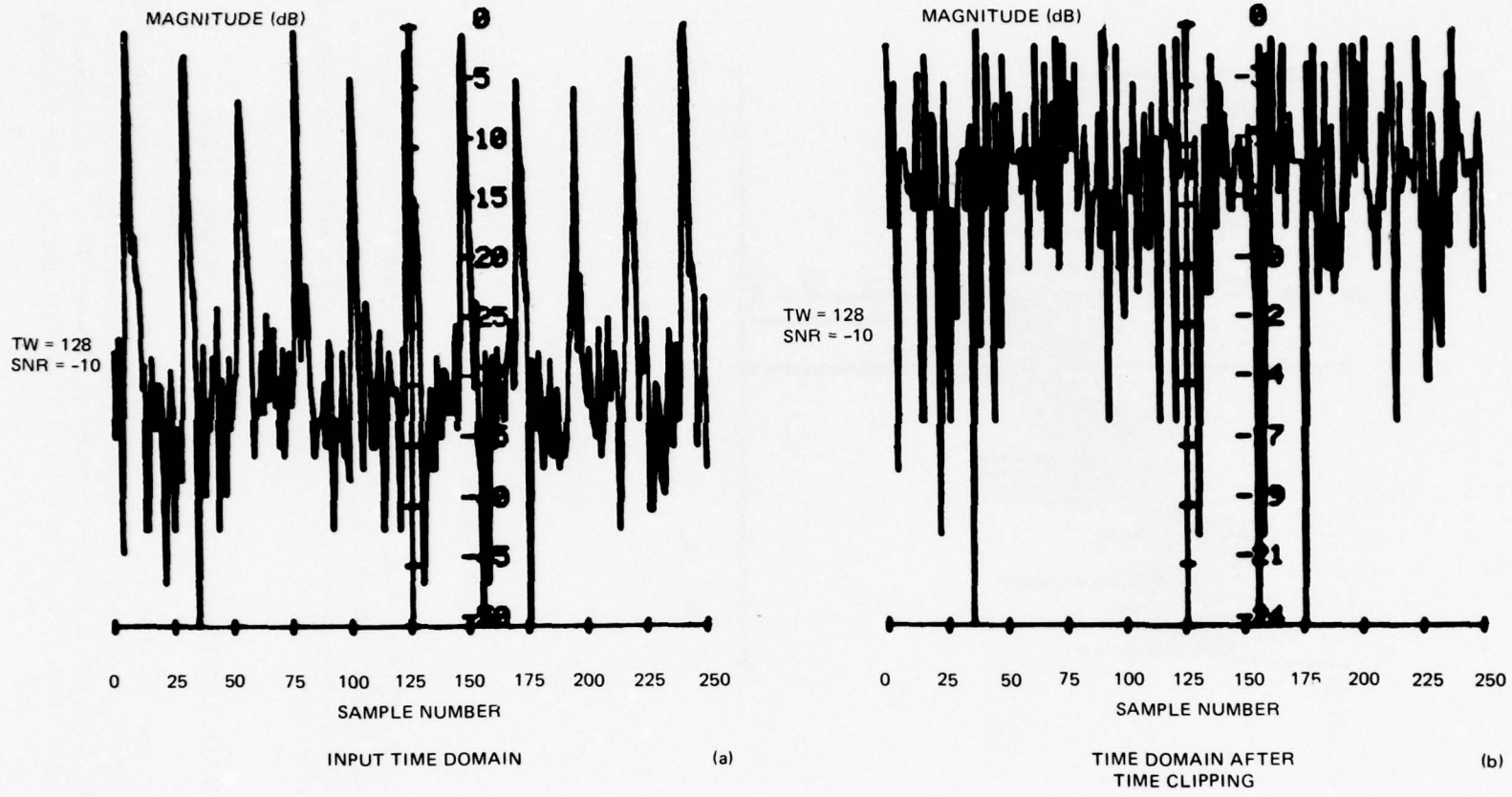

Figure 8. Input time envelope.

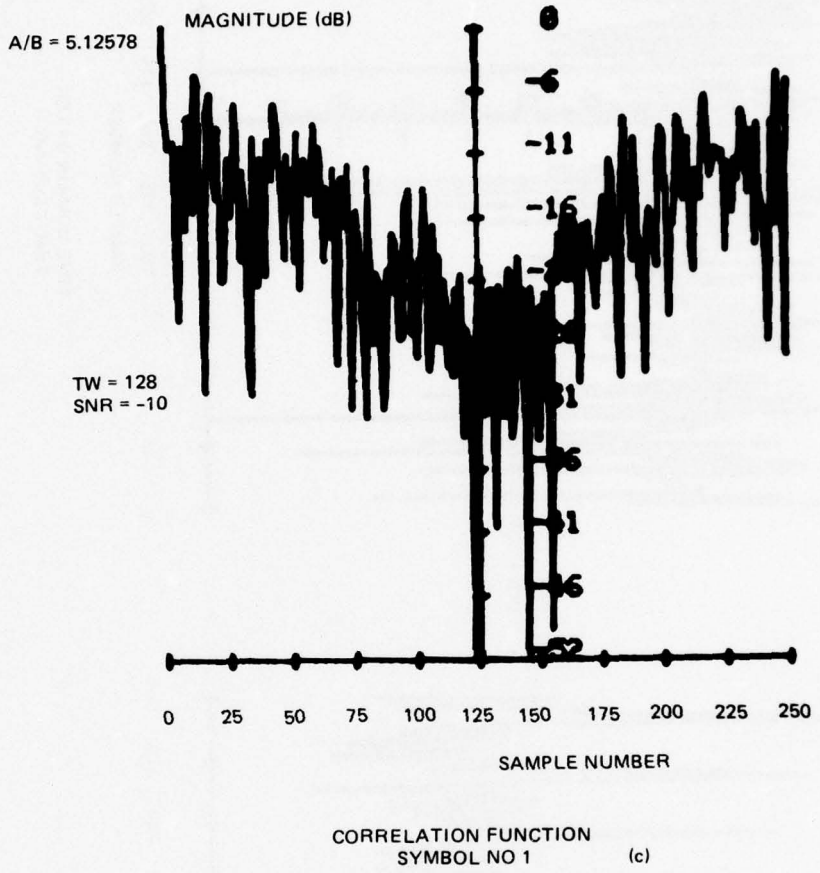

Figure 8. Continued.

As was the case for excision, the clipping threshold may also be optimized. This was done empirically and the optimum clipping threshold was found to be about one half of the optimum excision threshold. This threshold was used in all the simulations described under performance of burst-noise suppression algorithms.

BROADBAND NOISE SUPPRESSION USING A HALL-TYPE RECEIVER

The receiver-processing algorithm described here is based on an optimum receiver derived for the Hall model of impulsive noise.[2] The exact realization of this receiver is difficult because a logarithmic function is required. However, for a low signal-to-noise ratio (which is typically the case for moderate TW products) the test statistic reduces to

$$\Lambda_i = \left| \int_0^T \frac{x(t)\,\mu_i^*(t)}{|x(t)|^2 + \alpha(m)}\,dt \right|, \qquad (5)$$

where i = 1, 2, . . ., M

M = alphabet size

Λ_i = test statistic for the i^{th} symbol

x(t) = input time waveform

$\mu_i(t)$ = i^{th} symbol reference waveform

$\alpha(m)$ = bias term (dependent upon noise statistics)

m = noise parameter

This test statistic[1] is an incoherent correlator receiver where the input waveform has been weighted by the instantaneous envelope and a bias term. The bias term changes the effect of the envelope weighting. For $\alpha(m) >> |x(t)|^2$, the receiver approaches a simple correlator. For $\alpha(m) << |x(t)|^2$, the receiver sets the magnitude of each complex sample pair equal to unity. The relationship between $\alpha(m)$, m, and the noise, is such that, in a highly impulsive noise background, m is set to a value of 1 or 2 and $\alpha(m)$ is small. In a nonimpulsive noise background, m is 3 or 4 and $\alpha(m)$ is large. The value of m must be determined a priori, but $\alpha(m)$ can be calculated using a recursive algorithm that provides a maximum likelihood estimate.[4] A diagram of the receiver structure that was implemented for simulation is shown in figure 9.

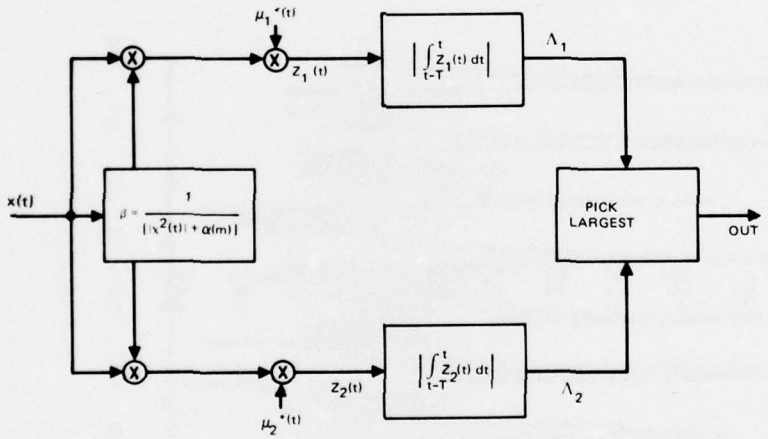

Figure 9. Simplified Hall receiver.

Figure 10 shows the time-domain waveform before and after Hall processing (Hall parameter, m = 3). The noise impulses are suppressed according to their magnitude; the larger the noise spike, the more it is suppressed. The performance of this receiver is given in the next section.

[4]Nirenburg, Lloyd M, Parameter Estimation for an Adaptive Instrumentation of Hall's Optimum Receiver for Digital Signals in Impulsive Noise, IEEE Transactions on Communications, COM-22, pp 798-802, June 1974

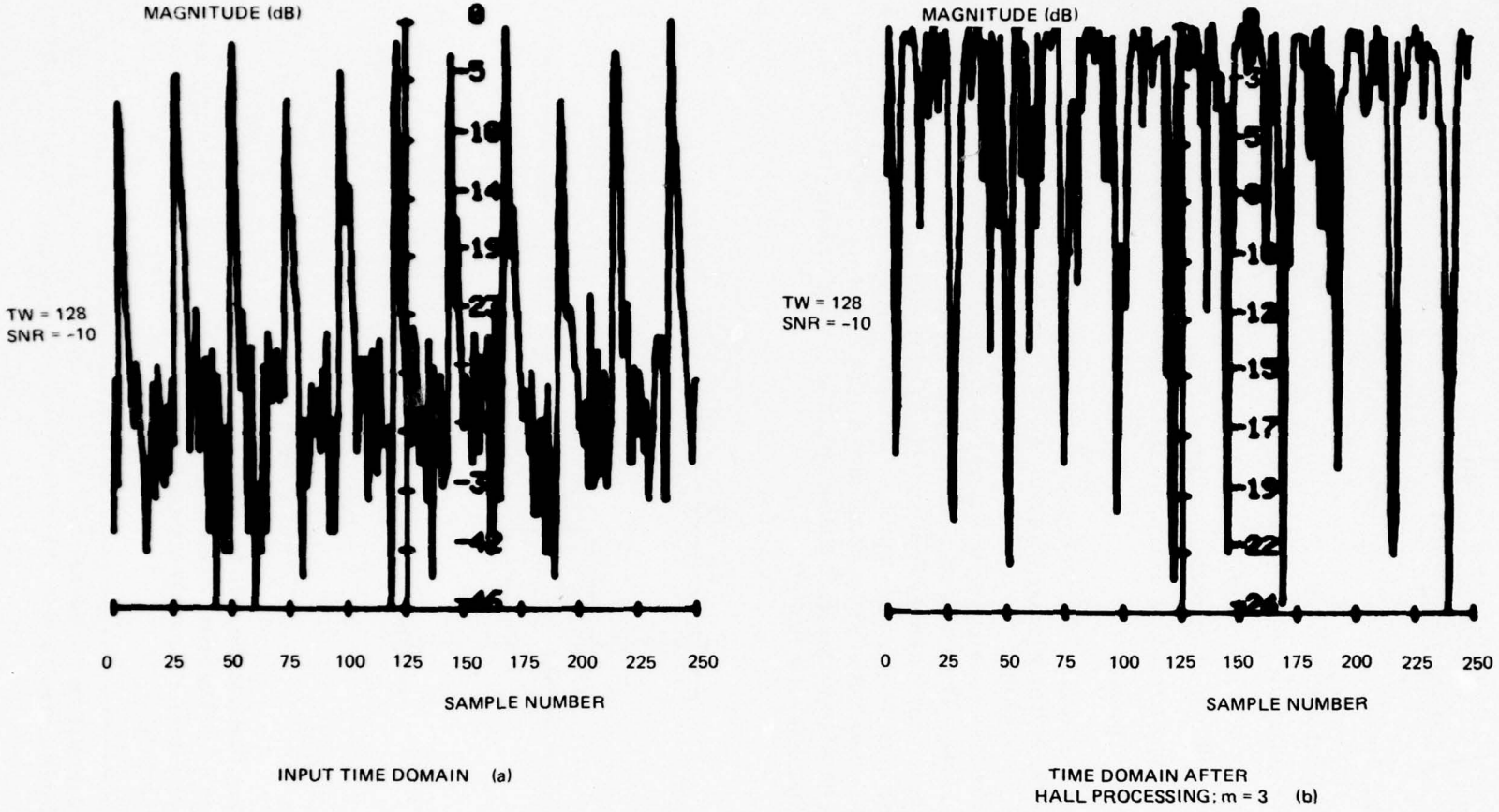

Figure 10. Input time envelope (SNR 10 dB).

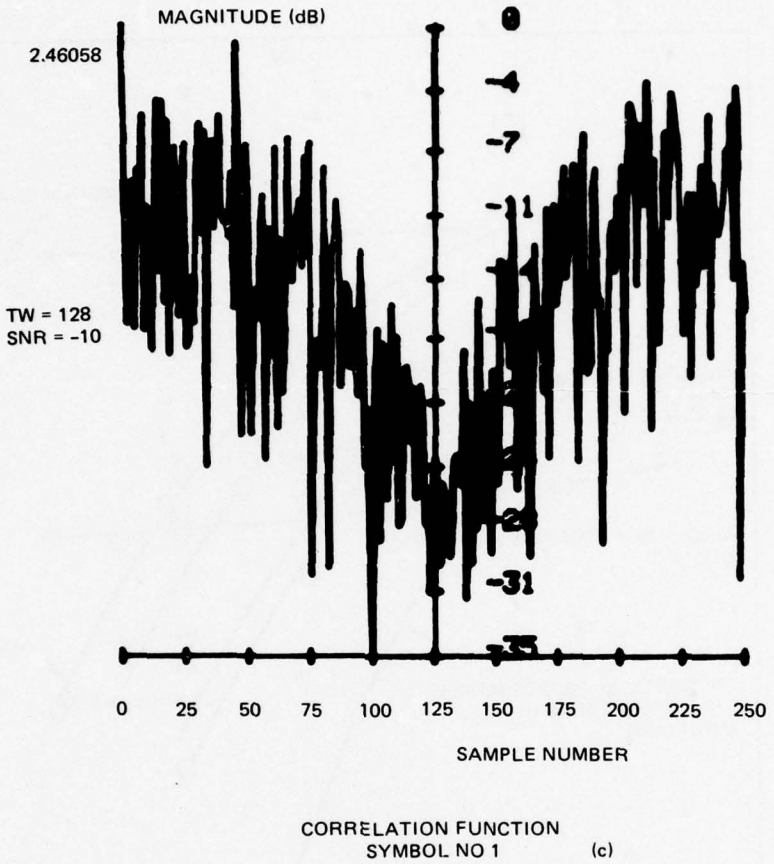

Figure 10. Continued.

PERFORMANCE OF BURST-NOISE-SUPPRESSION ALGORITHMS

PERFORMANCE IN STATIONARY WHITE GAUSSIAN NOISE

None of the three receiver structures is optimum in SWG noise to the extent that they perform nonlinear processing on the input time waveform when no burst interference is present. The performance curves from the STF for the processing alternatives are shown in figure 11. Also shown are the curves for the frequency-domain correlator where no nonlinear processing is performed, and the theoretical performance for binary incoherent signalling. There is a basic loss of 2 dB between the frequency-domain correlator and theory due to the input windowing, symbol non-orthogonality, and transform noise.[1] Above this, there is an additional 0.3-dB loss due to the excision algorithm. Some of this is a direct result of the signal energy loss (3.5 percent excision = 0.15 dB loss), and the rest is due to statistical estimation error and orthogonality loss.

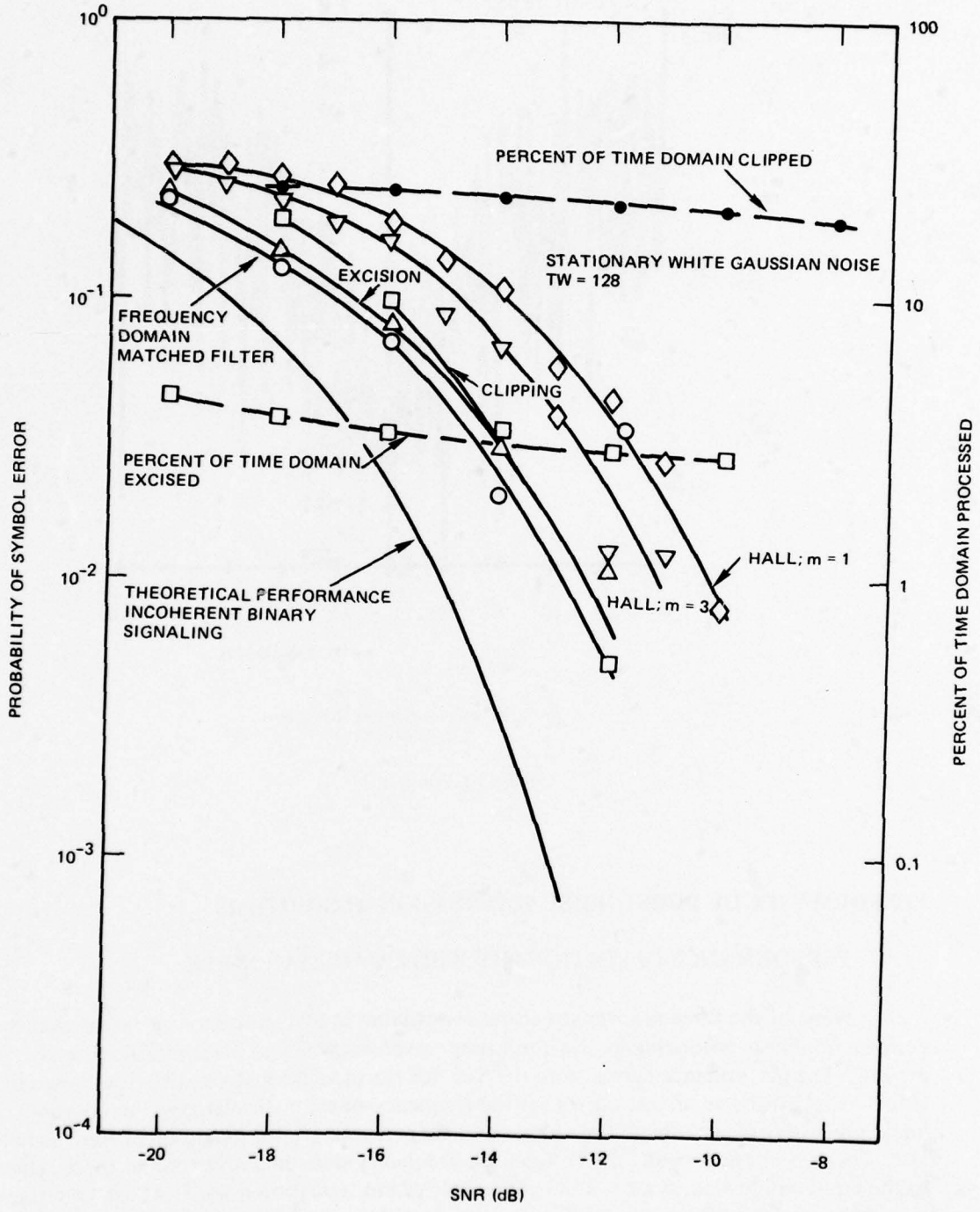

Figure 11. Burst-suppression algorithm performance in stationary white Gaussian noise.

The performance of the clipper was nearly identical to that of the excisor even though considerably more samples were clipped (20 percent versus 3 percent). Hall processing with m = 3, degrades performance by about 1.5 dB from the frequency-domain matched filter. This is significantly more degradation than in the excision and clipping experiments; not an unexpected result since the Hall receiver does not set a threshold, but instead processes all of the received samples in a nonlinear fashion.

For other values of the parameter m, the performance will differ, as was shown in reference 1. The curve for m = 1, taken from reference 1, shows an additional 1 dB loss.

PERFORMANCE IN SWGN PLUS BURST INTERFERENCE

Tests were run with the STF using a combination of stationary white Gaussian background noise, upon which the SNR was set, and a higher level of pulsed Gaussian interference, upon which the INR was set. The results of one of these tests is shown in figure 12 where the SNR was held constant at −12 dB while the INR was varied. The burst-interference parameters were held constant at 10-μs duration and a 4-kHz repetition rate, or approximately four pulses over the signal interval (figure 10a). The advantage of processing is clearly shown in figure 12, over the entire range of INR. Note that as the interference level increases, so does the percent of excised time domain since the bursts are somewhat sinx/x-shaped rather than perfect rectangles. As the percent excision increases, so does the loss due to lost signal energy. A curve based on this loss and the SWGN performance (figure 11) is also shown in figure 12. This curve comes close to the actual performance results, but an additional loss is still apparent. Again, excision is somewhat better than clipping. The Hall receiver's performance is the least sensitive to INR, even though it performs poorest in SWGN. Overall, excision performs better than clipping or the Hall receiver at all values of INR.

The performance of the time-domain processing algorithms was also analyzed as a function of interference pulse density. That is, the interference pulses were fixed at a peak power level and were varied in repetition rate. The resulting error probabilities for an SNR of −10 dB are shown in figure 13. The excision performance is close to that projected from the previous SWGN characteristics. The projected performance was calculated by estimating the energy lost and a loss of orthogonality (~0.5 dB in the region of 25-50 percent excision). Two problems occur; first, the threshold is pushed up by the additional interference, this, in turn, allows more interference to come through unsuppressed, and second, eliminating the "interfered" samples from the threshold estimation process leaves too few samples for a reliable estimate to be made. The excess loss thus incurred is about 2 dB.

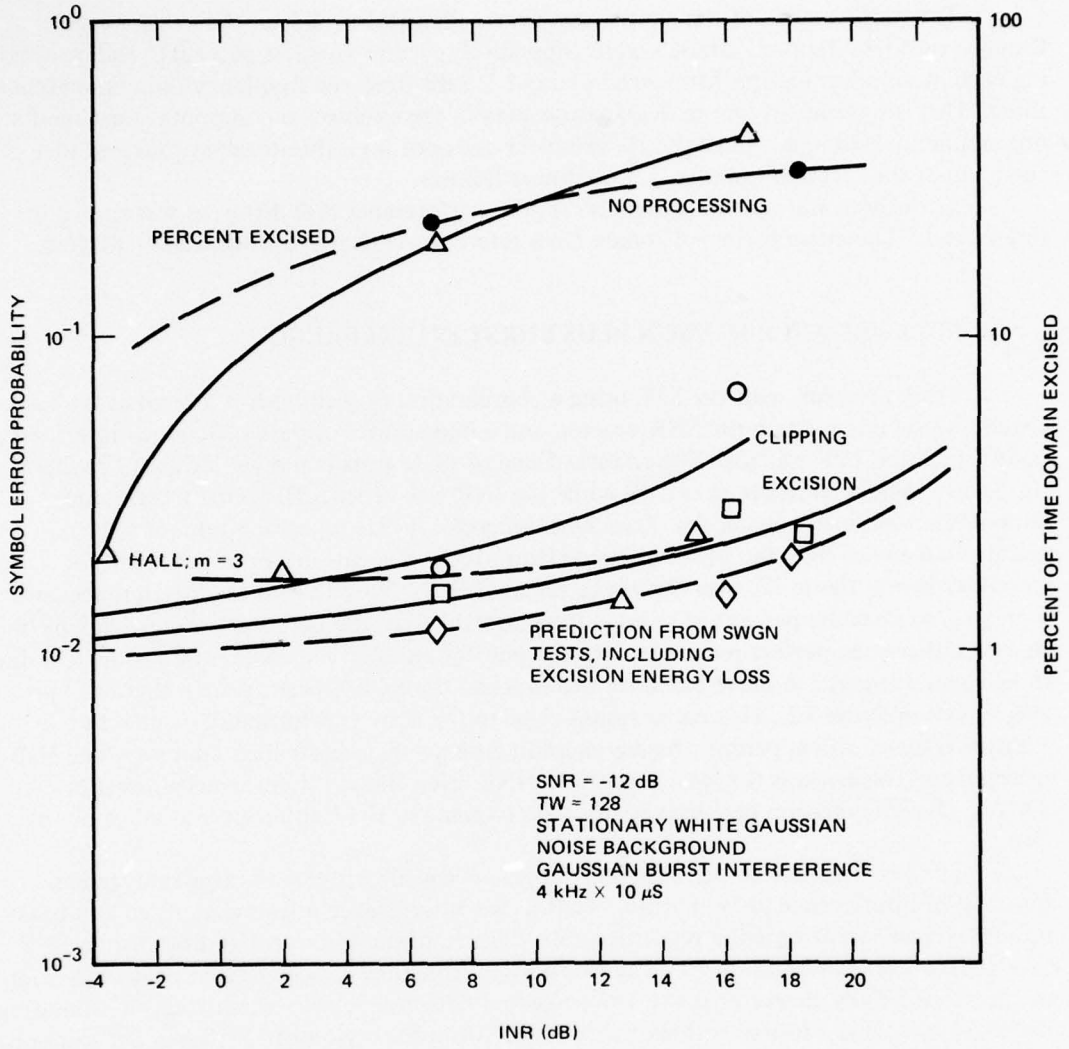

Figure 12. Algorithm performance in burst interference (SNR -12 dB).

Excision again performed better than clipping and Hall processing, although the parameter of m, picked for the Hall receiver, was probably not optimal. In addition, the particular type of interference picked for this simulation did not fit the Hall model description for interference.

The receiver operating curves are given in figure 14 for the same noise and interference when the INR is fixed at about 15 dB. Again, excision performs better than the other 2 techniques. Excision is also the easiest technique to implement, making it an attractive choice, however, the impact of frequency-domain processing (SIGNAL PROCESSING IN THE FREQUENCY DOMAIN) must be considered before a final choice can be made.

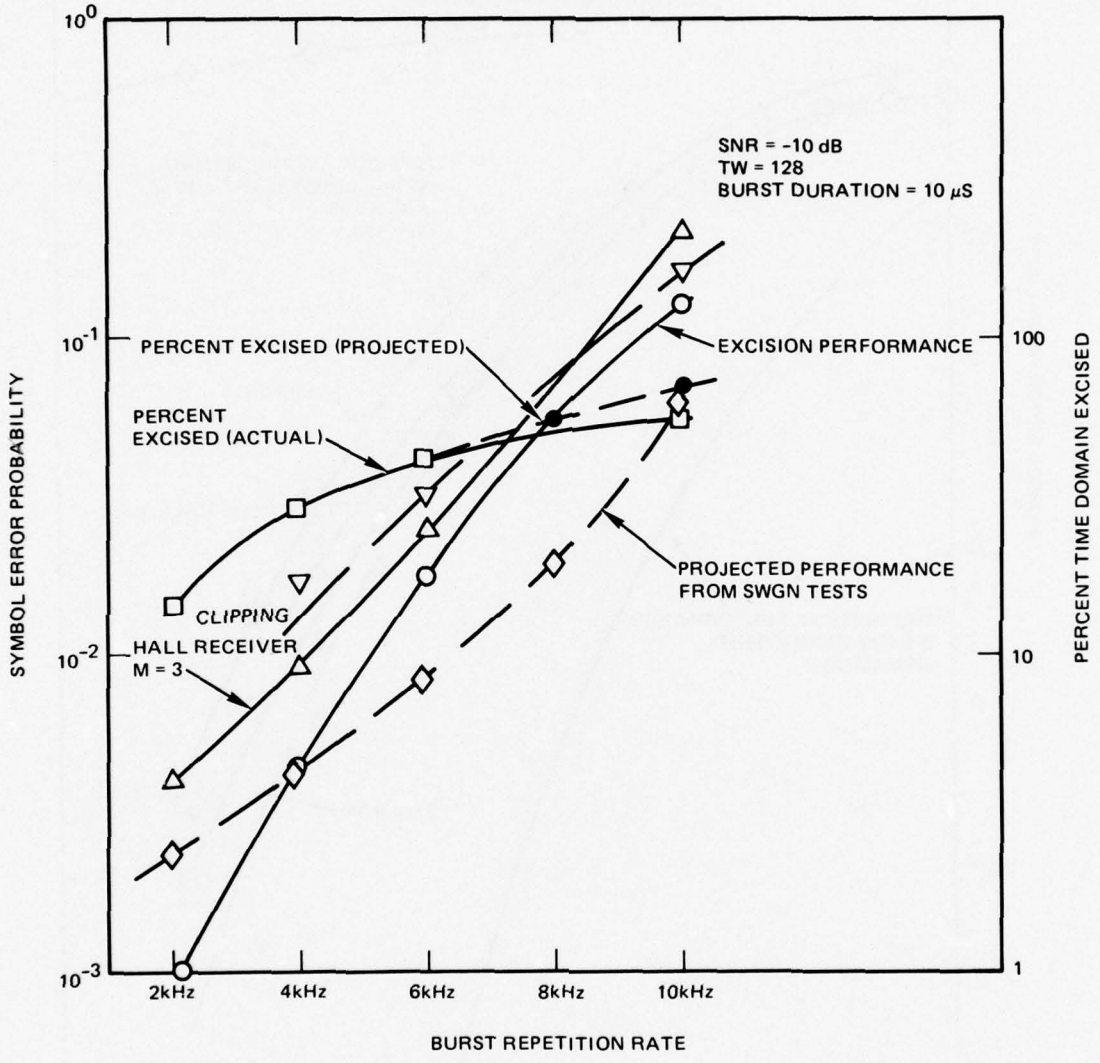

Figure 13. Algorithm performance in burst interference (SNR -10 dB).

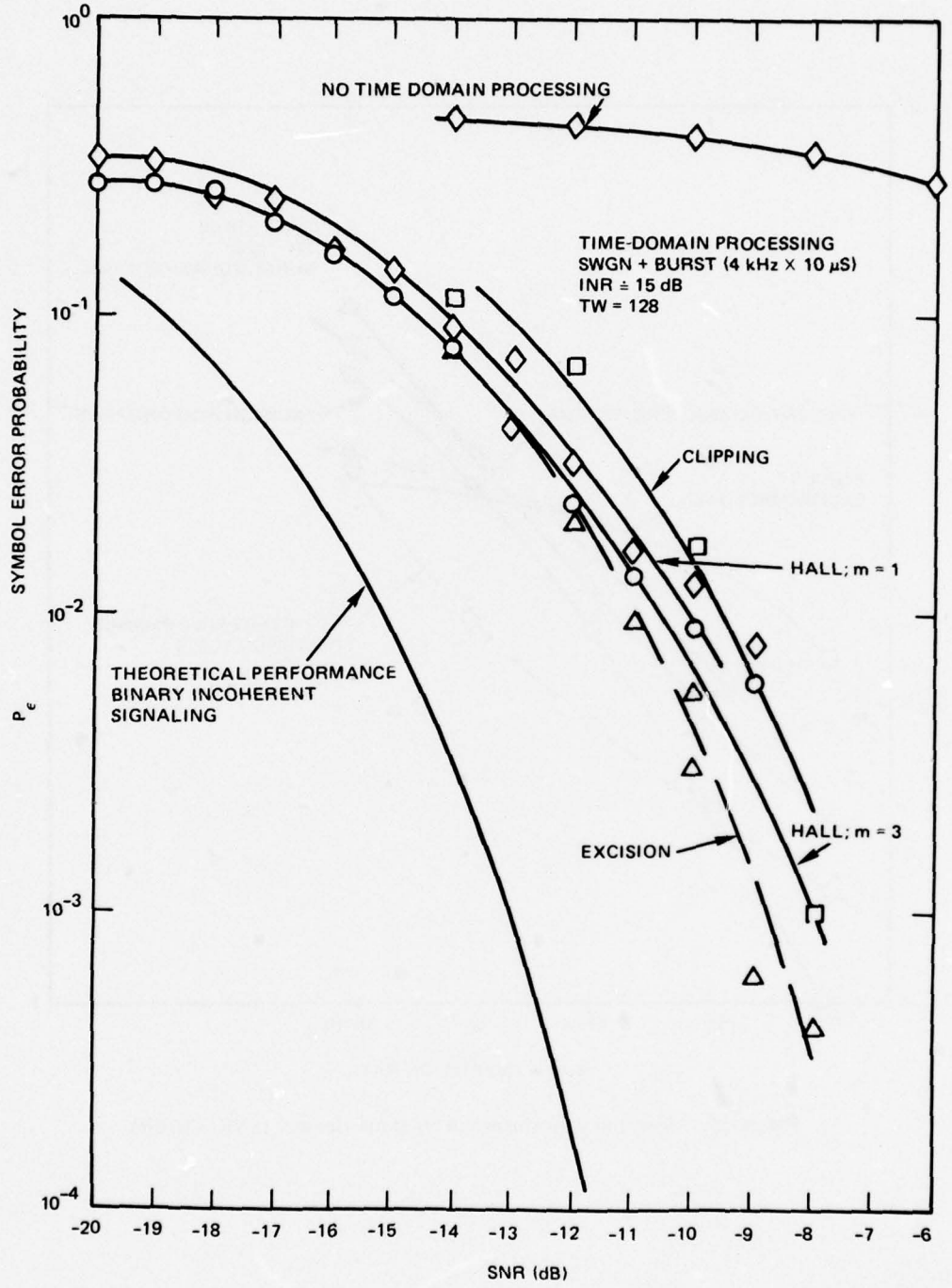

Figure 14. Receiver operating curves for burst interference.

TIME-DOMAIN EXCISION PROCESSING FOR SMALL TIME-BANDWIDTH PRODUCT SIGNALS

Several techniques are available for broadband noise suppression when small TW product signals are involved. One approach is to make "soft" symbol decisions on each signal and let a decoder do the interference suppression. Another approach is to use threshold excision, where the set threshold is based on statistics gathered over a time interval longer than the symbol itself. The first of these techniques places the interference-suppression burden on error-correction codes, a topic outside the scope of this report. The second approach involves additional processing complexity and memory, and does not address the problem of relatively short-duration interference.

The technique considered here is a simple extension of the excision algorithm presented previously (figure 5). The only difference is the manner in which the excision threshold is set. In this case, the threshold is based on the average envelope of all N sample pairs

$$z = \frac{1.5}{N} \sum_{i=0}^{N} y_i,$$

where

y_i = envelope of the i^{th} sample pair.

The multiplying factor of 1.5 was found empirically to give good performance over a wide range of interference parameters.

A receiver operating curve for Gaussian plus burst-Gaussian interference with N = 32 is shown in figure 15. The excision performance is about 6 dB poorer than the theoretical performance in SWGN, and about 10 dB better than the correlator receiver alone. The performance loss from optimum is about 2 dB more than occurred for a TW product of 128 (see figure 14).

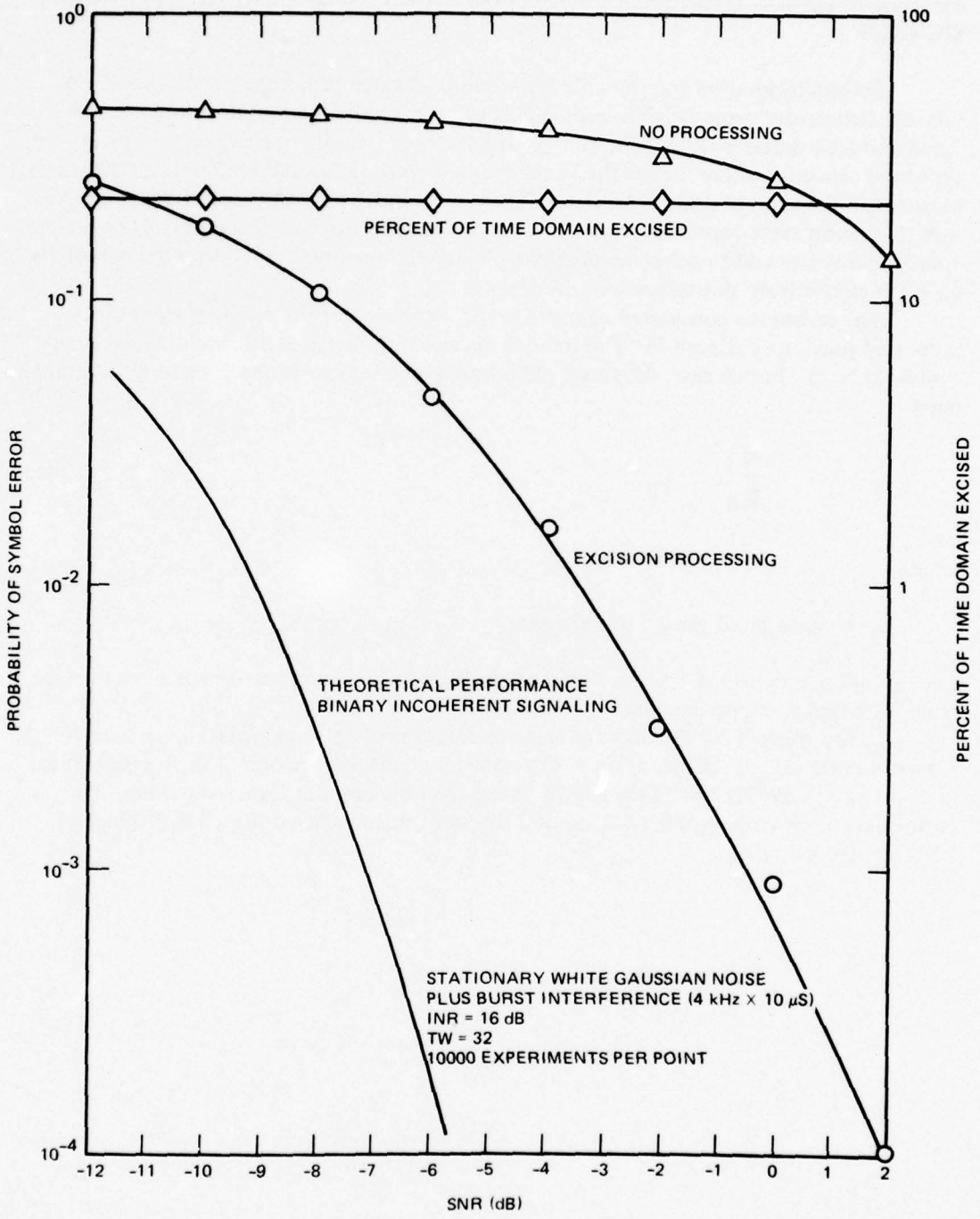

Figure 15. Receiver operating curve for small TW burst suppression.

SIGNAL PROCESSING IN THE FREQUENCY DOMAIN

The frequency-domain signal processing presented here used the fast Fourier transform (FFT) to provide a sampled frequency-domain representation of the received signal plus noise. Like time-domain processing, frequency-domain processing takes place on a symbol-by-symbol basis, and does not make use of memory to establish estimates of noise and interference conditions.

Previously,[1] three techniques were considered for frequency-domain interference suppression; true spectral whitening, whitening above a threshold (threshold whitening), and excising above a threshold (threshold excision). It was shown in reference 1 that true whitening required a better estimate of the spectrum than was possible over the short symbol interval. The other two techniques are examined in this report.

NARROWBAND NOISE SUPPRESSION (NBNS) USING THRESHOLD TECHNIQUES

The rationale for using a threshold is that signals above the threshold are high powered and can be identified readily.

In a spread-spectrum system, narrowband interference will have processing gain through the time-frequency transformation via the FFT. For example, figure 16 shows the frequency transform for 4 different interference-to-noise ratios (INR) where

$$\text{INR} = \frac{\text{Interference Power}}{\text{Noise Power}} = \frac{P_I}{P_N} \quad \text{and}$$

P_I = Power of CW tone (measured at baseband)

P_N = Power of stationary white Gaussian background noise, measured over ±50 kHz at baseband

Figure 16a shows that, at 0-dB INR, the tone is clearly visible. This is due to the coherent integration performed by the FFT, giving a processing gain of TW or 24 dB. This also illustrates why the dynamic range of the FFT processor must include an additional factor of TW over the dynamic range of its input. The example shows that the FFT processing, in conjunction with a threshold, can effectively pick out narrowband tones without excising the background noise, even at low INRs, given sufficient TW sizes.

Figure 16d shows another interesting characteristic. In this example, the large tone exceeds the dynamic range of the system's analog to digital (A/D) converter. When this happens, many spurious components are generated (the main peak has changed position because a slowly sweeping tone was used). This distributes the noise power over the signal bandpass, effectively increasing the background noise level, and also causing more of the spectrum to be excised.

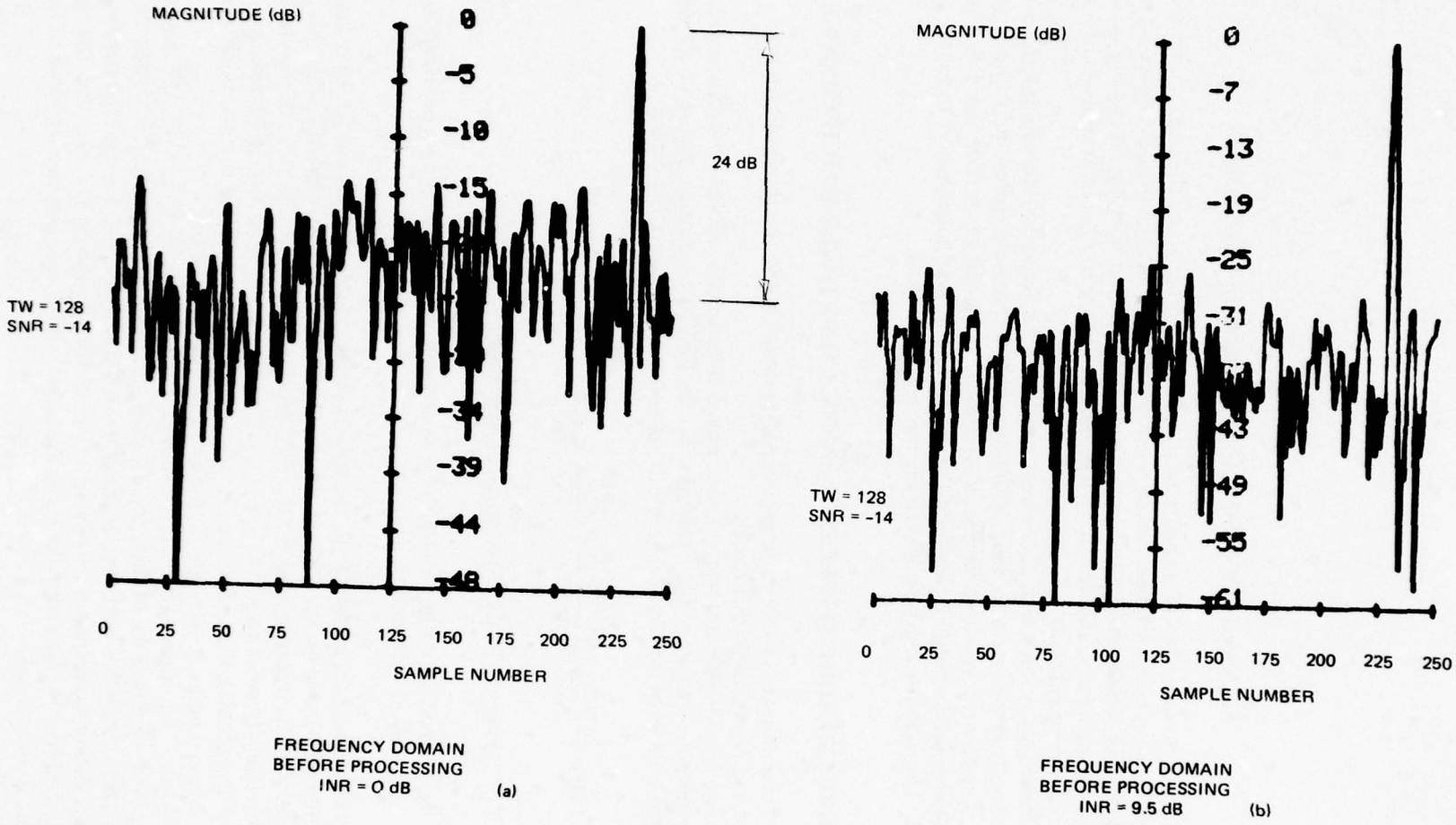

Figure 16. Spectrum for SWGN plus tone.

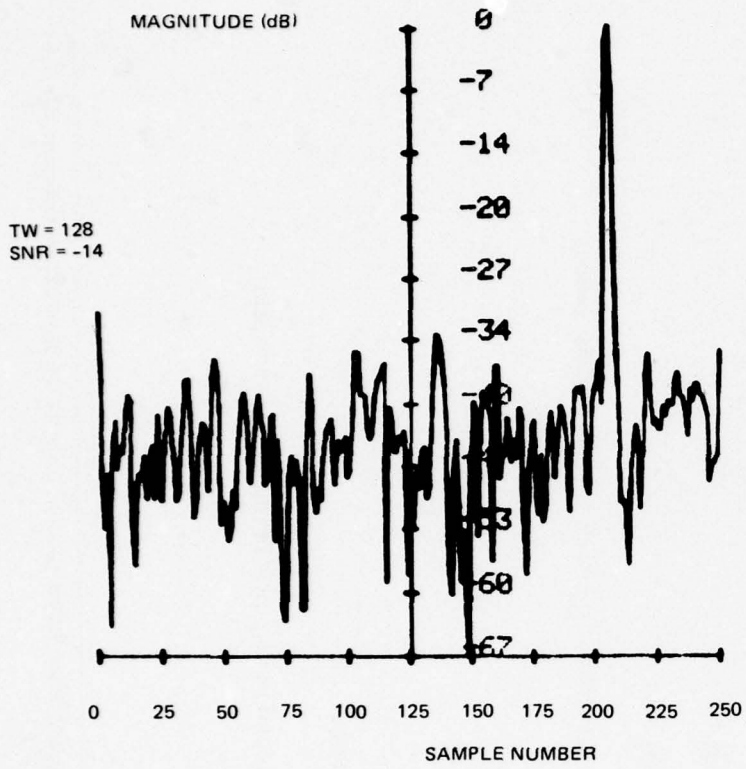

FREQUENCY DOMAIN
BEFORE PROCESSING
INR = 20 dB (c)

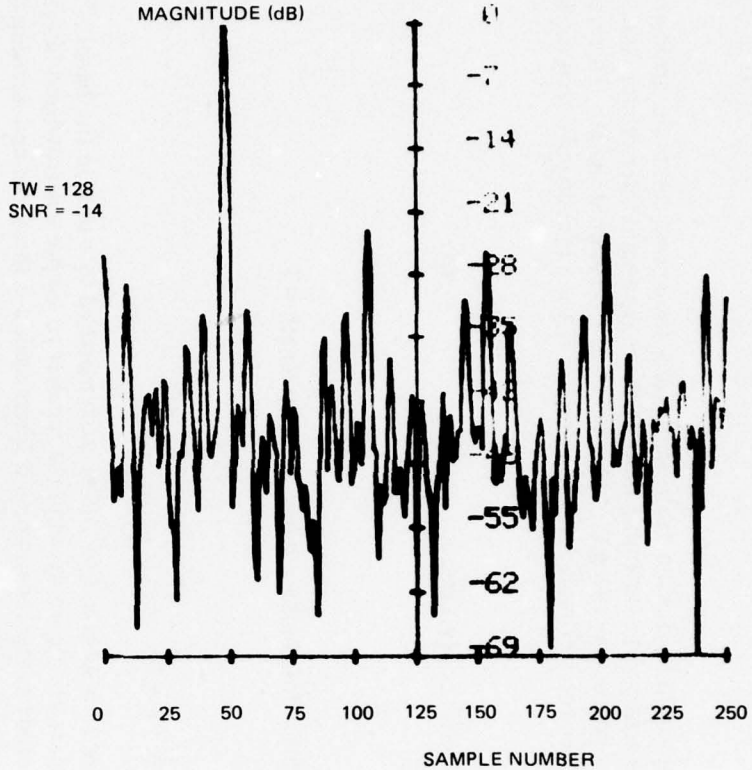

FREQUENCY DOMAIN
BEFORE PROCESSING
INR = 25 dB (A/D DYNAMIC RANGE EXCEEDED) (d)

Figure 16. Continued.

The best threshold level is the one that provides the lowest communication-error probability. This is achieved by detecting most of the narrowband interference (low threshold) without overexcising the rest of the spectrum (the desired signal). This trade-off was analyzed using the receiver model shown in figure 17 for a broadband signal consisting of multiple tones[5]

$$S(t) = \sum_{k=1}^{N} a(t) \cos (w_{\Delta} kt), \qquad (6)$$

where

$a(t)$ = pseudorandom biphase sequence, chip length = T

$w_{\Delta} = 1/T$

$TW = w_{\Delta} \cdot N \cdot T = N$

The receiver in figure 17 is a bank of N filters, each matched to a tone in the signal. The "test and excise" boxes are incorporated in the receiver to suppress narrowband interference by testing the magnitude of the tone-matched filters against a threshold and excising those that exceed the threshold. If the threshold is set at z (bar notation denotes a complex sample pair),

$$\bar{x}_j = \begin{cases} \bar{g}_j & \text{IF } |\bar{g}_j| \leqslant z \\ o & \text{IF } |\bar{g}_j| > z \end{cases}$$

If tone interference is excised, the effective signal-to-noise ratio is

$$SNR_o = \frac{P_S}{P_N},$$

where

P_S = Signal Power

P_N = Background noise power in the signal bandwidth

[5]NELC TN 2461, Signal and Noise Representations for a Multi-Channel Phase-Coherent Signal, by CS Fuzak, 23 August 1973

If the interference is not suppressed, the effective signal-to-noise ratio is

$$SNR_1 = \frac{P_S}{P_N + P_I} ,$$

where P_I = power of the interfering tone. The effect of the interfering power will, on the average, be the same as an equivalent amount of Gaussian noise when N(=TW) is larger than about 10.

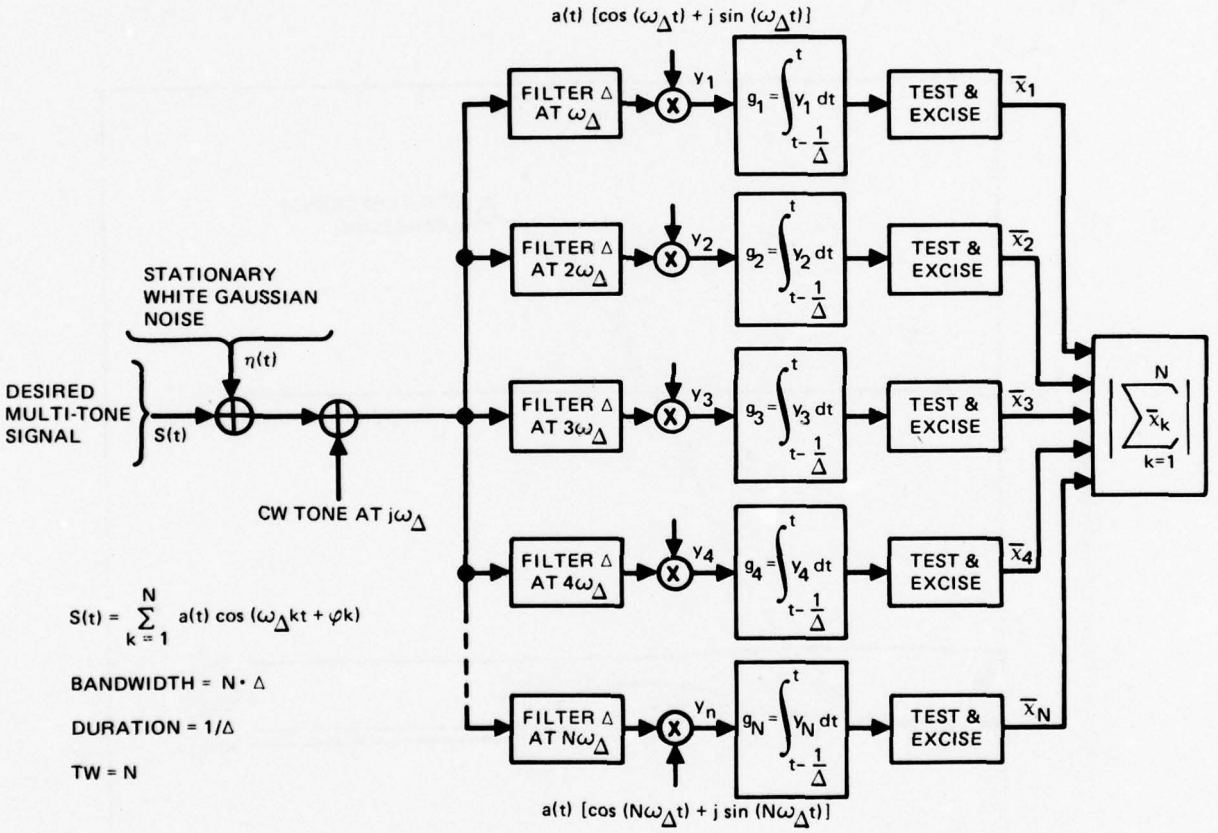

Figure 17. Receiver for a multitone signal.

The model in figure 17 was analyzed with the results shown in figures 18a and 18b. The plots represent error probability versus interference-to-noise ratio for a fixed SNR and symbol time-bandwidth product size, N. The curves are plotted parametrically with excision threshold, and a binary orthogonal symbol set was assumed. Figure 18a shows that performance improves over the total INR range as the threshold increases from $1\,N_{01}^{1/2}$ to $3\,N_{01}^{1/2}$ (N_{01} is the background unilateral noise power spectral density).

Above 3 $N_{01}^{1/2}$, the performance degrades in the region of INR about -8 dB. This is the region where the interference is not large enough to exceed the threshold, but is large enough to cause significant performance loss. This effect becomes more pronounced as the symbol duration (hence TW product) decreases. Figure 18b shows the results when N = 16 (the SNR has been adjusted to compensate for the decrease in processing gain). The decrease in N is reflected as a wider filter Δ (figure 17) and less processing gain with respect to the interfering tone, requiring a higher INR for effective interference suppression. Figure 18b shows that a threshold of 3 $N_{01}^{1/2}$ is still nearly optimum over the INR range. It also shows that it is possible to have poorer performance at a low INR, say -2 dB, than at an INR of 20 dB because the interference cannot be separated from the desired signal at the low INR.

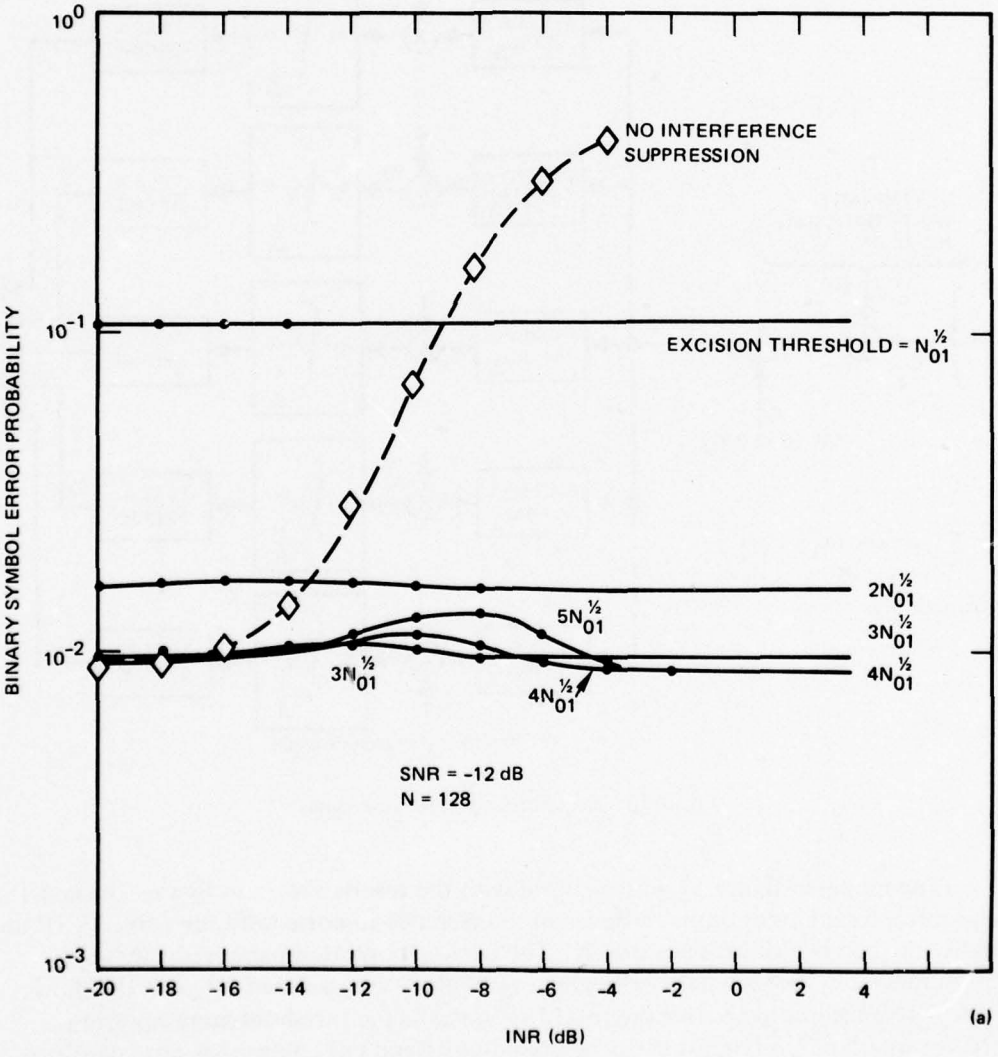

Figure 18. Narrowband excision characteristics.

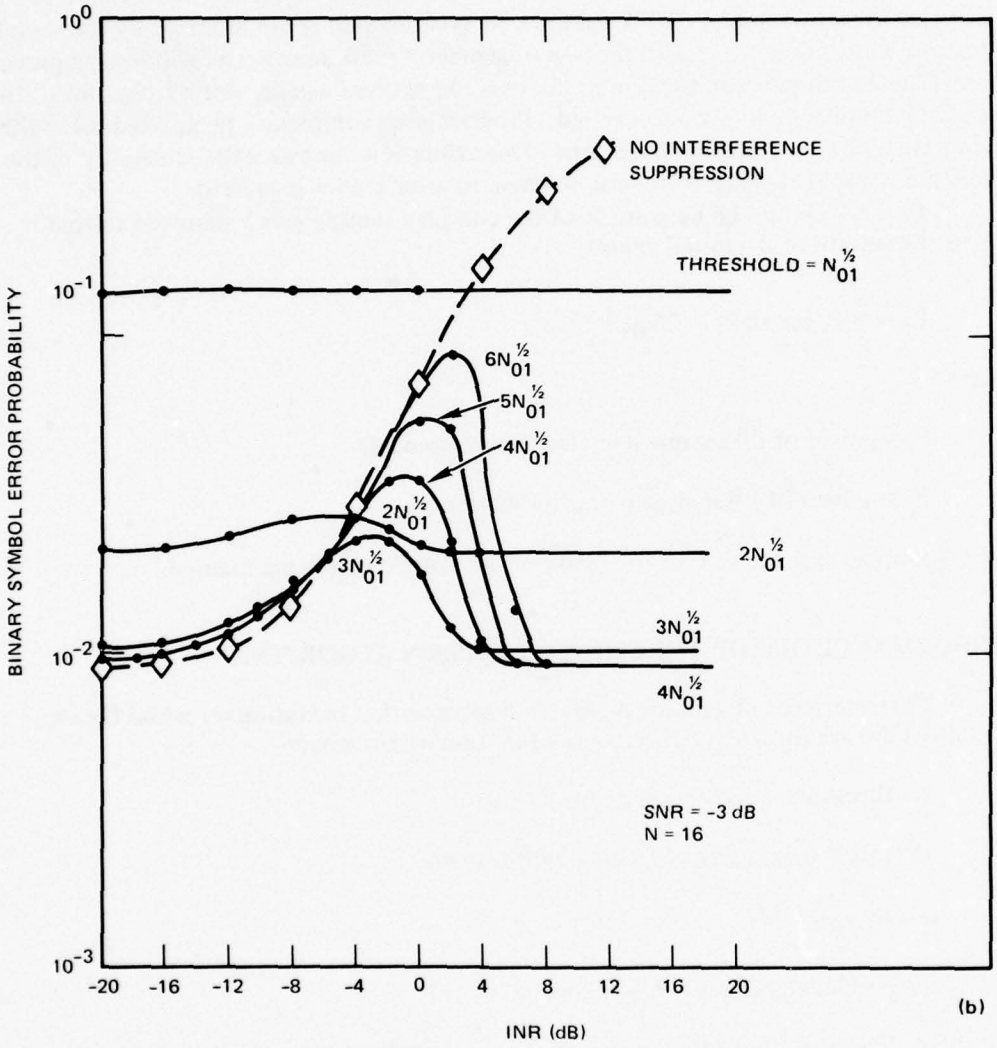

Figure 18. (Continued).

When several interfering tones are present, the resulting performance tends to be that shown in figure 18b, even for large values of N. In the limit of many interfering tones, the interference is actually broadband and this type of suppression technique is no longer effective.

Several methods for setting the threshold level were discussed in the previous section of this report. Since the quantile algorithm was chosen for the time-domain threshold, it is reasonable to also use it for the frequency-domain threshold.

Flow diagrams for the two threshold NBNS techniques are shown in figure 19. Note that twice as many samples (2 TW complex pairs) are taken as are required by the sampling theorem. This is done to reduce the loss of signal by the Kaiser-Bessel windowing process.[1, 6] There is an additional modification in the excision process where samples adjacent to those exceeding the threshold are also excised. Programming complexity prohibited using this technique with the whitening algorithm. This effectively increases the sensitivity of the algorithm without causing overexcision when no interference is present.

For whitening, the magnitude of the complex sample pair is adjusted so that it equals the inverse of it's initial value

$$P_j' = 1/P_j \text{ for all } P_j > 2N_{01}^{1/2},$$

where

P_j = power of j^{th} sample pair (frequency domain)

P_j' = power of j^{th} sample pair after whitening

The adjustment is made so that the phase of the sample pair is maintained.

PERFORMANCE OF THE THRESHOLD-EXCISION ALGORITHM

Characteristics of the threshold excision algorithm in stationary white Gaussian noise (SWGN) are shown in figure 20 as a function of z/σ where

z = threshold value operating on $|F(\omega)|$

$|F(\omega)|$ = magnitude of frequency transform

$\sigma = (N_{01}/2)^{1/2}$

N_{01} = Unilateral noise power spectral density

The curves flatten at about the same point for all 3 SNRs shown. At this point, only about 0.01 percent of the band was excised. The percent of the band excised was within 1 percent of the theoretical calculations. Since so little spectrum was excised, the Gaussian-noise performance curve for the frequency-domain matched filter (figure 11) could also be used here to characterize the performance when z/σ exceeded 4 ($z = 2.8\sqrt{N_{01}}$).

---

[6] NUC TP 532, Windows, Harmonic Analysis and the Discrete Fourier Transform, by Frederic J Harris, September 1976

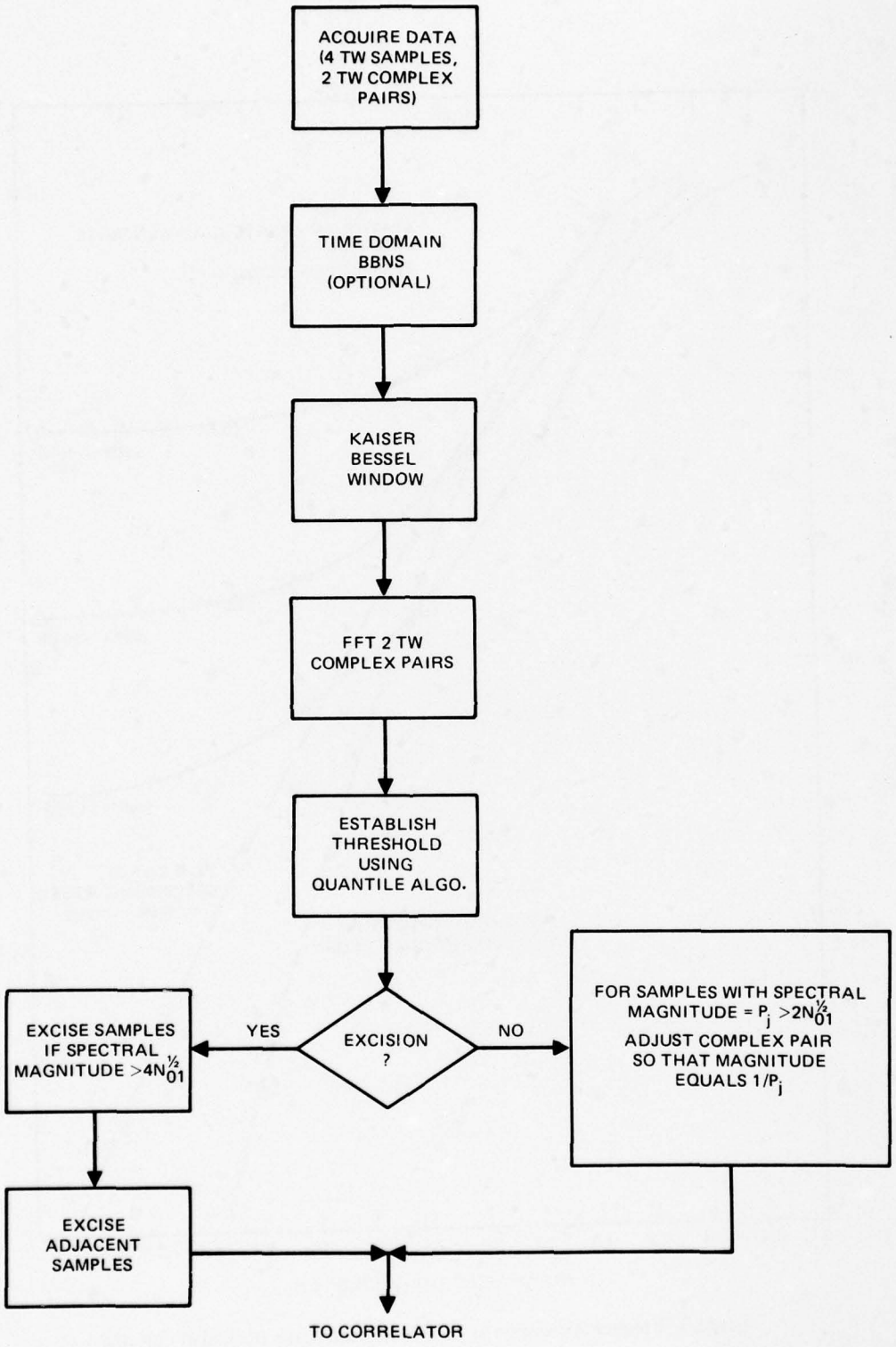

Figure 19. Narrowband-suppression algorithm flow diagram.

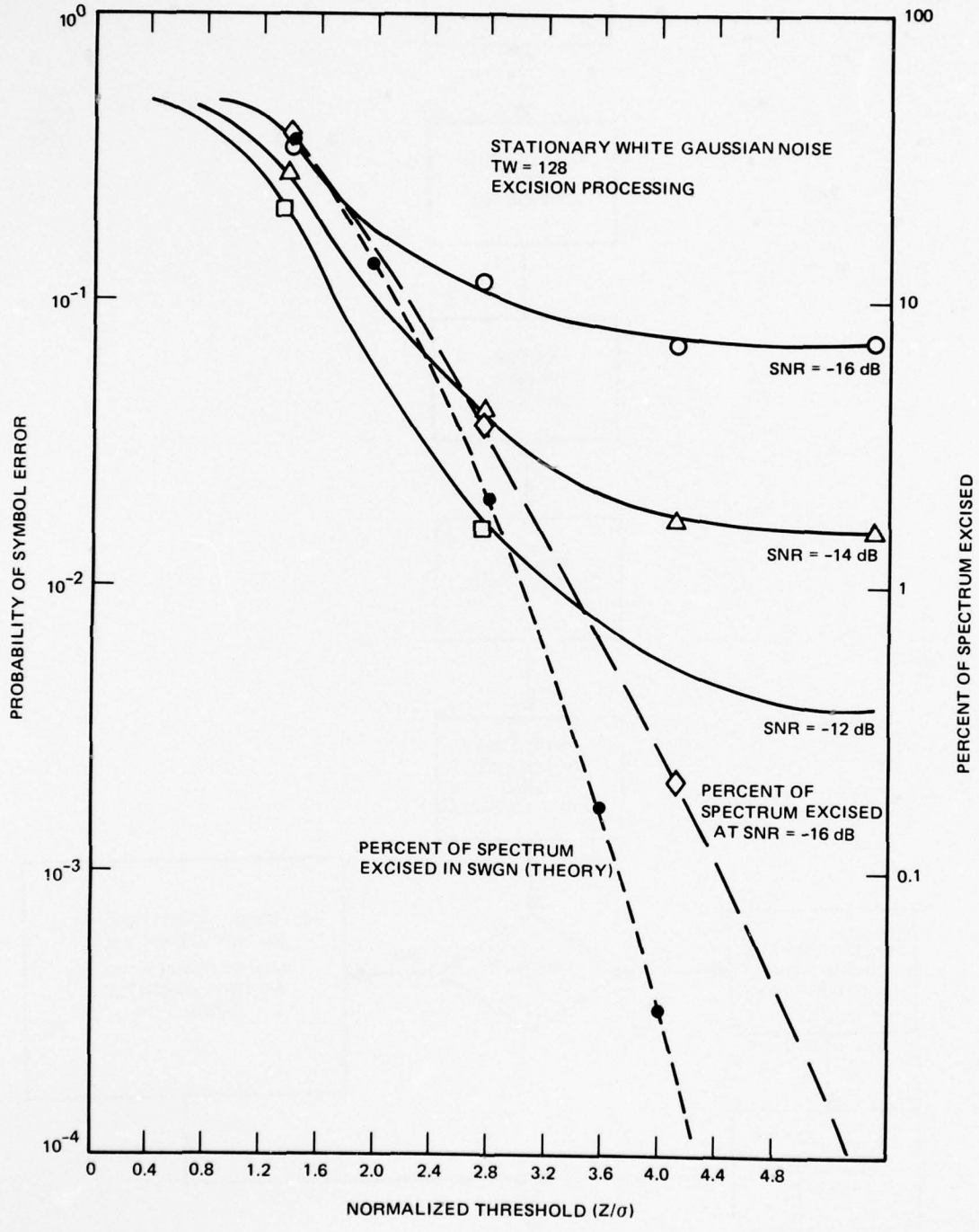

Figure 20. Frequency-excision algorithm characteristics (Gaussian noise).

Figure 21 shows the performance characteristics for stationary white Gaussian noise (SWGN) background plus a single slowly sweeping CW tone. (A slow sweeping tone was used because previous experiments indicated that the error probability when no excision is used is strongly dependent upon the placement of the tone. Slowly sweeping the tone gives an average performance measure). In this case, the threshold never exceeded the tone level and all the curves flattened out at $z/\sigma = 6$. This was the point where the excision percentage also flattened out, indicating that only the tone interference was being excised. With the Kaiser-Bessel windowing, [6] a CW tone should occupy about 3 frequency slots. For the 256-point transform used here, this means a 1.2-percent occupancy. This is close to the percentage excised in figure 21. Because of the TW processing gain, the excision threshold was exceeded even for a 0-dB INR when a single tone was present. This condition is shown in figure 22.

When several tones are present in the passband, the total interference power is divided between the tones. For M equal power tones, the interference cell energy-to-noise ratio is

$$\frac{E_I}{N_{01}} = \frac{P_I}{P_N} \cdot \frac{TW}{M}$$

In this case, the excision threshold may exceed the tone level if M is large enough. In the limit where M approaches TW, the interference is essentially broadband and the frequency-domain excision algorithm is ineffective.

Figure 23 shows the performance curves for 5 interfering tones plus SWGN where the total INR was about 7.6 dB, or 0.61 dB per tone. The "percent of band excised" curve shows that at $z/\sigma = 5$, most of the tone interference was excised (5 tones occupy about 6 percent of the band). At $z/\sigma = 10$, the threshold starts to exceed the tone amplitudes and at $z/\sigma = E_I/M \cdot \sigma = 12$, the error rate starts to noticeably increase. The effect was more pronounced for a smaller INR, as shown in figure 24. In this figure, the minimum P_e point occurs at $z/\sigma = 5$, the same as in figure 23; in fact, for all the examples, the optimum threshold point appeared at about

$$z = 5\sigma = 3.5\sqrt{N_{01}}. \qquad (7)$$

Receiver operating curves are shown in figures 25 and 26 for a fixed threshold at

$$z = 5\sigma.$$

In the case of a slow-sweep CW interfering signal, the performance was equal to that expected in SWGN; that is, the tone was completely suppressed. The difference in performance between the 0-dB INR and 11-dB INR curves was within the experimental repeatability error of the STF (< 1 dB). Figure 26 shows that the suppression of multiple tones was less than ideal, with a loss of 1.5 to 2 dB from SWGN performance at an INR of 7.6 dB. The explanation for this loss is that not all of the interference was always suppressed. This would be expected when the interfering signal was actually some type of wideband interference, multi-tone or otherwise.

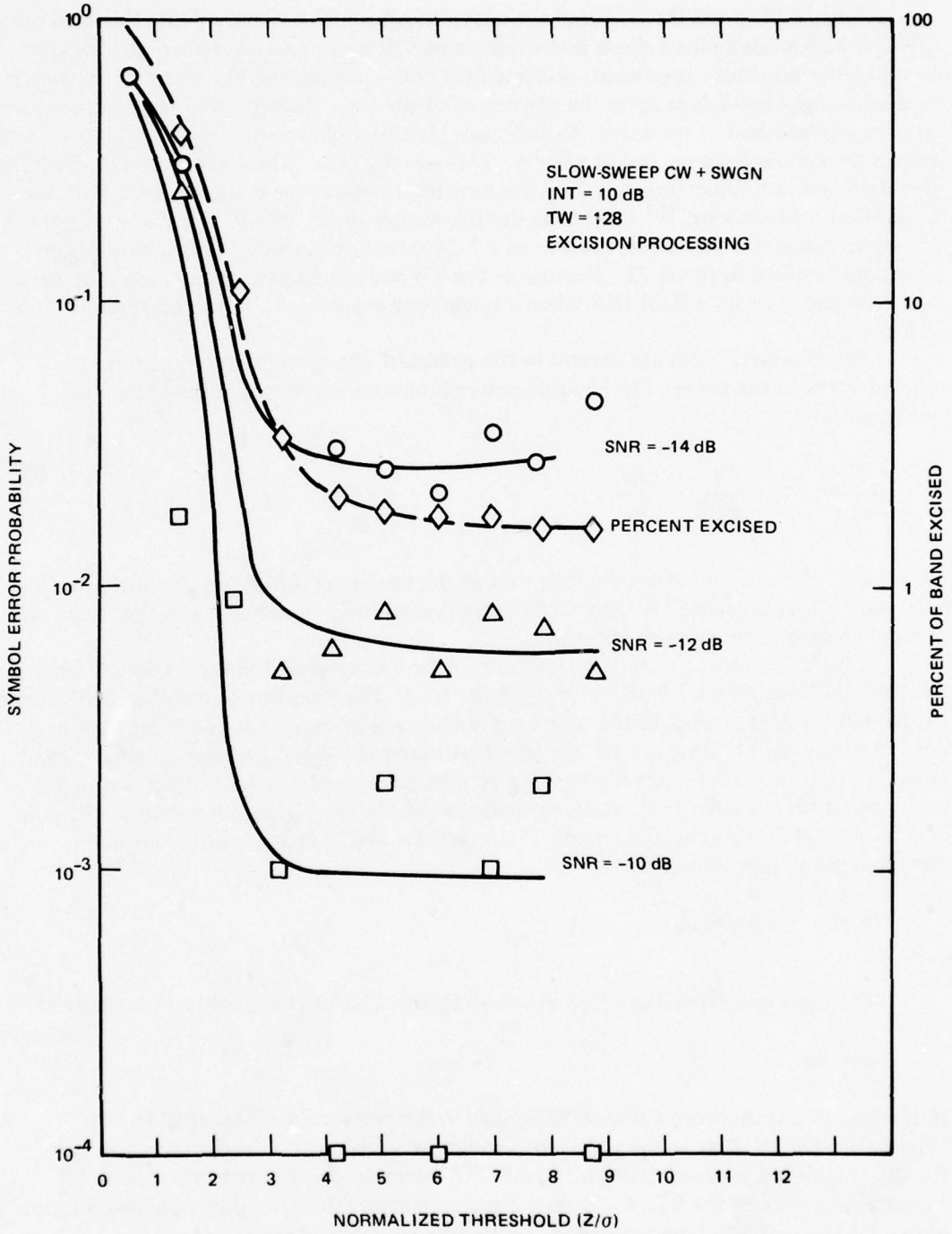

Figure 21. Frequency-excision algorithm characteristics (slow-sweep CW and SWGN, INR 10 dB).

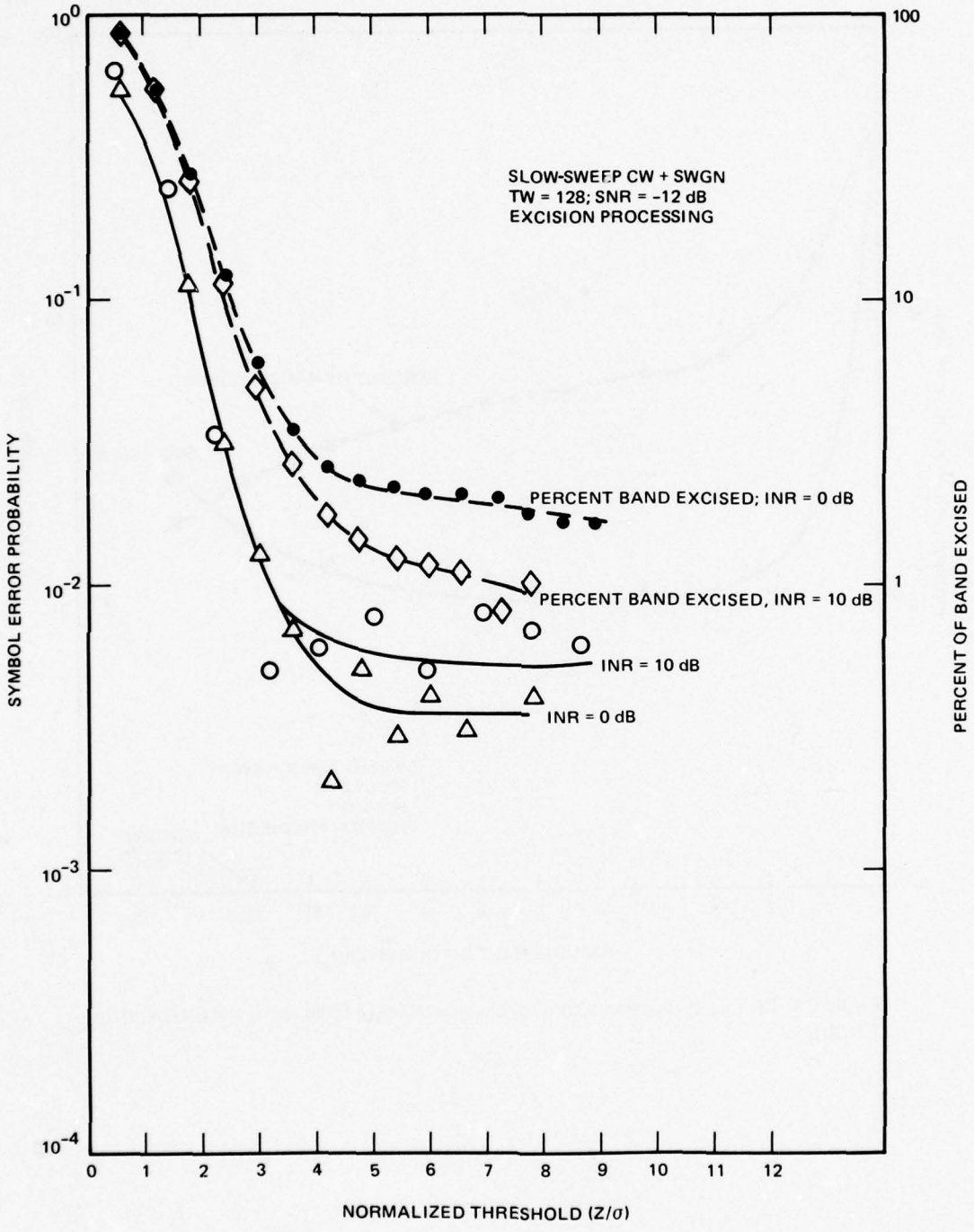

Figure 22. Frequency-excision algorithm characteristics (slow-sweep CW and SWGN, SNR -12 dB).

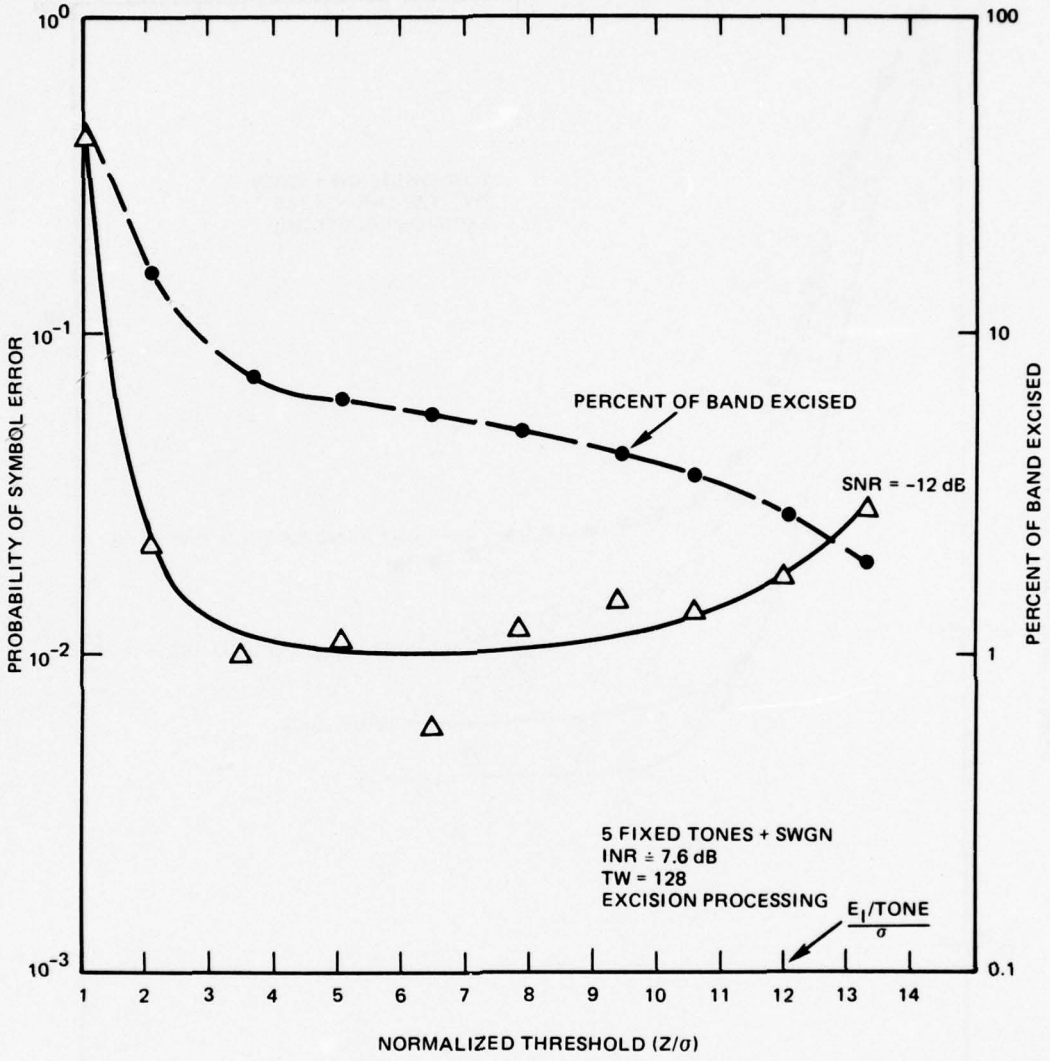

Figure 23. Frequency-excision algorithm characteristics (5 fixed tones and SWGN, INR 7.6 dB).

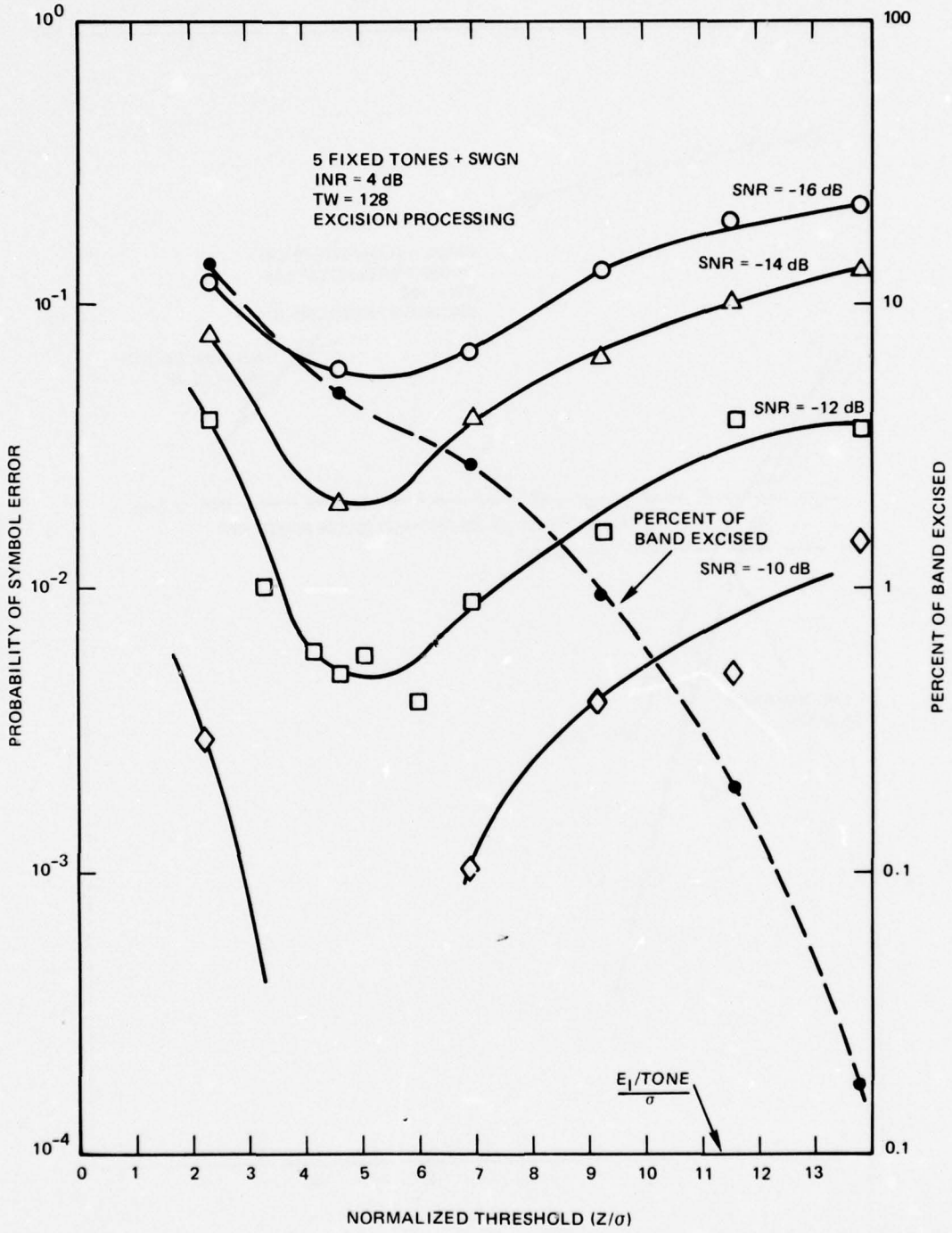

Figure 24. Frequency-excision algorithm characteristics (5 tones and SWGN, INR 4 dB).

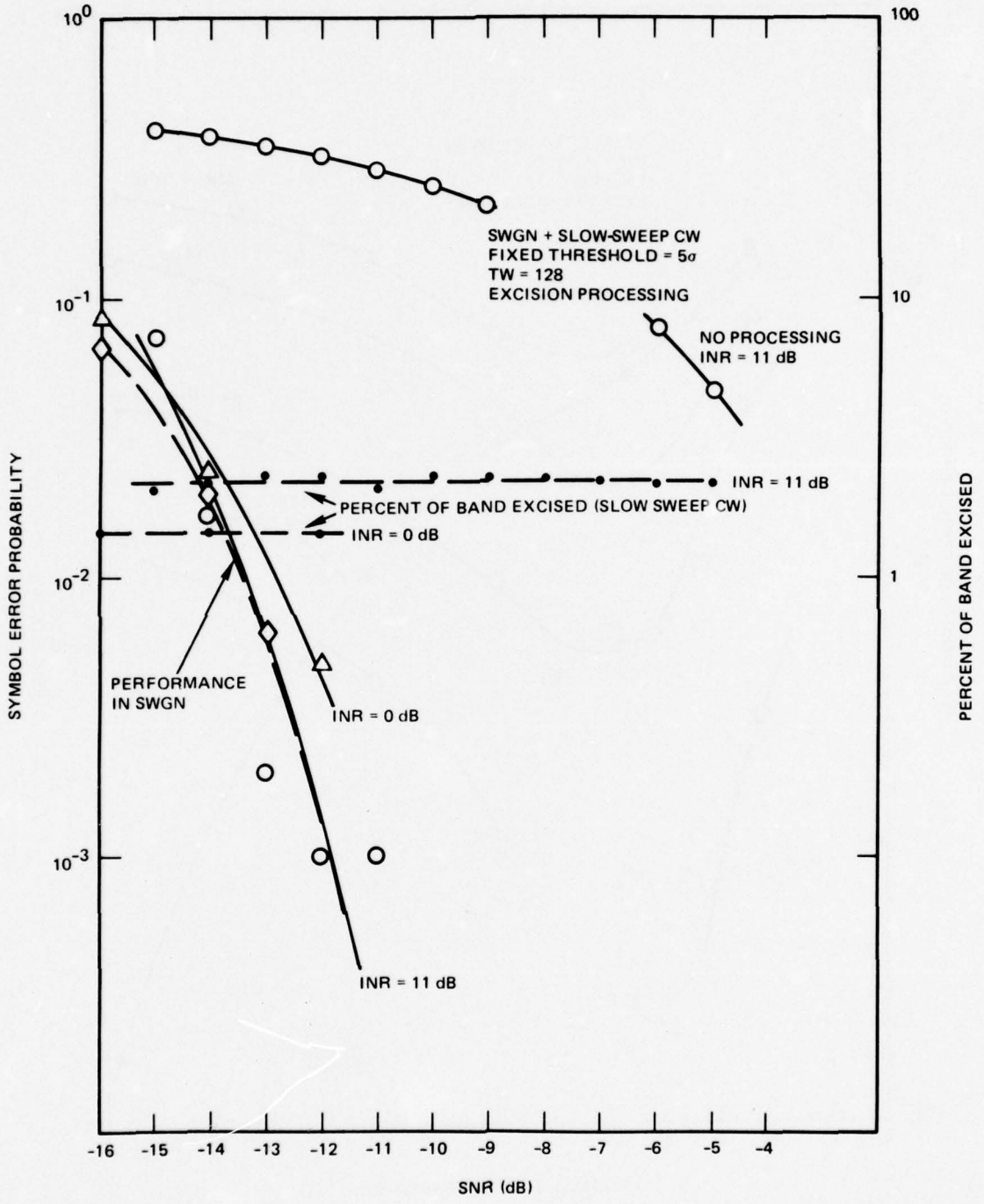

Figure 25. Receiver operating characteristics for frequency-domain excision (SWGN and slow-sweep CW).

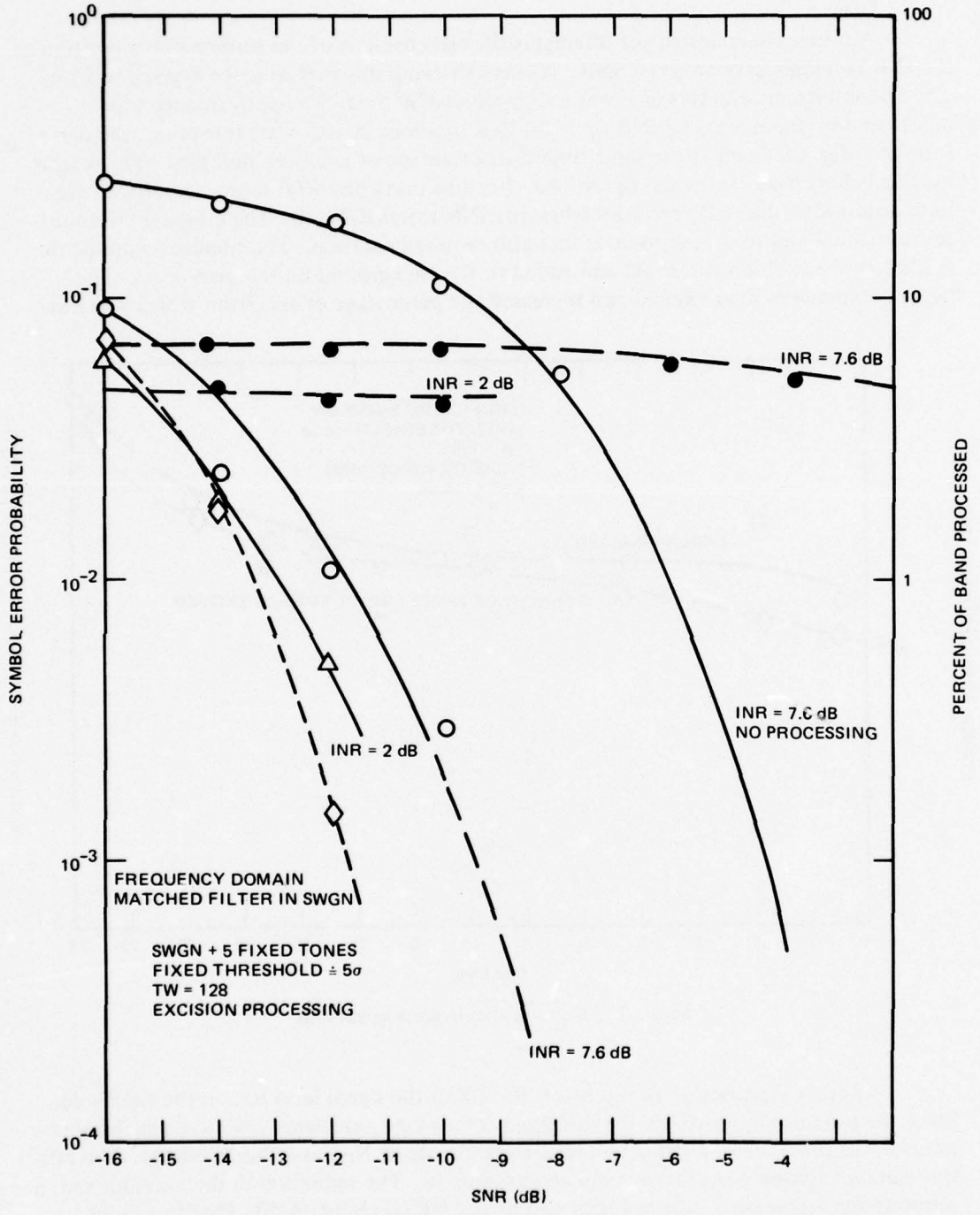

Figure 26. Receiver operating characteristics for frequency-domain excision (SWGN and fixed tones).

Another characteristic of interest is the effectiveness of the suppression algorithm as the INR increases, given a fixed SNR. A curve showing this performance is given in figure 27. The interference in this case was a slow-sweep CW tone. The performance was unaffected by the increasing INR up to an INR of about 20 dB. Past this point, the performance degraded and at the same time the percentage of excision increased. The reason for this behavior was shown in figure 16d. For this particular STF setup, clipping of the tone occurred at the A/D converter when the INR reached 20 dB. The clipping produced additional in-band tone components that also required excision. The smaller components fell below the excision threshold and added to the background noise power level. The larger components were excised and increased the percentage of spectrum which was lost.

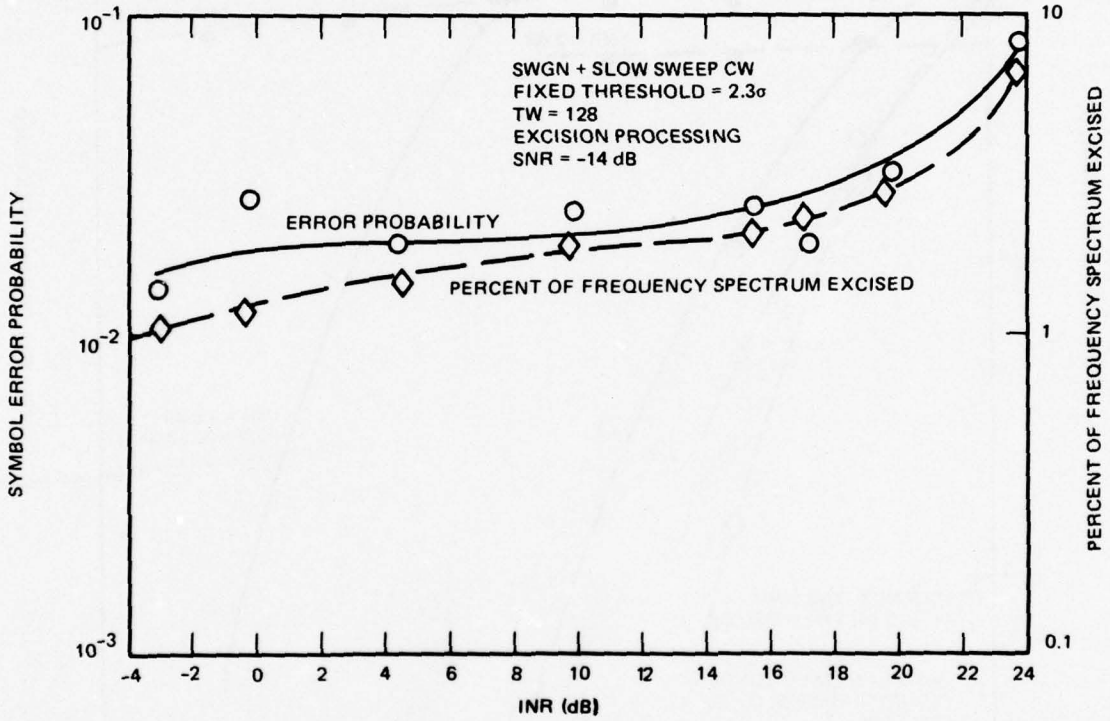

Figure 27. Excision effectiveness versus INR.

Another relationship of interest is the effect the signal level has on the threshold. Since the statistics upon which the threshold is based are calculated over the signal-to-noise interval, the presence of a signal will raise the estimate of N_{01} and the threshold. The effect this had on excision percentage is shown in figure 28. The reduction in the excision and, hence, interference suppression, was negligible up to an SNR of about -4 dB. Past this point, significant degradation of interference suppression took place; however, this was a necessary result if the signal was not to be suppressed itself.

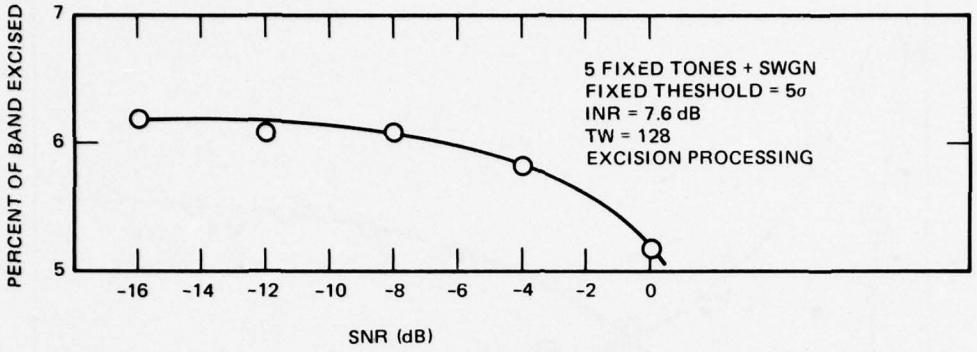

Figure 28. Excision characteristic versus SNR.

PERFORMANCE OF THE THRESHOLD-WHITENING ALGORITHM

Characteristics of the threshold-whitening algorithm in the presence of stationary white Gaussian noise plus interference made up of five fixed equal power tones is shown in figure 29 for several values of SNR. The optimum threshold appeared at about $z = 3\sigma$, significantly less than for the excision case. This was to be expected since the nonlinearity is less severe than excision. In comparing figures 29 and 24, it is interesting that the performance sensitivity to a change in threshold is just as strong with threshold whitening as it is with excision.

The threshold-whitening and excision-performance characteristics are compared in figures 30 and 31, which show little difference in performance between the two techniques. Considering the increased complexity of the whitening algorithm, excision is the best choice for suppressing narrowband interference.

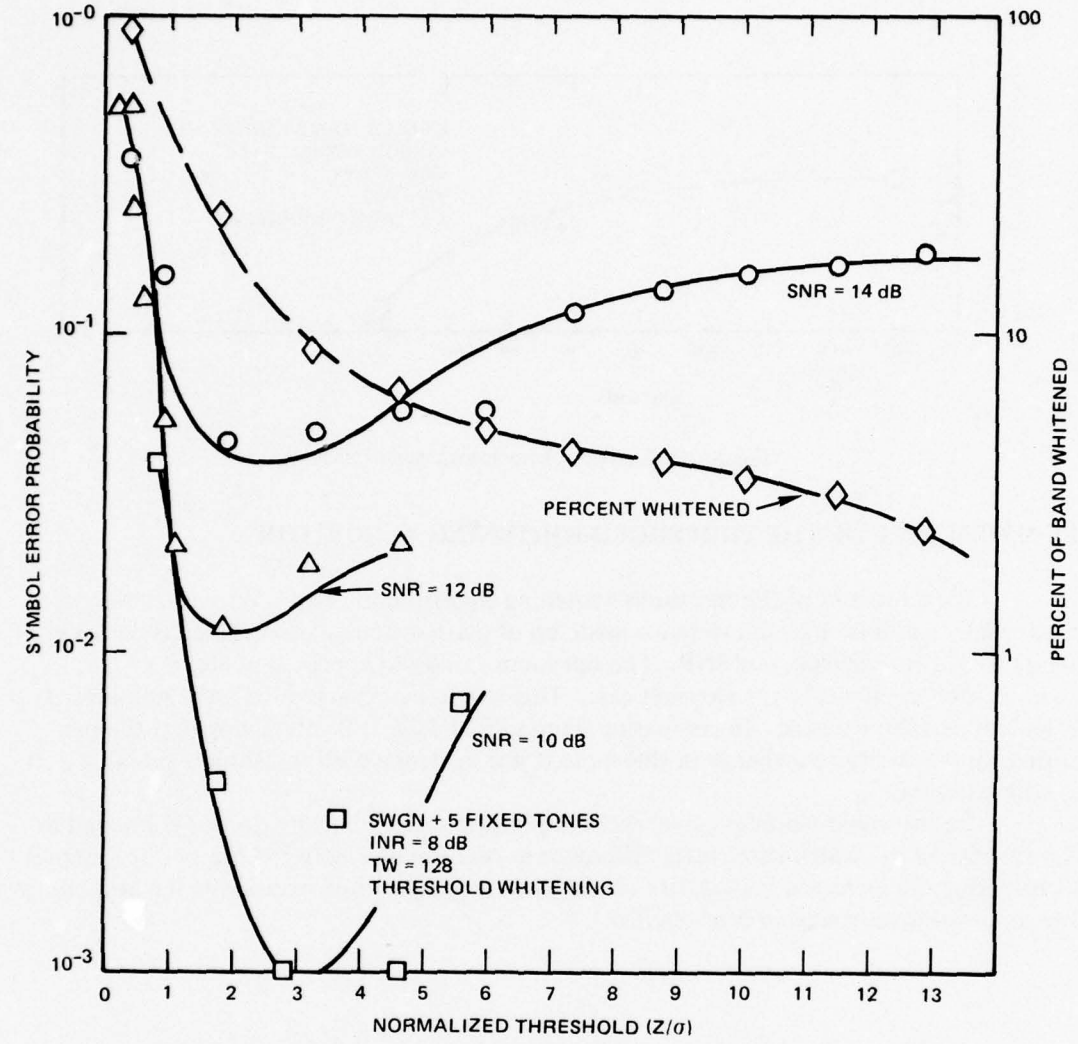

Figure 29. Frequency-whitening algorithm performance characteristics.

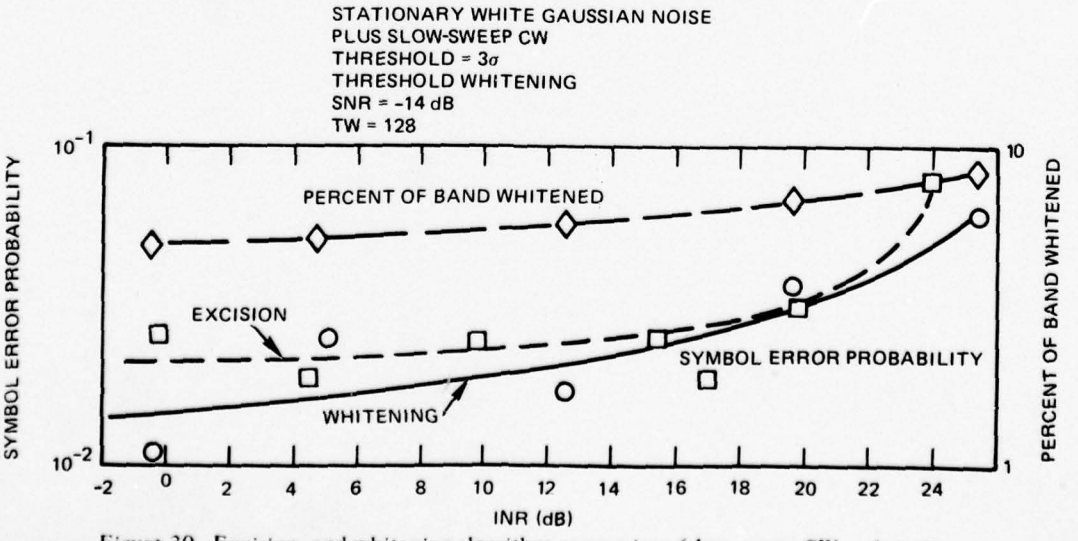

Figure 30. Excision- and whitening-algorithm comparison (slow-sweep CW and stationary white Gaussian noise).

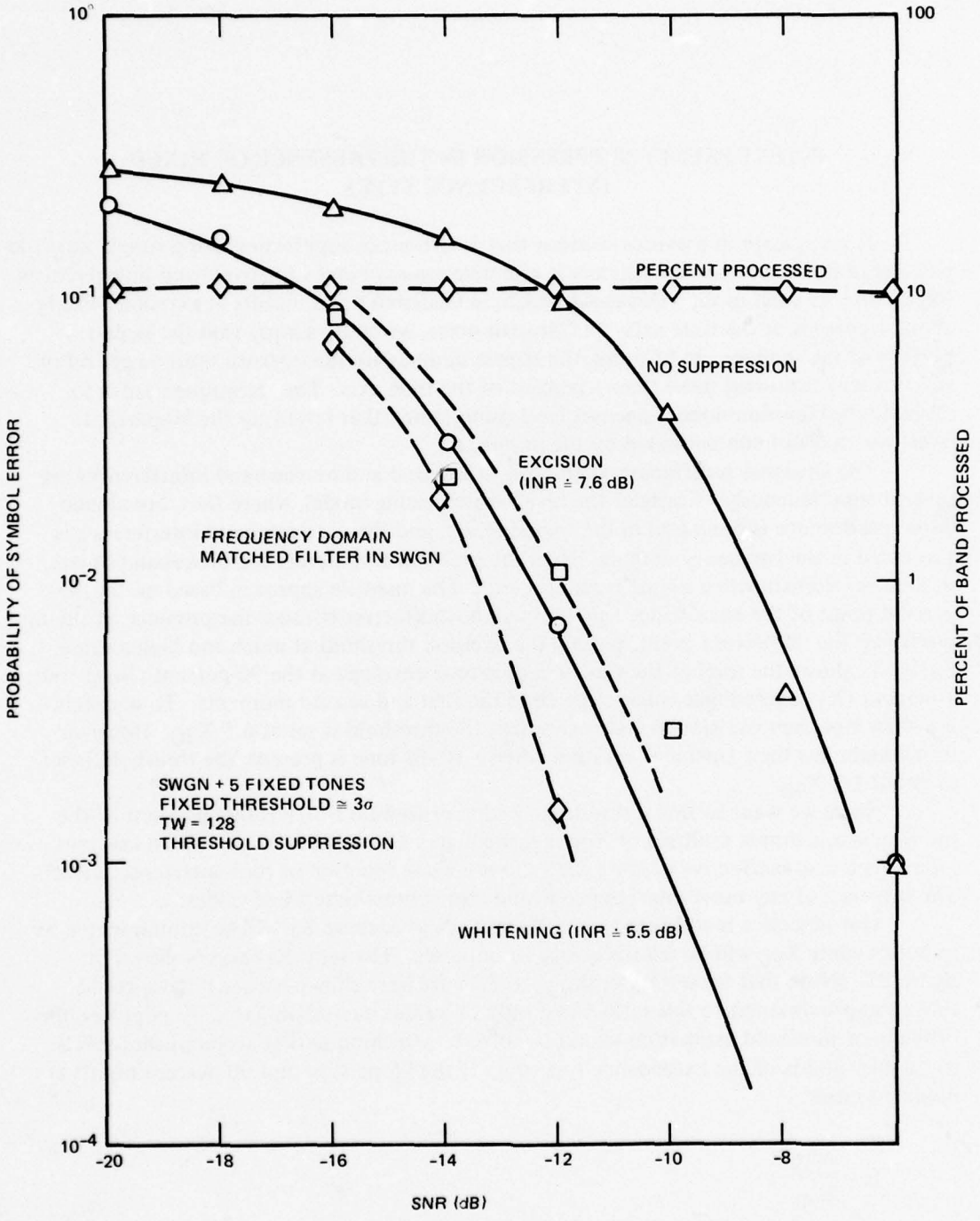

Figure 31. Excision- and whitening-algorithm comparison (SWGN and fixed tones).

INTERFERENCE SUPPRESSION IN THE PRESENCE OF MIXED INTERFERENCE TYPES

It was shown in previous sections that interference suppression using simple quantile-based threshold and excision schemes is effective against burst or narrowband interferences. Recall that we wish to set a threshold which, in Gaussian noise, results in excision of only about 1 percent of the time axis. In Gaussian noise, we could simply find the largest 1 percent of the samples. In hf noise, the largest samples are the ones we want to get rid of, and this may represent more than 1 percent of the time axis. The technique used is to estimate the Gaussian-noise 1-percent level using some other level (say the 90-percent level) which is not contaminated by the impulses.

The situation is different when both broadband and narrowband interferences are present simultaneously. Consider the receiver-processing model, where first, broadband-burst interference is processed in the time domain, and then, narrowband interference is processed in the frequency domain. Here the problem is to detect the broadband bursts in the time domain when a tone is also present. The quantile approach based on the 90-percent point of the exceedance function will be ineffective because the presence of the tone pushes up the 90-percent point, placing the excision threshold at much too high a value. Figure 32 shows the level of the Gaussian-plus-tone envelope at the 90-percent (X_{90}) and 1-percent (X_1) exceedance values, as well as the first and second moments. To maintain less than 1-percent excision in Gaussian noise, the threshold is set at 6.5 X_{90}. However, to maintain less than 1-percent excision when a 10-dB tone is present, the threshold is set at about 1.2 X_{90}.

Since we want to find a threshold-setting procedure which is independent of the interference, a simple multiple of X_{90} is inadequate. Using the ratio of first and second moments is also ineffective because the ratio is a weak function of tone-interference level. The presence of any burst interference would also contaminate these values.

Our objective is still to estimate X_1 from X_{90} because X_1 will be contaminated by impulses while X_{90} will be relatively free of impulses. The ratio X_1/X_{90} is shown on figure 32. (Note that for $\alpha = 0$, $X_1/X_{90} = 6.5$, as we have shown earlier.) If we could find an approximation to this ratio based only on values uncontaminated by impulses, the problem of threshold estimation would be solved. A technique that accomplishes this is to use two points of the exceedance function. If the 95-percent and 90-percent points are used as a ratio,

$$R = \frac{X_{95}}{X_{90}} ,$$

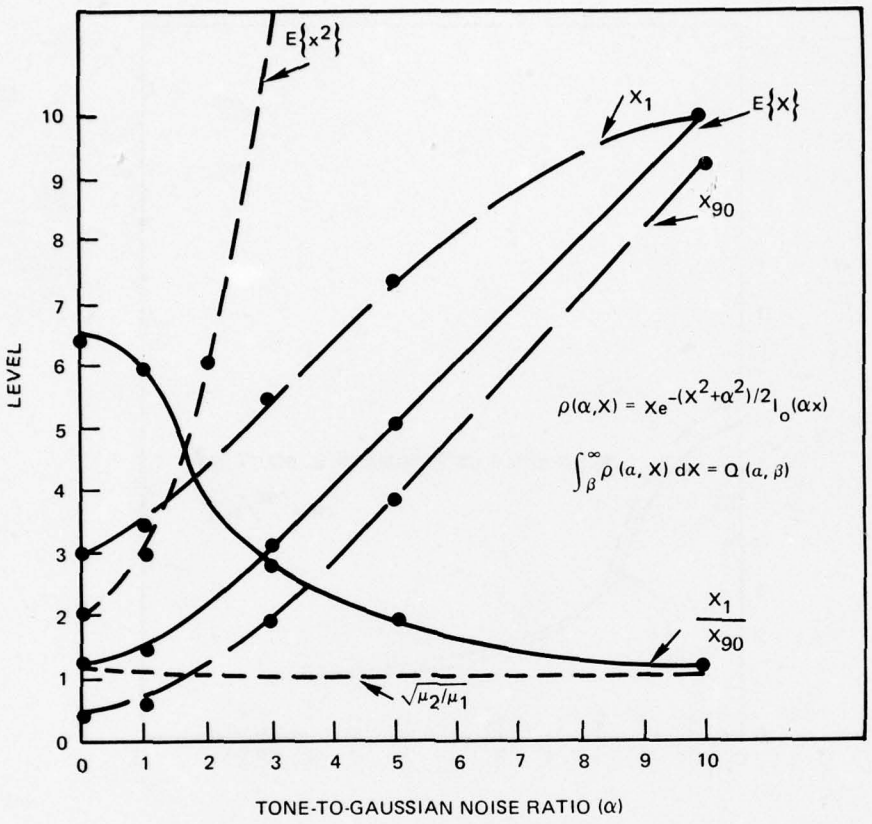

Figure 32. Statistic characteristics of tone plus Gaussian noise.

then an approximation to the ratio X_1/X_{90} can be made as,

$$\frac{X_1}{X_{90}} \cong 5\ (2.5 - 2R)^3.$$

The comparison is shown in figure 33. A 1-percent excision value can be maintained by setting the excision threshold at the level X_1 or,

$$T = X_1 \cong X_{90} \cdot 5\ (2.5 - 2R)^3. \qquad (8)$$

A comparison of actual algorithm performance is given in figure 34. This figure shows the density function of symbol excision percentages taken from the STF in several noise and interference environments. The upper figures of 34a and 34c show the characteristics in stationary white Gaussian noise (SWGN) for the original single-point quantile algorithm and the modified two-point algorithm respectively. The single-point algorithm never excised more than 0.4 percent of the samples. The two-point algorithm excised an average of 0.36 percent, and occasionally up to 24 percent. The lower figures of 34a and 34c show

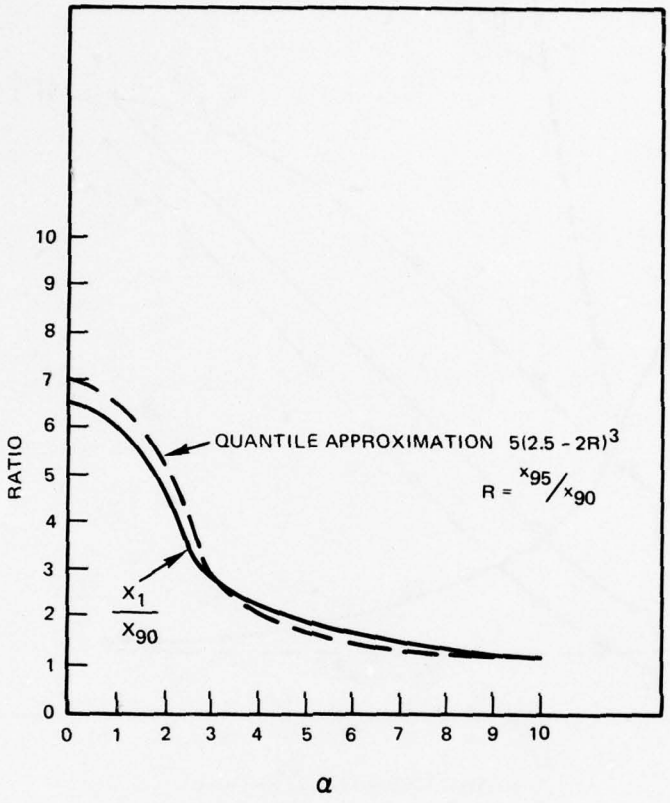

Figure 33. Ratio approximation.

characteristics when noise bursts of the type previously used (figure 10) are added to the SWGN. The two-point algorithm shows a larger spread compared to the single-point algorithm, again occasionally excising a large number of samples. Figures 34b and 34d show what happens when a CW tone is also added. With a low-level tone (upper figures) the average excision percentage of the single-point algorithm drops to less than 3 percent as the tone pushes up the threshold; however, the modified algorithm still excises most of the bursts. Increasing the tone level (lower figures) does not affect the modified algorithm performance, but the unmodified algorithm is completely ineffective.

Even if the excision threshold is set close to the 1-percent exceedance level, the burst interference may go undetected if the tone is large enough to mask it. The only alternatives in this case are to either use a "grid" processing technique to separate the two types of interference, or to double the number of required transforms and process in the frequency domain before processing in the time domain.

The reverse situation may also occur where, in the frequency domain, the narrowband interference is masked by the burst interference. The frequency-domain ratio of in-band burst power to CW power in the tone cell is (figure 35).

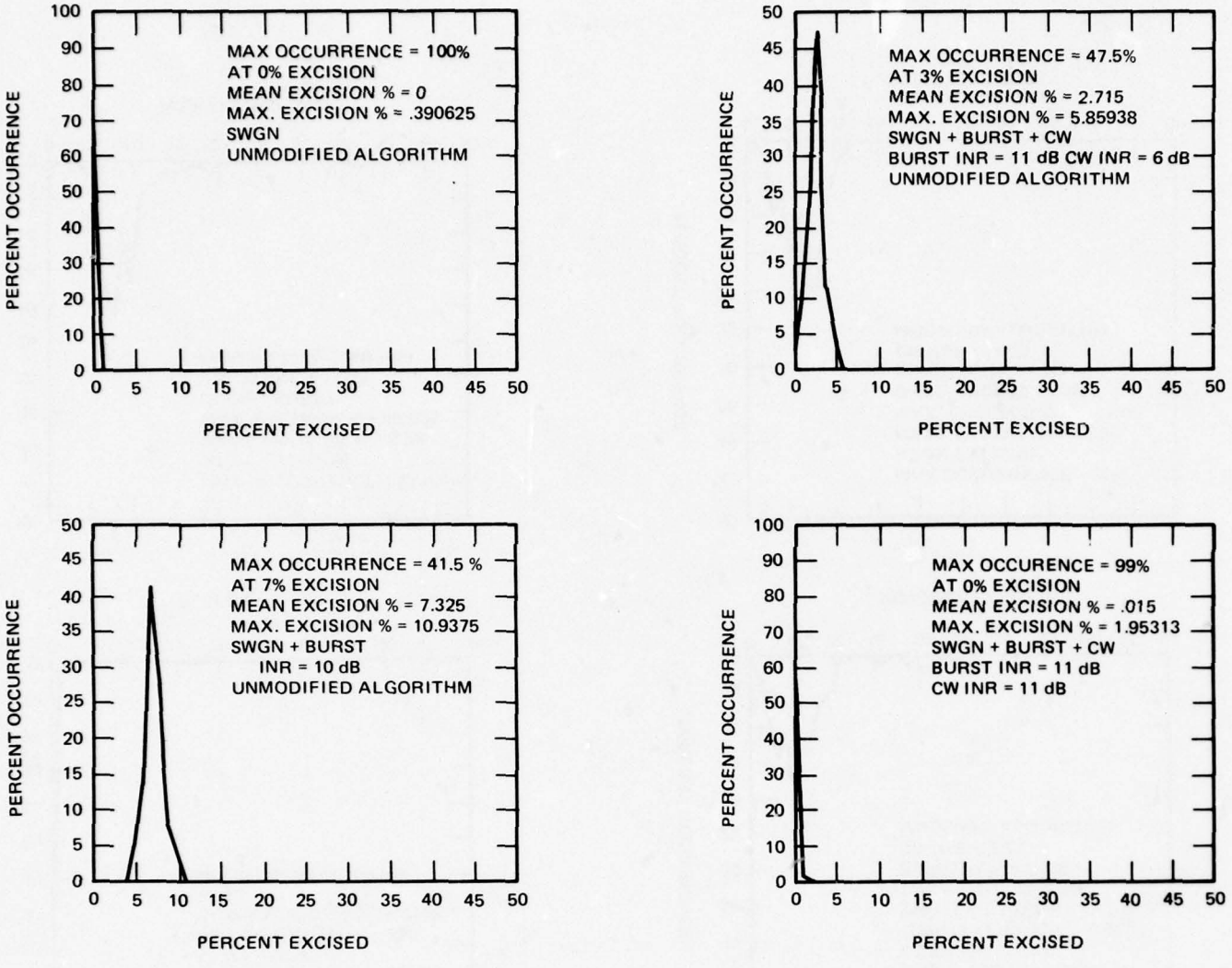

Figure 34. Threshold algorithm performance.

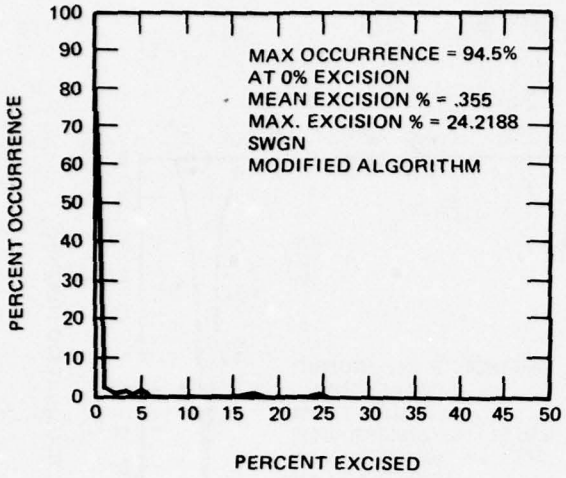

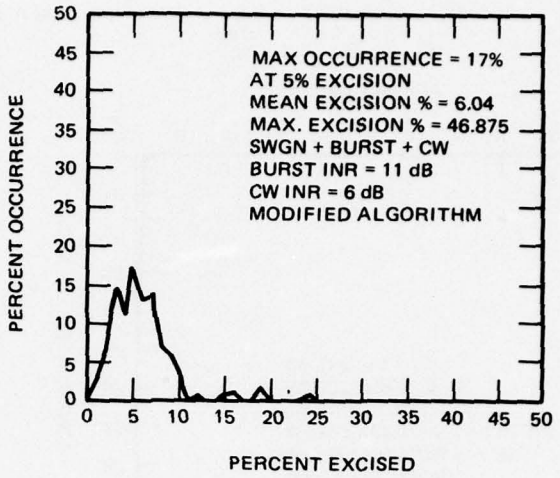

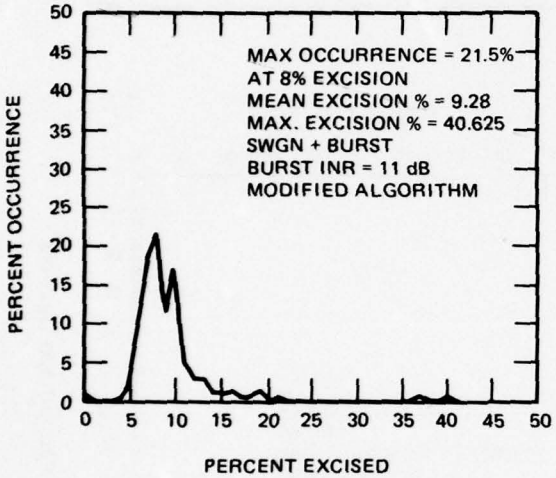

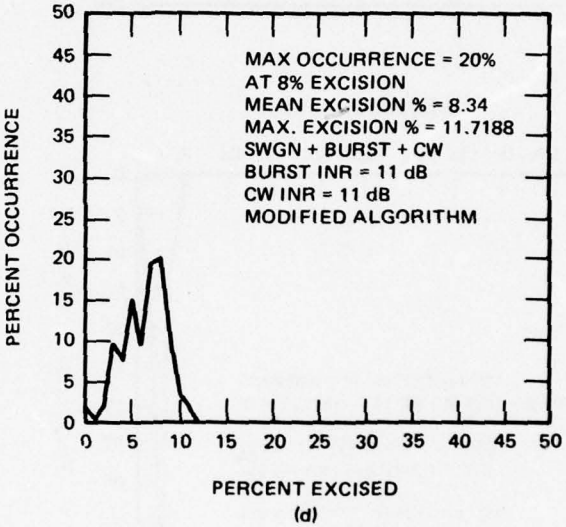

Figure 34. Continued.

$$\frac{P_B}{P_{CW}} \cong TW\left(\frac{T}{T_B}\right) ,$$

where

TW = time-bandwidth product processed

T_B = burst duration, $T_B \leqslant T$.

For short bursts and moderate or large TW products, the burst must be very large compared to the CW tone for it to be masked. Since large CW tones are common in the hf spectrum, the masking of burst interference by tone interference is more likely to occur than will the converse. It would appear, from this argument, that narrowband suppression should be performed ahead of broadband interference suppression.

Another possible solution to this dilemma of time-frequency suppression is to use a time-domain technique that does not require a threshold. The Hall processing described earlier would be a candidate, together with frequency-domain excision. Table 2 summarizes the techniques available in the Simulation Test Facility, and their applicability and problems.

TABLE 2. SUMMARY OF SUPPRESSION TECHNIQUES FOR MIXED TYPES OF INTERFERENCE.

Technique	Application	Problems
Time-Domain Excision or Clipping with Simple Quantile-Set Threshold	Gaussian Noise + Broadband Bursts	Ineffective in Mixed Types of Interference Common at HF
Frequency-Domain Excision or Whitening with Simple Quantile-Set Threshold	Gaussian Noise + Narrow-band	Ineffective When a High Powered Burst is Also Present
Reverse Processing Order (Frequency, Time)	Mixed Interference. Large Narrowband, Small Power Bursts	Requires Two Additional Transforms for Frequency Domain Correlation
Time Domain With Modified Quantile-Set Threshold Plus Frequency-Domain Excision	Mixed Interference, Large Bursts	Threshold Setting More Complex
Hall Processing Plus Frequency-Domain Excision	Mixed Interference, Large Bursts	Hall Processing is More Complex Than Excision
Grid (Hybrid) Processing	Mixed Interferences of all Types	Requires Large TW Product

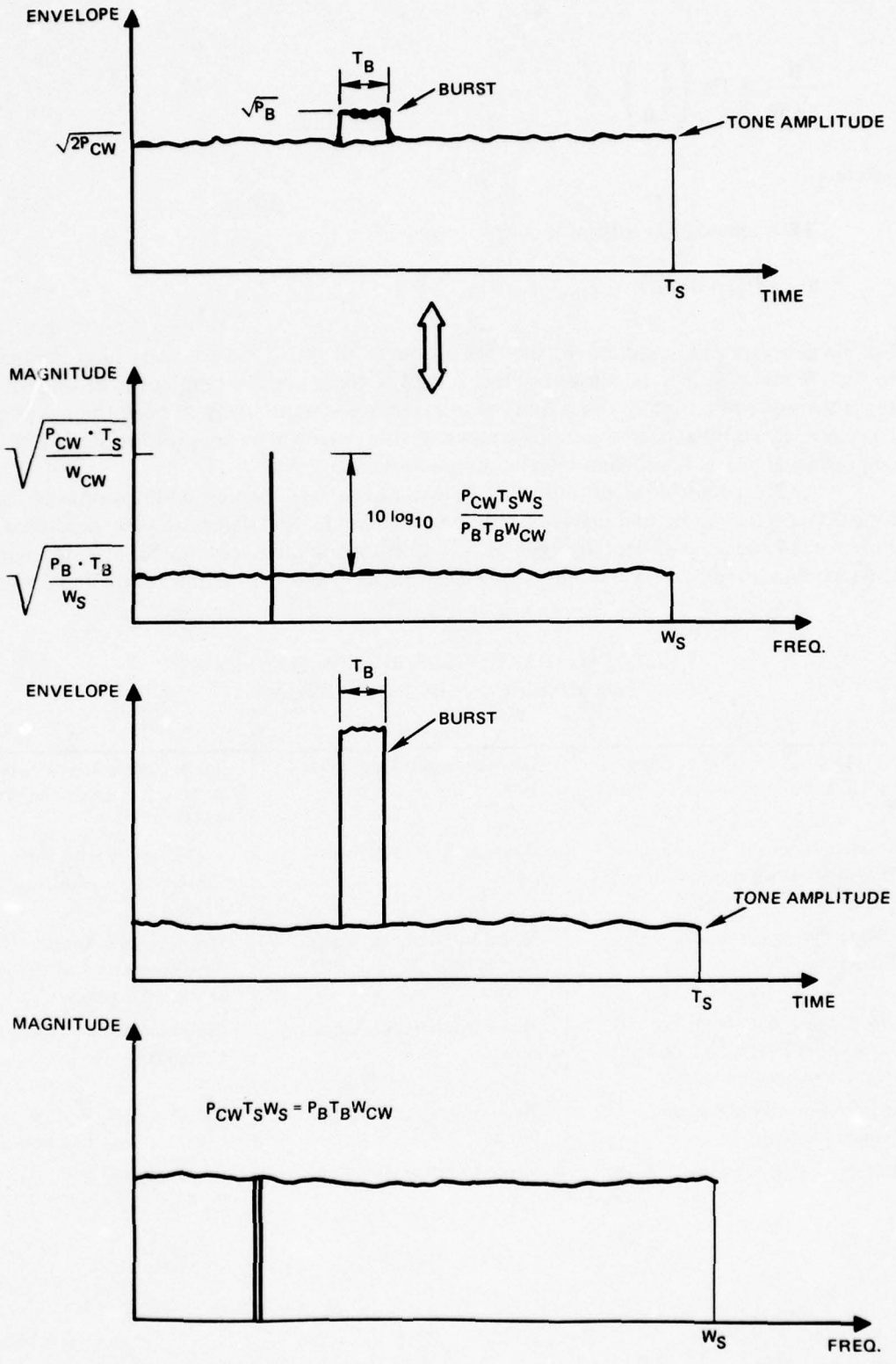

Figure 35. Time-frequency relations for broadband and narrowband interferences.

GRID OR HYBRID PROCESSING

The most straightforward approach for integrating the time- and frequency-domain processing in a mixed noise environment is to use the "grid" approach whereby the received signal, time-frequency space is divided into a time-frequency grid (figure 36). This may be particularly convenient when an analog filter bank is used rather than a discrete or fast Fourier transform. In the latter case, the time samples must be blocked into T-second groups and weighted by a window function to prevent narrowband "leakage." To avoid significant processing loss, the windowing must be done in an overlapping fashion as shown in figure 36b. Thus a total of K transforms, each of size 2TW/K complex samples is required. The resulting Fourier transforms have the grid structure of figure 36a, with half the frequency resolution and twice the time resolution of the grid shown. Excision or clipping can then be used on the total grid, allowing one or more elements in a row or column of the grid to be processed. The excision or clipping threshold is set based on a quantile level calculated over the entire grid. Correlation is most easily performed in the frequency domain by using reference symbols with the same grid structure, and then summing the respective components of the product blocks (figure 36c). The IFFT of this product-sum array will give the correlation function for delays of up to 2T/K seconds. For large K, this could be small and would only work if the system were nearly synchronized. An alternate scheme for delays up to T seconds, requires that the grid be put together again in the frequency domain after the interference suppression step (figure 37). This requires an additional set of IFFT and FFT transforms.

GRID-PROCESSING TRADEOFFS

Although the grid processing requires a lot of data shuffling, it also uses smaller, more efficient transform sizes. Table 3 compares the processing times for a TW product of 2048 (1024 complex samples) with the data block broken into 1, 2, 4, 8, and 16 time slots. Overall, grid processing with grid correlation is faster than the standard time-frequency processing and the improvement increases as the number of slots increases. The time requirements for setting the threshold and excising were not included but, if they were, the grid processing would show an additional advantage because this process is done only once over the grid instead of once in the time domain and once in the frequency domain.

If the alternate (total symbol) correlation is done with the grid processing, additional time is required for reassembling the grid in the time domain and transforming back into the frequency domain for correlation. This will always take more time than the time-frequency (non-grid) processing.

One of the trade-offs between grid processing and time-frequency processing is the loss in frequency resolution when the grid method is used. Assuming a processed time-bandwidth space of TW, K grid time slots, and Nyquist rate sampling, the frequency resolution will be

$$\Delta = \text{frequency resolution} = \frac{K}{T}\ H_z.$$

Also assuming Kaiser Bessel windowing, the effective resolution degrades (due to the narrowbanding effect of the window) to

$$\Delta \doteq \frac{3K}{T}.$$

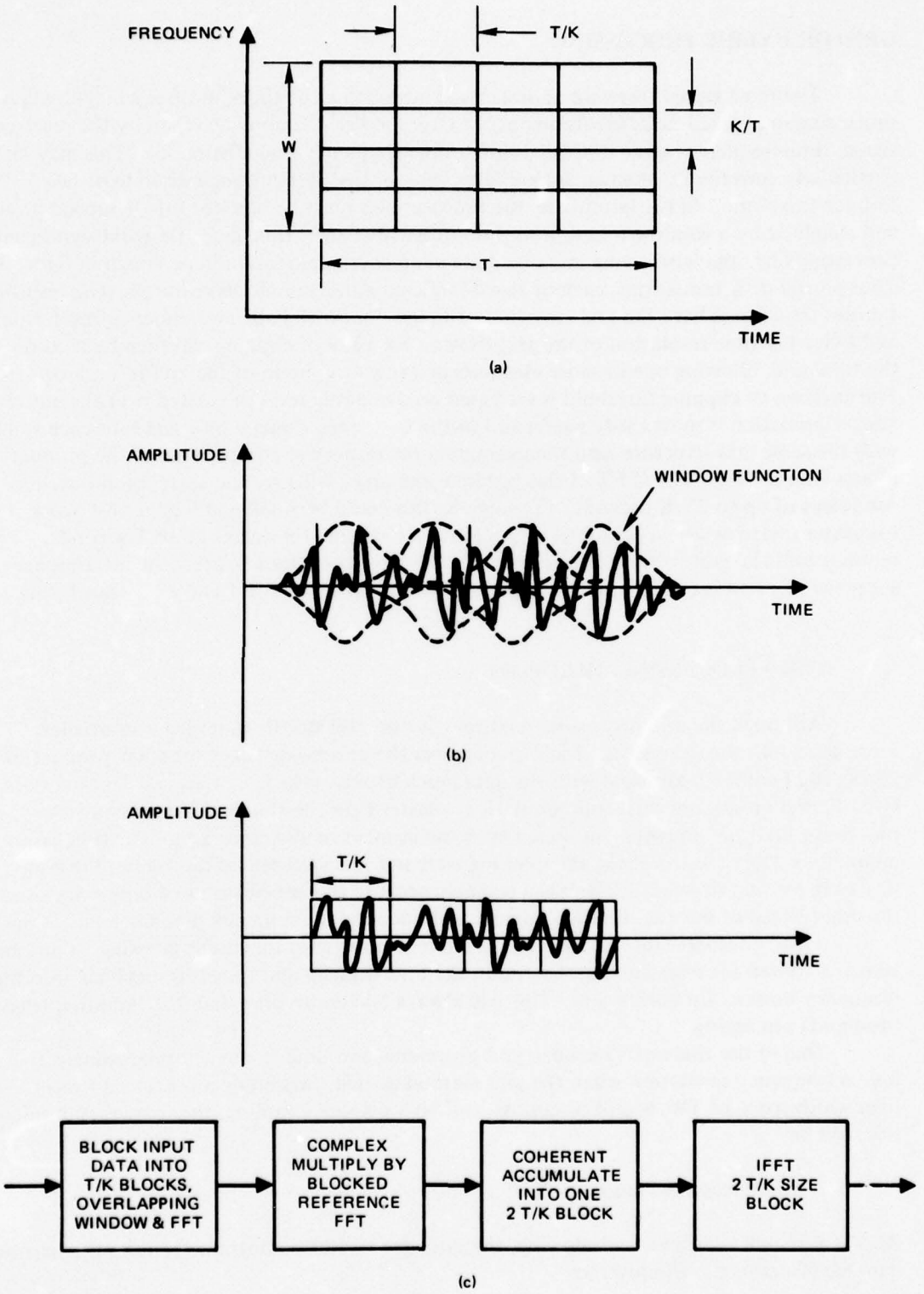

Figure 36. Grid technique, version one.

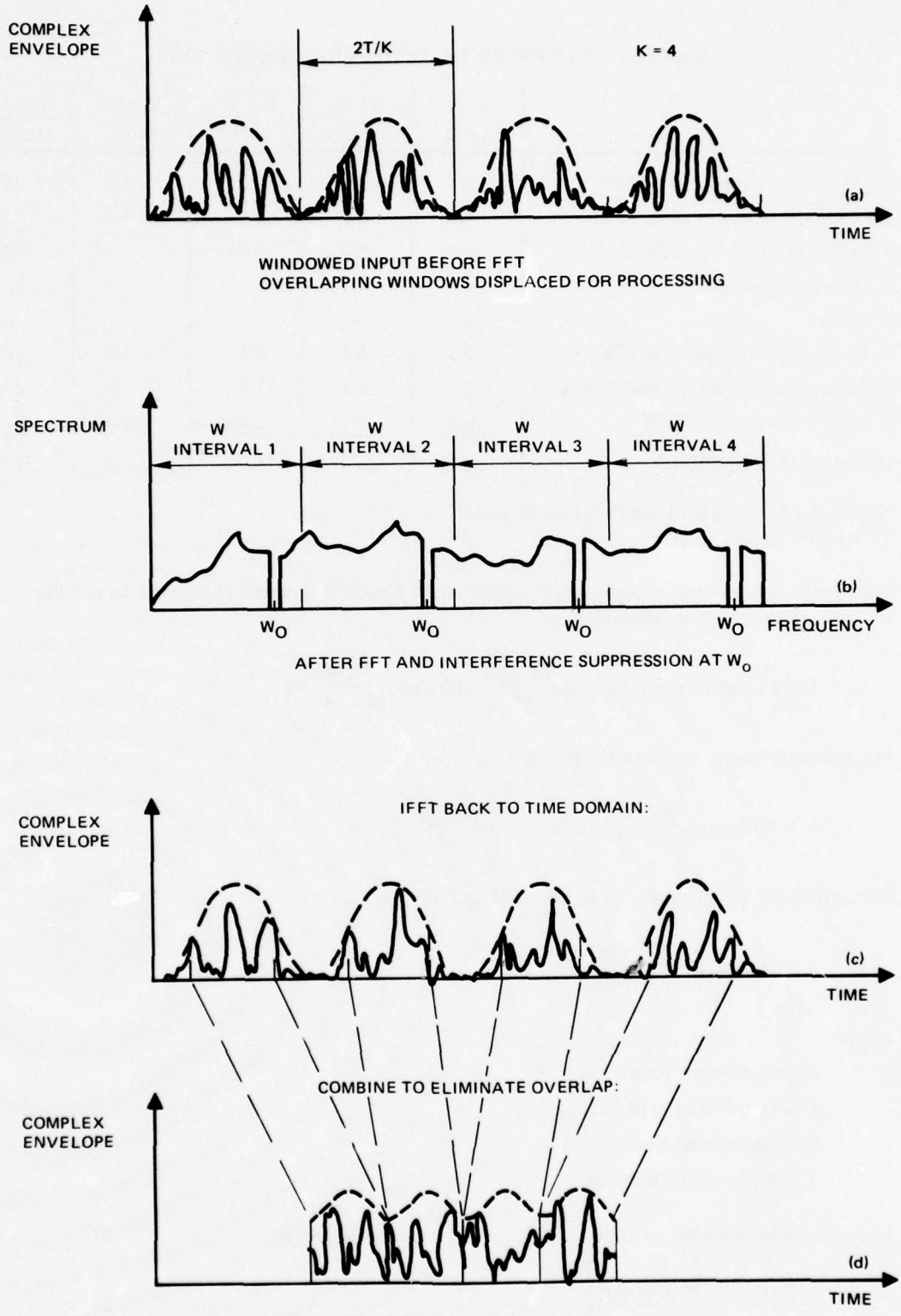

Figure 37. Grid technique, version two.

TABLE 3. GRID PROCESSING WITH GRID CORRELATION.

	K = 1 (ms)	K = 2 (ms)	K = 4 (ms)	K = 8 (ms)	K = 16 (ms)
1. Duplicate K Arrays of Size 2TW/K	0	2.2	2.2	2.2	2.2
2. Window K Arrays of Size 2TW/K	3.3	3.3	3.3	3.3	3.3
3. FFT K Arrays of Size 2TW/K	10.8	9.5	9.04	7.76	7.52
4. Determine Threshold	–	–	–	–	–
5. Excise	–	–	–	–	–
6. Ref Multiply 1 Array, Size 2TW	5.5	5.5	5.5	5.5	5.5
7. Accumulate K-1 Arrays, Size 2TW/K	0	1.1	1.6	1.9	2.1
8. IFFT 1 Array, Size 2TW/K	10.8	4.75	2.26	0.97	0.47
TOTAL TIME REQUIRED*	30.4	26.4	23.9	21.6	21.1

*Times Based on FPS AP-120B With Fast Memory
TW = 1024 Complex Points

For simplicity, assume a single tone present, with bandwidth small compared to Δ. The amount of excess processing loss is

$$L = \text{excess loss} = 10 \log_{10}\left(\frac{W-\Delta}{W}\right) - 10 \log_{10}\left(\frac{W-\Delta/K}{W}\right).$$

For multiple tones, the worst-case loss is

$$L = 10 \log_{10}\left(\frac{W-n\Delta}{W}\right) - 10 \log_{10}\left(\frac{W-n\Delta/K}{W}\right),$$

where n tones are present. In terms of N and T,

$$L = 10 \log_{10} \frac{TW-3nK}{TW-3n}, \tag{9}$$

where

n = number of tones
K = number of grid time slots
W = processing bandwidth
T = processing duration.

The maximum number of time slots for a loss of 2 dB or less is,

$$K = \left[\frac{0.12\,TW + 0.63\,n}{n}\right], \tag{10}$$

where [x] is the largest integer less than or equal to x, but at least 1. The performance of the grid algorithms will be given at the end of this section along with the other algorithm performances. Equation (10) is plotted in figure 38.

When the grid approach is used, the effect of having many tones present becomes important because even a single tone appears K times (K = the number of time slots). This multiplicity of tones has two effects; the presence of the tones biases the threshold estimate higher and also increases the loss due to signal-energy excision.

Given n tones, all of which are excised, the processing loss due to excision is

$$L_X = \left(\frac{TW - 3nK}{TW} \right) , \tag{11}$$

where we have assumed the tones are large compared to the background noise and the noise-excision effects are negligible.

If the threshold is set too high, the tones will not be excised and the effective SNR will be degraded by the interference power. The maximum interference loss occurs when the interference is just below the threshold level, z,

$$L_I \text{ (max.)} = \frac{\sigma^2}{z^2\, nK/2TW + \sigma^2} , \tag{12}$$

where σ^2 is the background noise variance.

The excision strategy is,

If $L_X > L_I \rightarrow$ Do Not Excise,

If $L_X \leq L_I \rightarrow$ Excise.

Therefore, the correct threshold can be found by solving for z,

$$L_I \text{ (max)} = L_X$$

$$\frac{\sigma^2}{z^2 nK/2TW + \sigma^2} = \frac{TW - 3nK}{TW} \tag{13}$$

$$z = \left(\frac{6\sigma^2}{1 - 3nK/TW} \right)^{1/2} * .$$

As the number of time segments increase, the desired threshold should also increase as,

$$\frac{z_K}{z_1} = \left(\frac{TW - 3n}{TW - 3nK} \right)^{1/2} , \quad 3nN < TW, \tag{14}$$

*For K=1 and TW>>n, $z = 2.45\sigma$. This is less than the optimum value found previously (5σ in equation (7)). If background noise had been considered, a larger value for z would have been found.

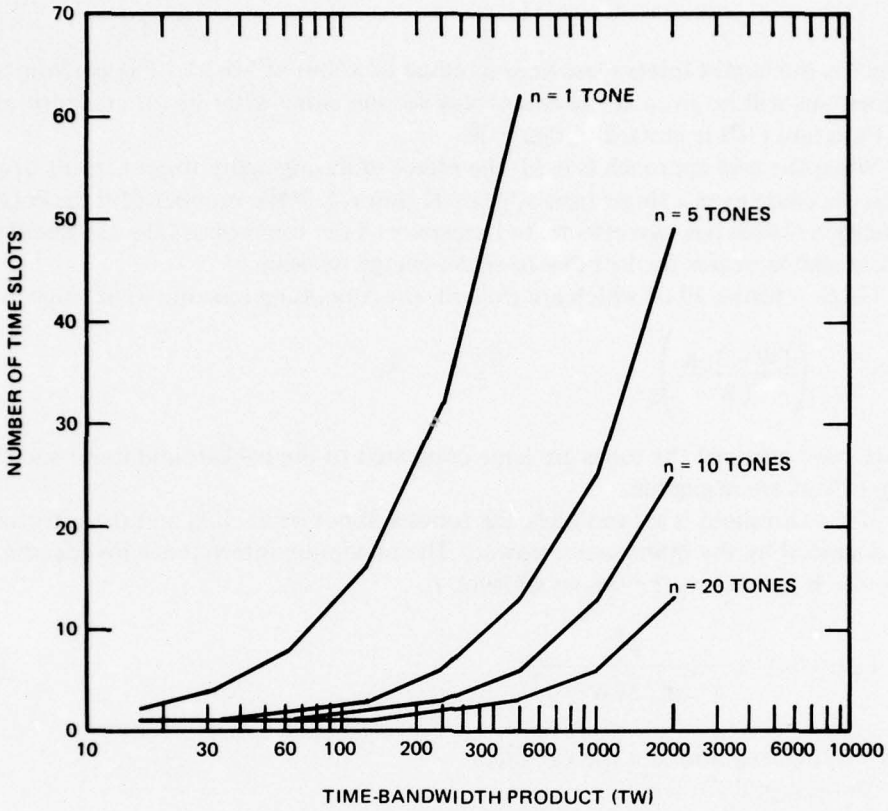

Figure 38. Number of grid time slots allowed for 2 dB loss.

where z_i is the threshold for i time segments.

Now consider what happens then the quantile algorithm is used to set the threshold. When large tones are present in the data sample, the 90-percent exceedance-value estimate is biased upward. The biased estimate may be calculated as follows: take the total number of grid samples as 3nK; assume that the interference is large enough to ensure that none of these samples will occur in the lowest 10 percent of overall samples; since these samples are randomly selected, 10 percent of them would have occurred below X_{90} without interference and 90 percent above X_{90}; assuming they are now well above X_{90}, a new 90-percent exceedance value is calculated ($=X'_{90}$) as:

$$0.9 = \frac{[(TW - 3nK) \int_{X'_{90}}^{\infty} \frac{x}{\sigma^2} e^{-x^2/2\sigma^2} dx] + 3nK}{TW}, \qquad (15)$$

$$X'_{90} = X_{\beta},$$

where

$$\beta = \left(\frac{0.9\,TW - 3nK}{TW - 3nK}\right), \; 3nK < TW,$$

and the threshold is set at

$$z = CX_{\beta}. \tag{16}$$

The threshold calculated by the quantile method (equation (16) is compared in figure 39 to the threshold resulting from the previous analysis (equation (14)). Both thresholds have been normalized by the values for K = 1 to show the relative threshold increase as K increases. The figure shows that the quantile algorithm does what it should; increases with increasing K to keep the excision loss from becoming too large.

The results in the following section for grid processing were achieved using the quantile algorithm described by equation (16), where C was set at 8 to avoid over excising on the SWGN channel.

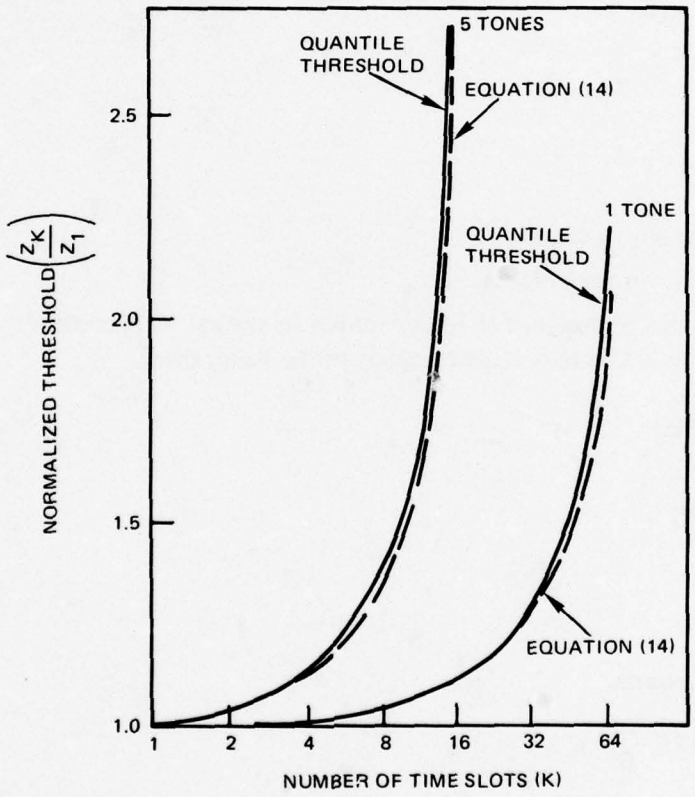

Figure 39. Threshold behavior for grid processing.

GRID-PROCESSING PERFORMANCE

The results of grid processing in the presence of narrowband interference are shown in figures 40 and 41 for a single slow-swept tone and five fixed tones, respectively. With a

single tone present, grid processing is effective with up to 16 time slots (blocks) when TW is 128. Figure 42 shows that only minimal excision took place with 32 or 64 time blocks, balancing off the excision loss against the interference loss. With five interfering tones, the algorithm was capable of effective interference suppression only up to four time blocks before the excision loss surpassed the interference loss (figures 41 and 43).

Figure 43 shows that, in a narrowband interference environment, the performance is governed by excision loss. Since this loss rapidly increases when more than 50 percent of the spectrum is excised, the grid format should be designed so that excessive excision is avoided under typical hf interference conditions. The spectral characteristics of an hf transmitter, as defined by FCC standards[7], is shown in figure 44. The figure shows that the spectral resolution of the grid processor should be around 3 kHz,

$$\frac{3W}{TW/K} = 3 \text{ kHz},$$

or

$$K \approx 3 \text{ kHz} \cdot T,$$

where T = processing duration

K = number of time blocks.

The signal should also be designed to limit excision to around 50 percent. If we assume one frequency user each X kHz in occupied regions of the band, then,

$$n = \frac{W \text{ (kHz)}}{X},$$

$$3nk \leqslant \frac{TW}{2},$$

$$K \leqslant \frac{TX}{6}.$$

Combining these criteria,

$$K = \min \left(3T, \frac{TX}{6}\right), \quad T \text{ in ms.} \tag{17}$$

7. Stein Associates Inc, ONR Contract N00014-76-C-0650, Final Report, Spread-Spectrum Concepts, by Roger R Reed and John F Pieper

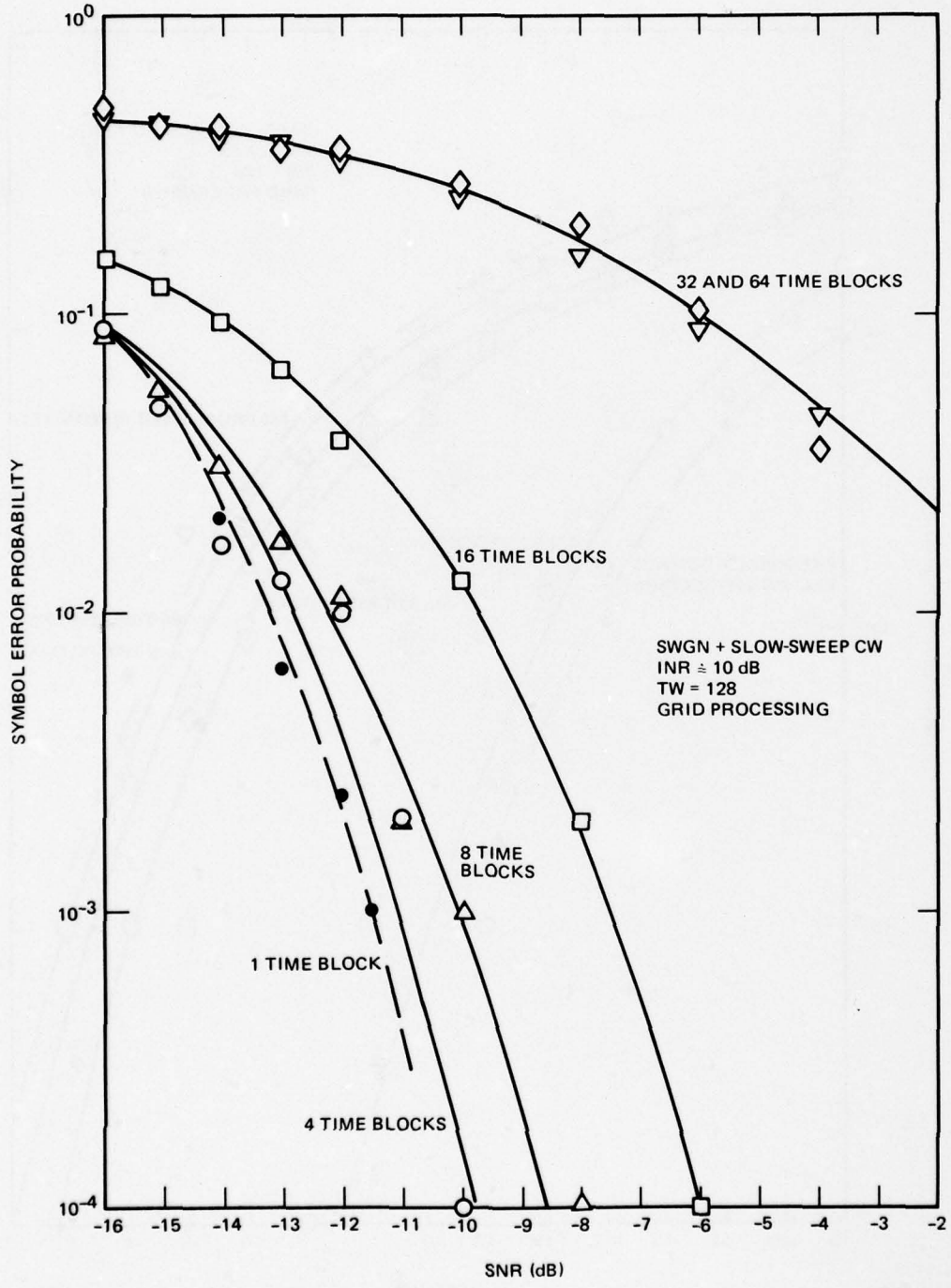

Figure 40. Grid-processing performance characteristics (SWGN and slow-sweep CW).

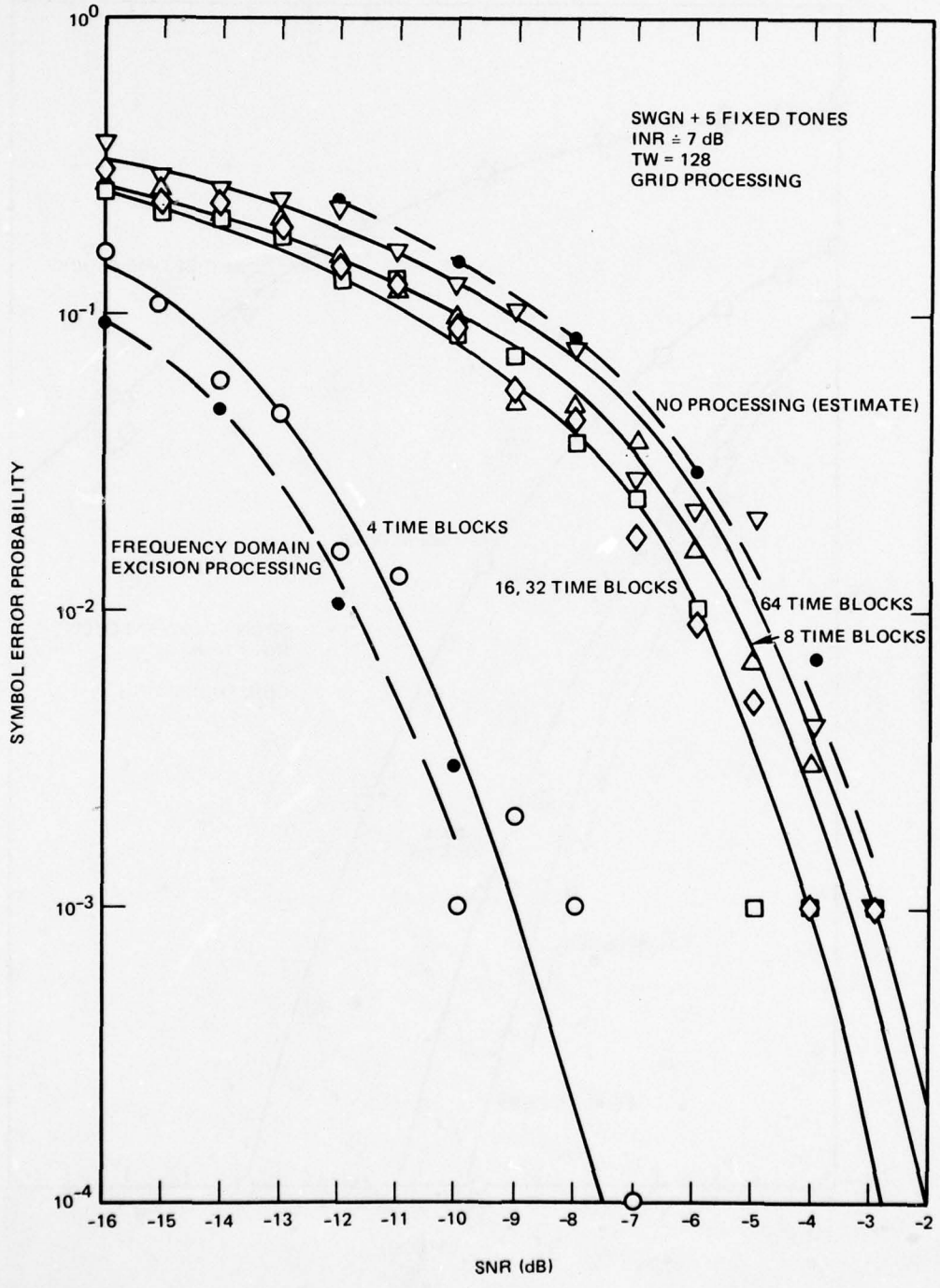

Figure 41. Grid-processing performance characteristics (SWGN and fixed tones).

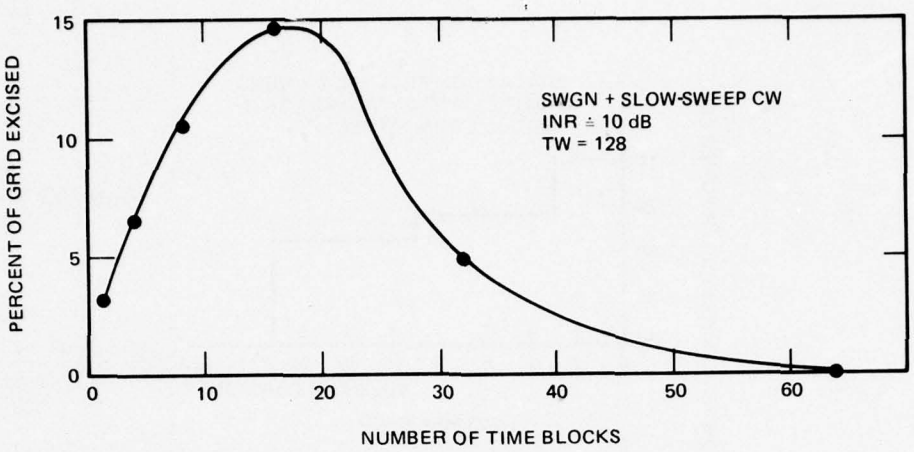

Figure 42. Grid-processing excision characteristics.

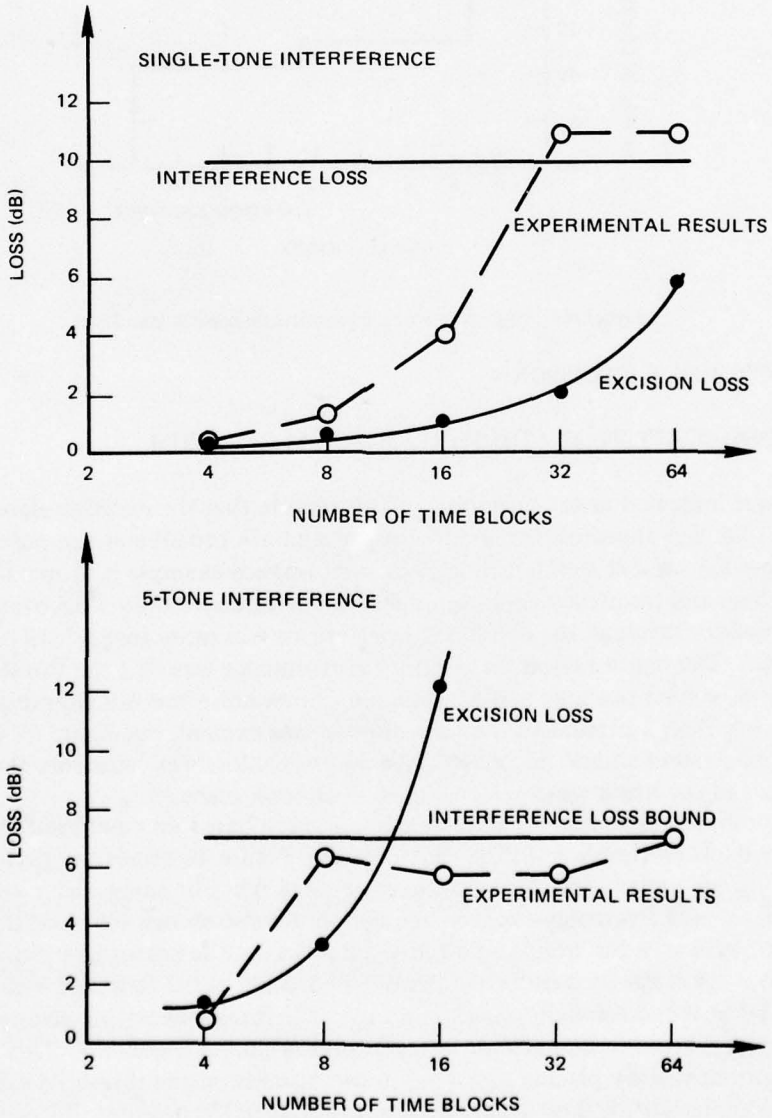

Figure 43. Grid-processing loss characteristics.

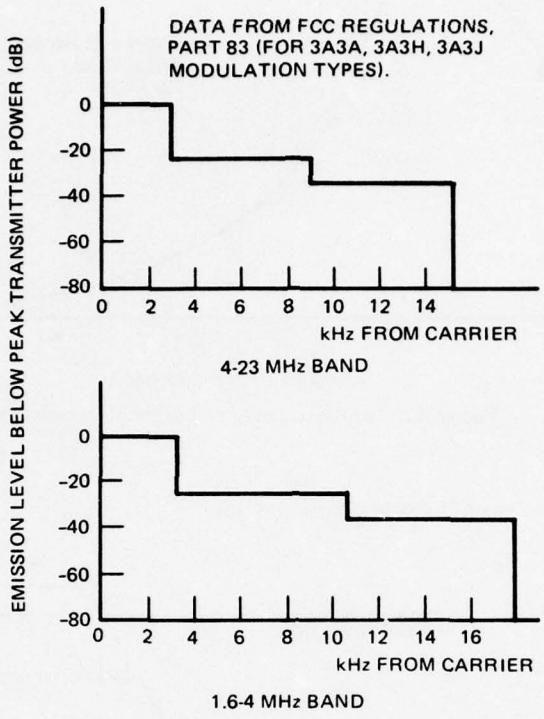

Figure 44. High-frequency transmitter emission standards.

TIME/FREQUENCY EXCISION

MODIFICATION OF THE THRESHOLD ALGORITHM

It was indicated at the beginning of this section that the excision algorithms used previously (9.8 X_{90} threshold) are ineffective when both broadband and narrowband interference types are present simultaneously. A performance example is shown in figure 45, where the use of time and frequency excision improved performance only 3 dB over no interference suppression, although the combined interference was more than 15 dB above the background noise. The major reason for the poor performance was that the threshold for burst-noise excision was set too high and consequently burst noise was not suppressed. Figure 45 shows that less than 1 percent of the time domain was excised, but figure 13 indicated that more than 10 percent should be excised. An additional loss was caused by the distortion of the narrowband spectrum when wideband excision took place.

A modified algorithm for time-domain excision based on equation (8) was used to set the time-excision threshold in the time domain. Figure 46 shows the performance of this algorithm on a mixed-interference channel (curve A). For comparison, the performance of the old time- and frequency-excision algorithms are also shown for conditions of narrowband and broadband interference only (curves B and C). The performance of the modified algorithm was significantly better than the old algorithm, but it flattened out at about $P_\epsilon \simeq 10^{-2}$ because, occasionally, the 2-point quantile threshold-setting algorithm set the threshold too high and underexcised, or set it too low and over-excised. This problem may be reduced somewhat by placing upper and lower bounds on the threshold estimate. It is conjectured here that this limit would decrease for larger TW product processing and more accurate threshold estimates.

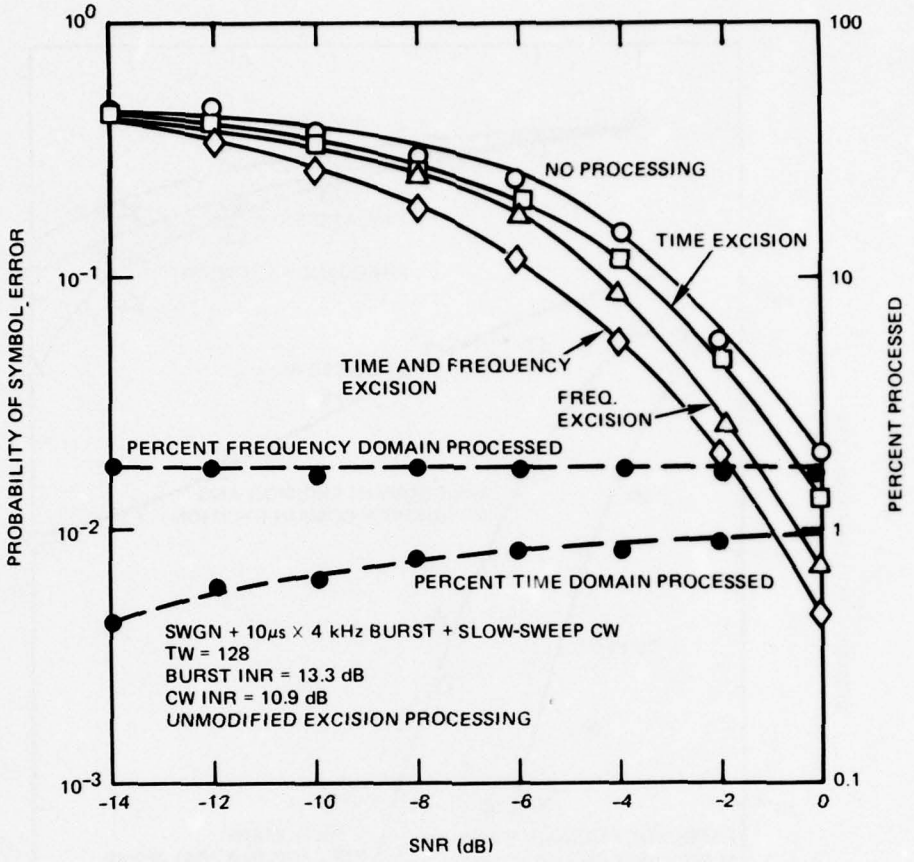

Figure 45. Unmodified time-excision/frequency-excision performance.

SMOOTHING THE EXCISION VECTOR

The second factor contributing a loss to the old time-excision/frequency-excision algorithm was the distortion caused to narrowband interference by prior time-domain excision. A simulation was run to estimate the loss when time-domain excision is done in the presence of a CW tone and frequency-domain excision is used to suppress the tone. The result showed that a loss of between 2 and 2.5 dB resulted from the tone spreading due to time excision. Figure 47a shows the tone and a signal in the frequency domain with a signal-to-tone ratio of −10 dB. In this figure, no prior time excision was performed and the tone occupies a single spectral region at 35 dB above the signal spectral peaks. Figure 47b shows a simulated time-domain excision of about 20 percent of the time domain. The resulting spectrum (47c) shows that the tone is now spread over the total bandwidth.

The objective of excision-vector smoothing is to reduce this tone spreading by limiting the steepness of the excision mask. This was done here by treating the excision vector as a sampled-time series of zeroes and ones. The time series was smoothed by low-pass filtering it to some fraction of its original bandwidth. To maintain a deep central null, the original excision vector was stretched (the zero intervals widened) as shown in figure 48b, low-pass filtered (figure 48c), and this vector was multiplied by the original vector to create the new excision vector that was used (figure 48d). Figure 49 is a flow diagram of how this

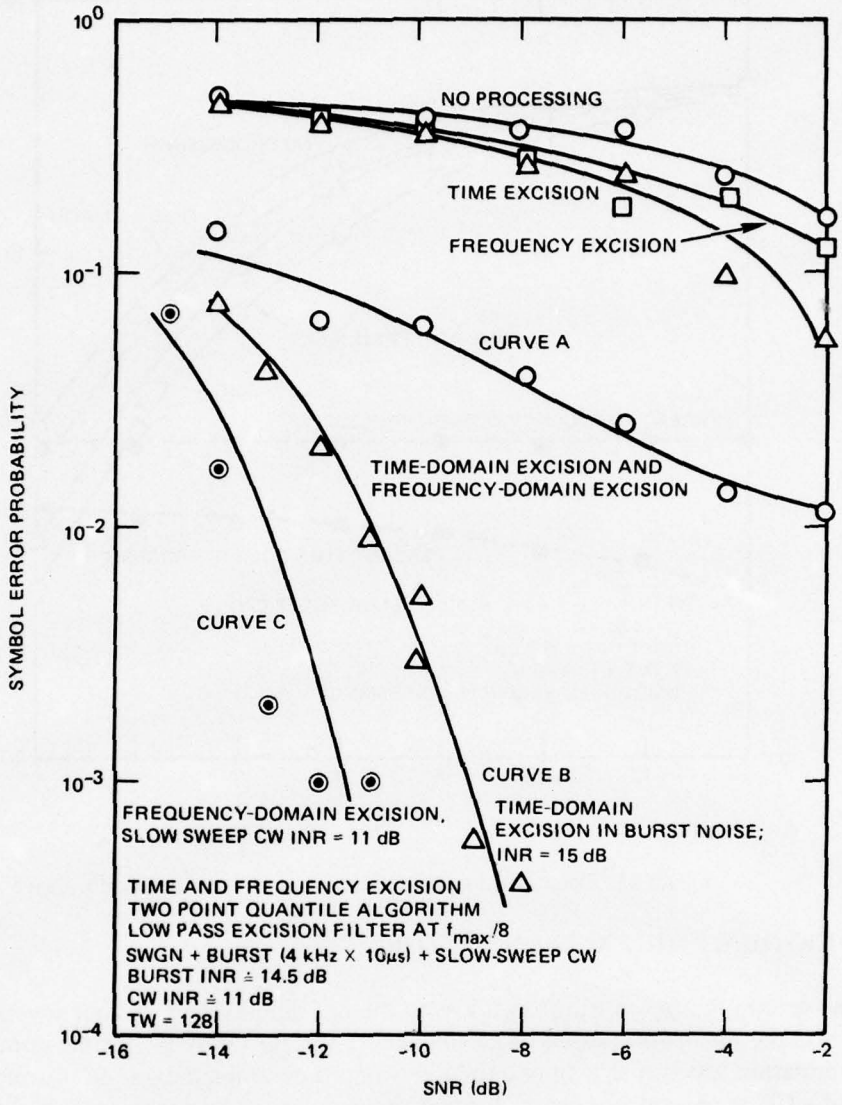

Figure 46. Performance examples on a mixed-interference channel.

was actually accomplished. Figures 47d and 47e, and figures 47f and 47g show the results with the vector's low-pass smoothing point set at $f_{max}/4$ and $f_{max}/8$, respectively.

A simulation test was run using different excision-vector smoothing points and noise consisting of a combination of stationary white Gaussian noise plus a slow-sweeping CW tone with an INR of 9 dB. The SNR was set at -12 dB. Table 4 gives the results of the simulation for four low-pass cut-off points and for no smoothing (cut-off at f_{max}). The final column of table 4 is the excess loss after the signal-energy loss has been accounted for. The excess loss is a significant factor when no vector smoothing is performed. By smoothing at $f_{max}/8$, the loss is reduced to 0.6 dB. The time-excision/frequency-excision simulation results which follow use this lowpass point for excision-vector smoothing.

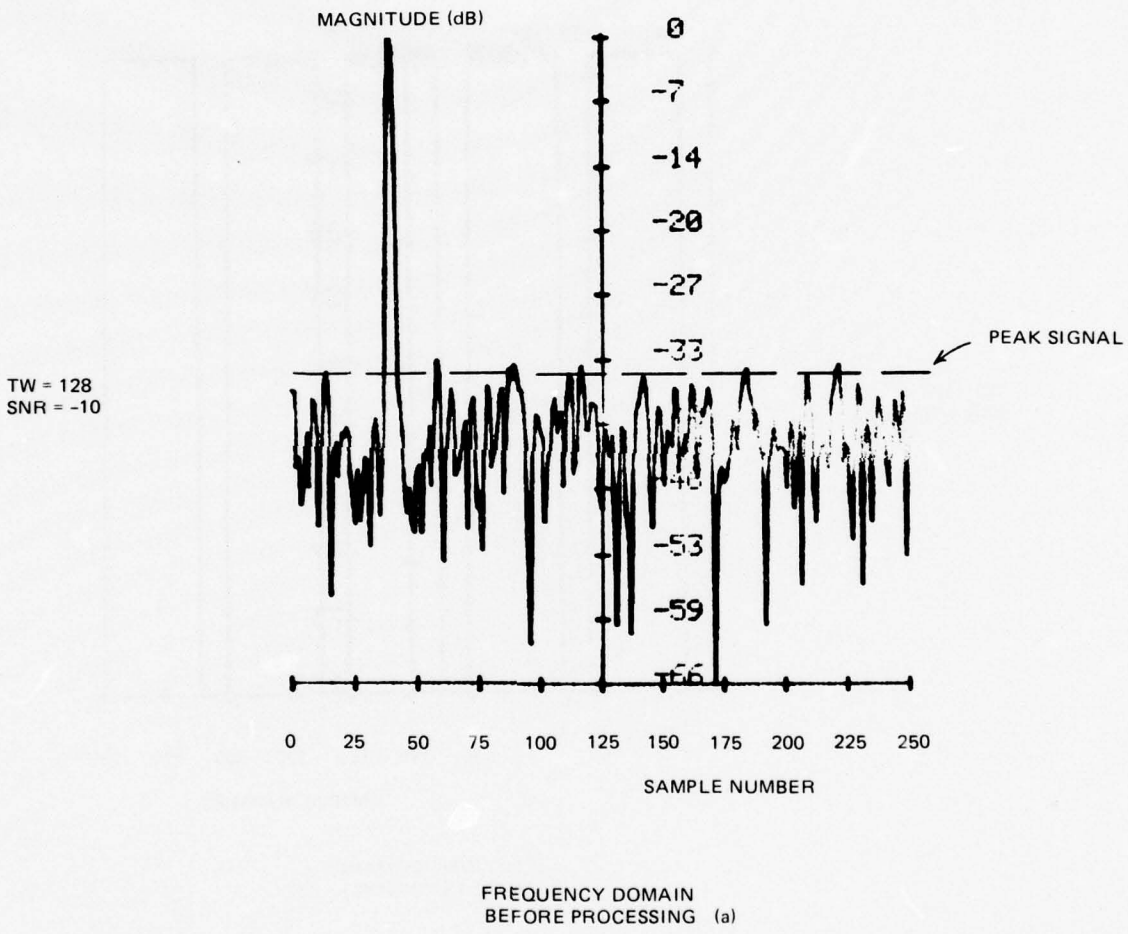

Figure 47. Frequency spectrum of SWGN plus CW tone.

TW = 128
SNR = -10

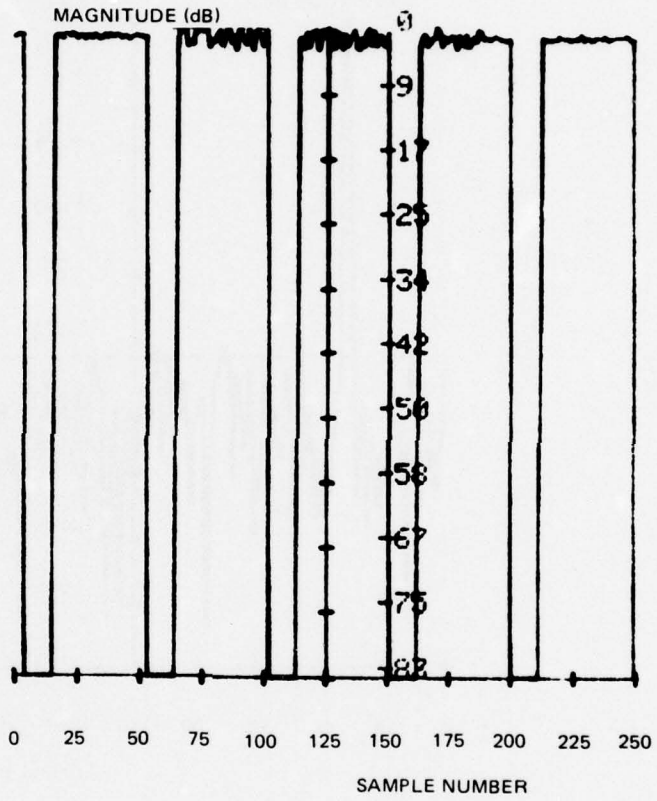

INPUT TIME DOMAIN
AFTER EXCISION (b)

Figure 47. Continued.

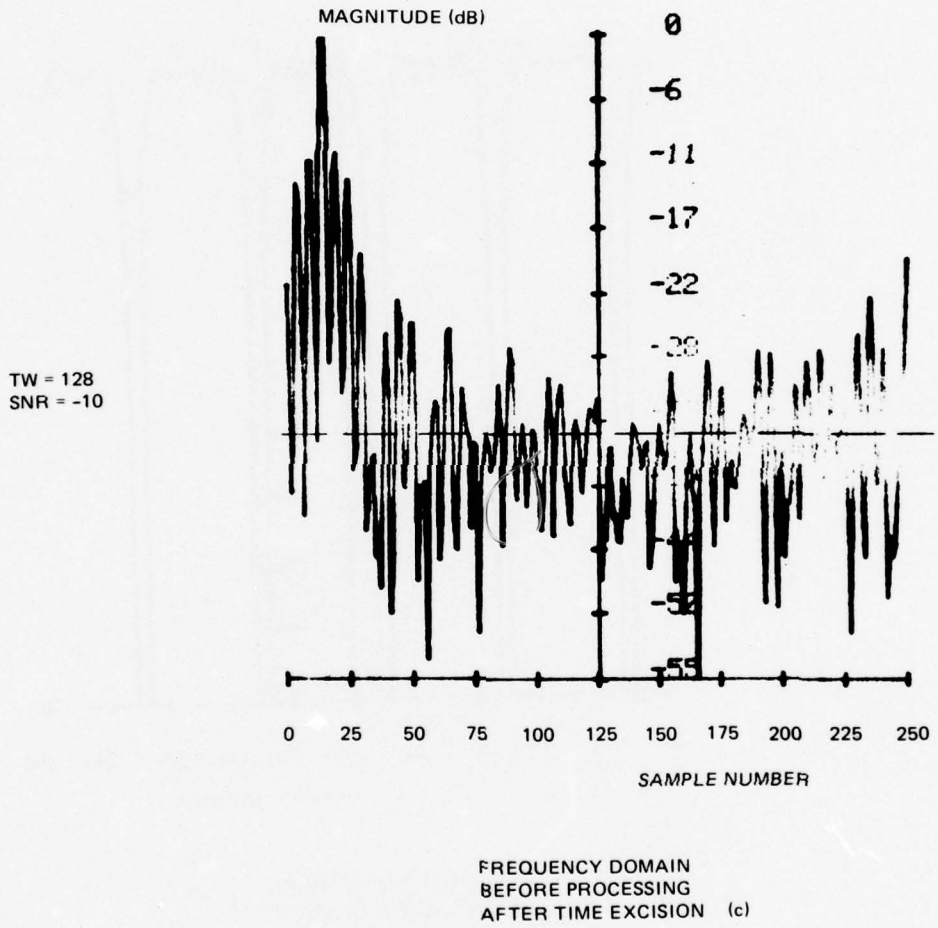

Figure 47. Continued.

TW = 128
SNR = -10

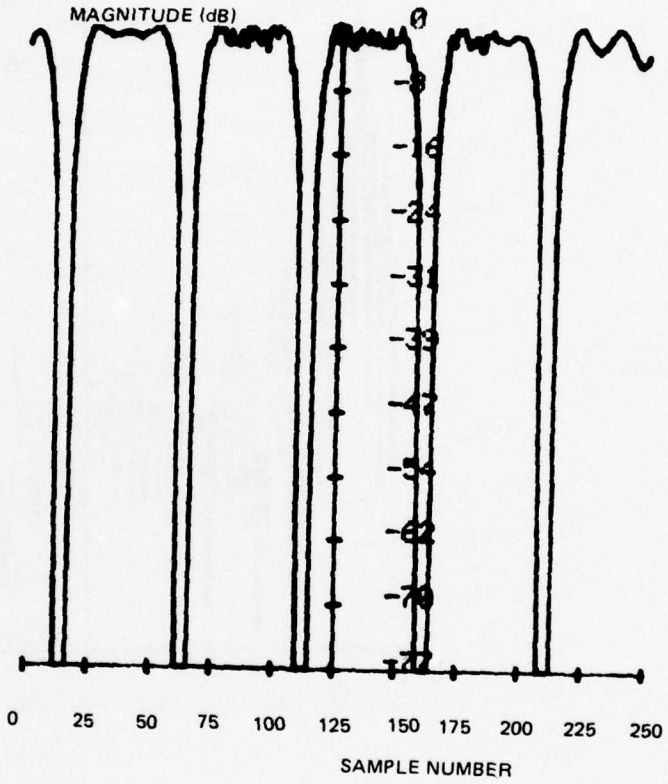

INPUT TIME DOMAIN
AFTER SMOOTH EXCISION (d)
(CUT OFF = f MAX/4)

Figure 47. Continued.

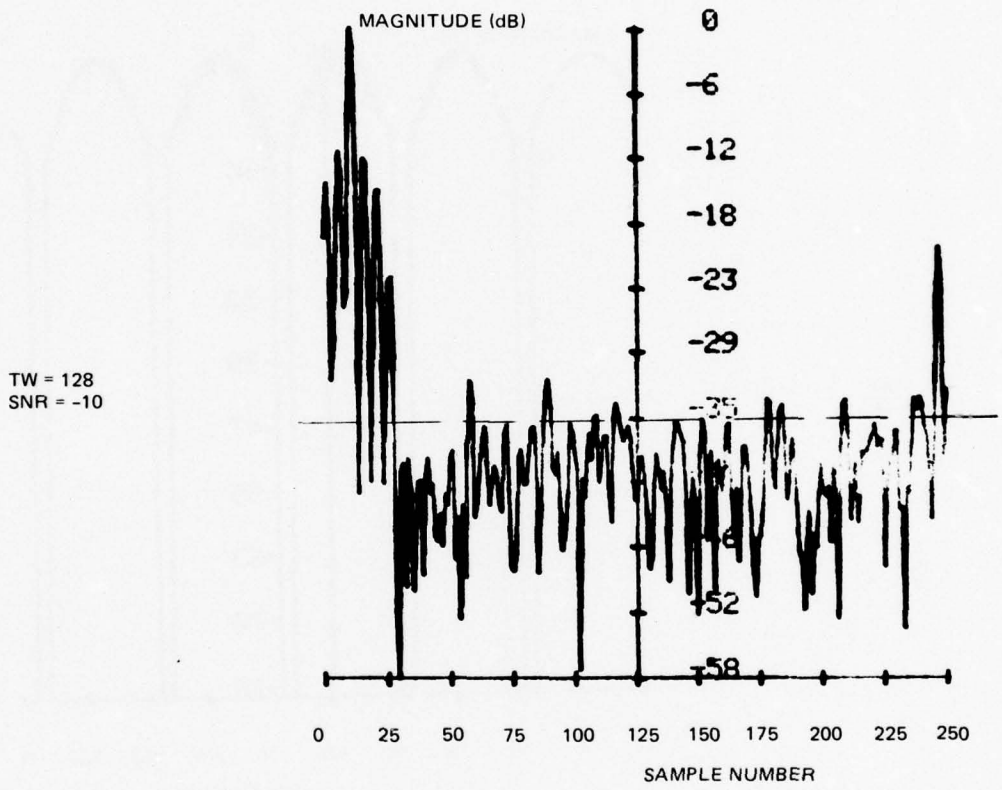

Figure 47. Continued.

TW = 128
SNR = -10

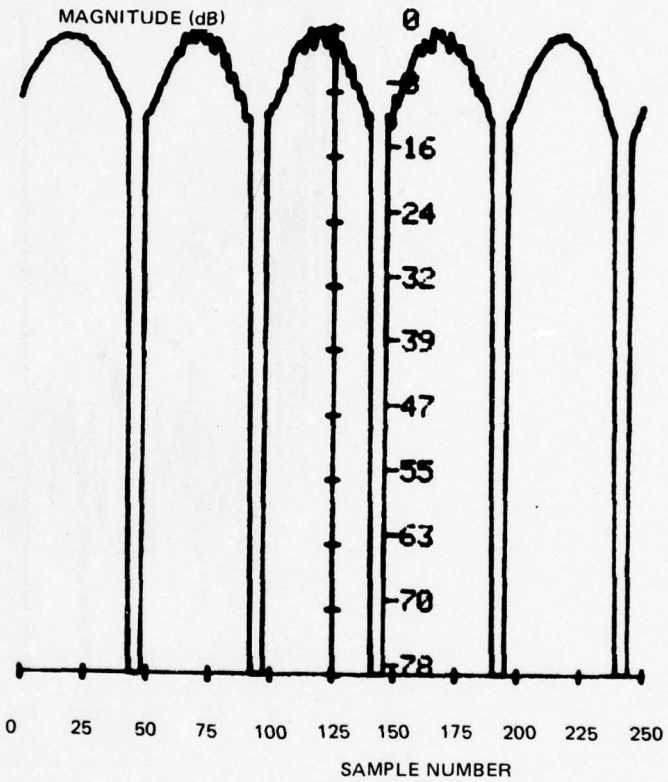

INPUT TIME DOMAIN
AFTER SMOOTH EXCISION (f)
(CUT OFF = f MAX/8)

Figure 47. Continued.

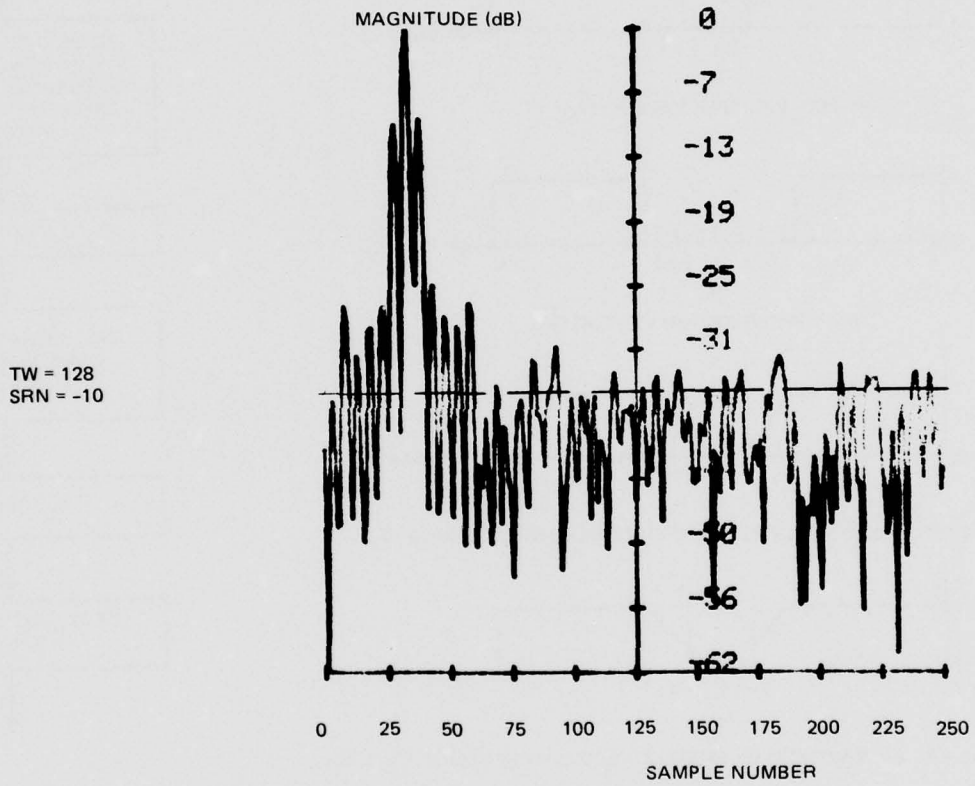

Figure 47. Continued.

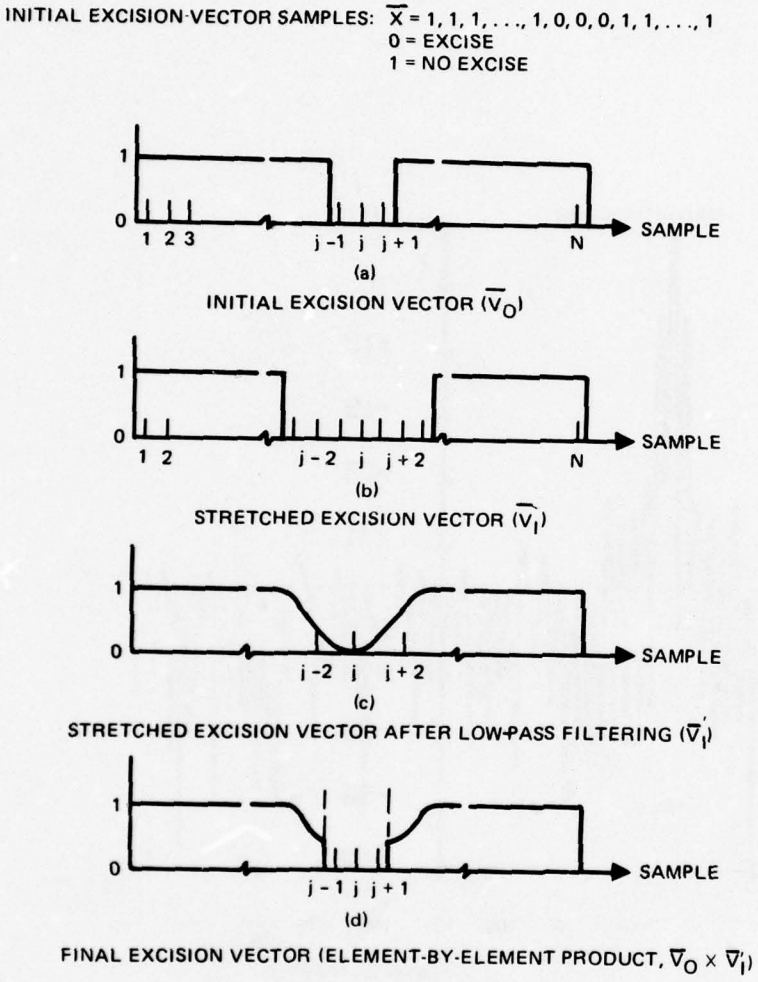

Figure 48. Excision-vector smoothing.

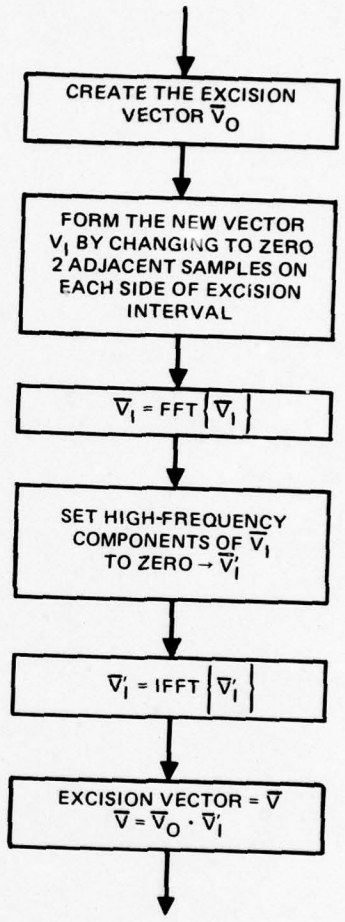

Figure 49. Excision-vector smoothing flow chart.

TABLE 4. EXCISION-VECTOR SMOOTHING SIMULATION RESULTS.

Lowpass Filtering Point	P_ϵ Before Frequency Excision	P_ϵ After Frequency Excision	Percent Freq Domain Excised	Loss Relative to no Time Excision	Excess Loss
f_{max}	0.351	0.072	9	3.6 dB	2.4 dB
$f_{max}/2$	0.352	0.053	9.5	2.8	1.6
$f_{max}/4$	0.354	0.048	9.5	2.6	1.4
$f_{max}/8$	0.348	0.033	8.7	1.8	0.6
$f_{max}/16$	0.342	0.030	7.8	1.7	0.5

TIME-DOMAIN CLIPPING, FREQUENCY-DOMAIN EXCISION

An alternative non-linearity to excision is time-domain clipping. Figure 50 (a, b, and c) shows the frequency domain after time-domain clipping at 3 different levels when the interference consists of a CW tone plus bursts of Gaussian noise in addition to the Gaussian-noise background. The tone spreading is still obvious in (a) and (b). In figure 50c, the threshold is low enough to cause the wideband noise floor to rise above the tone components. Figure 51 is the frequency domain when a smoothed excision vector is used with a lowpass cutoff at $f_{max}/4$. The background noise level is more than 10 dB lower than for clipping. In this case, clipping in the time domain does not appear to offer an improvement over excision. Table 5 shows results of a simulation test using time-domain clipping and frequency-domain excision. For comparison, the time-excision/frequency-excision algorithm with smoothed excision produced an error probability of 0.034.

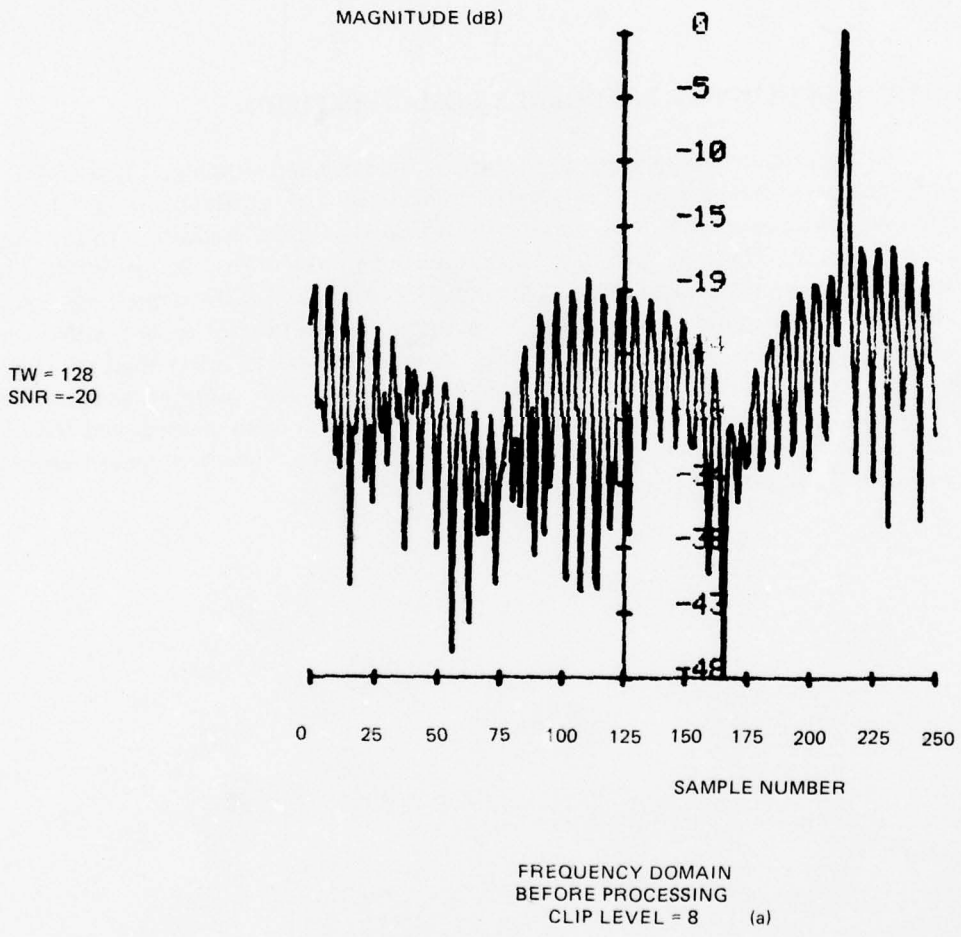

Figure 50. Frequency spectrum after time-domain clipping.

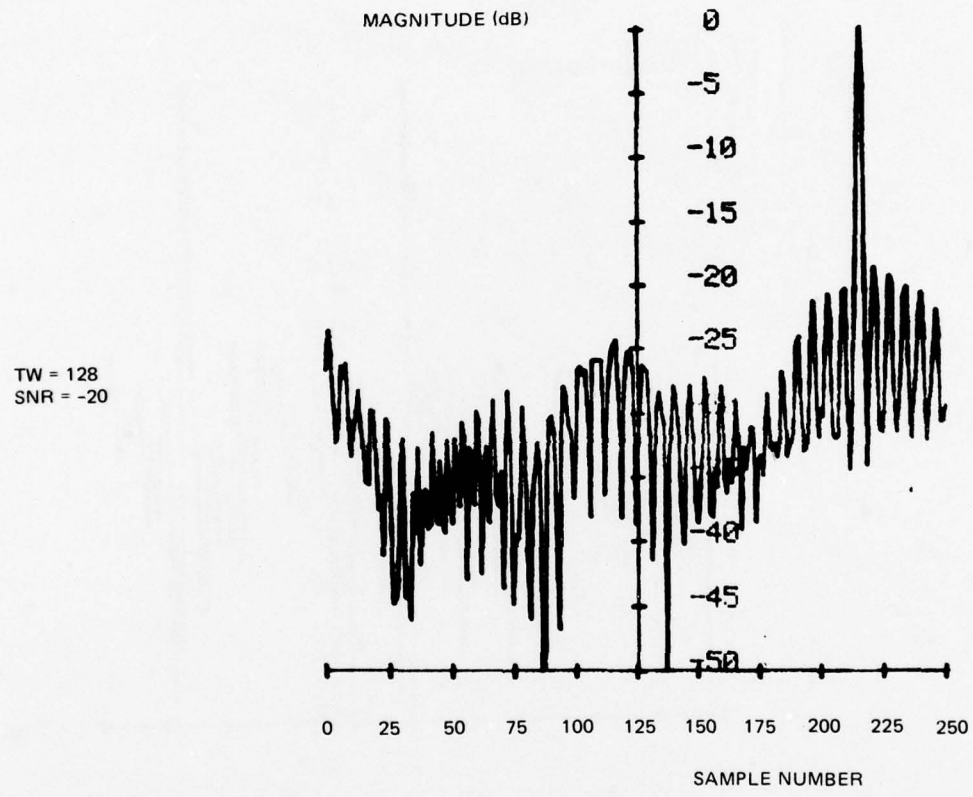

Figure 50. Continued.

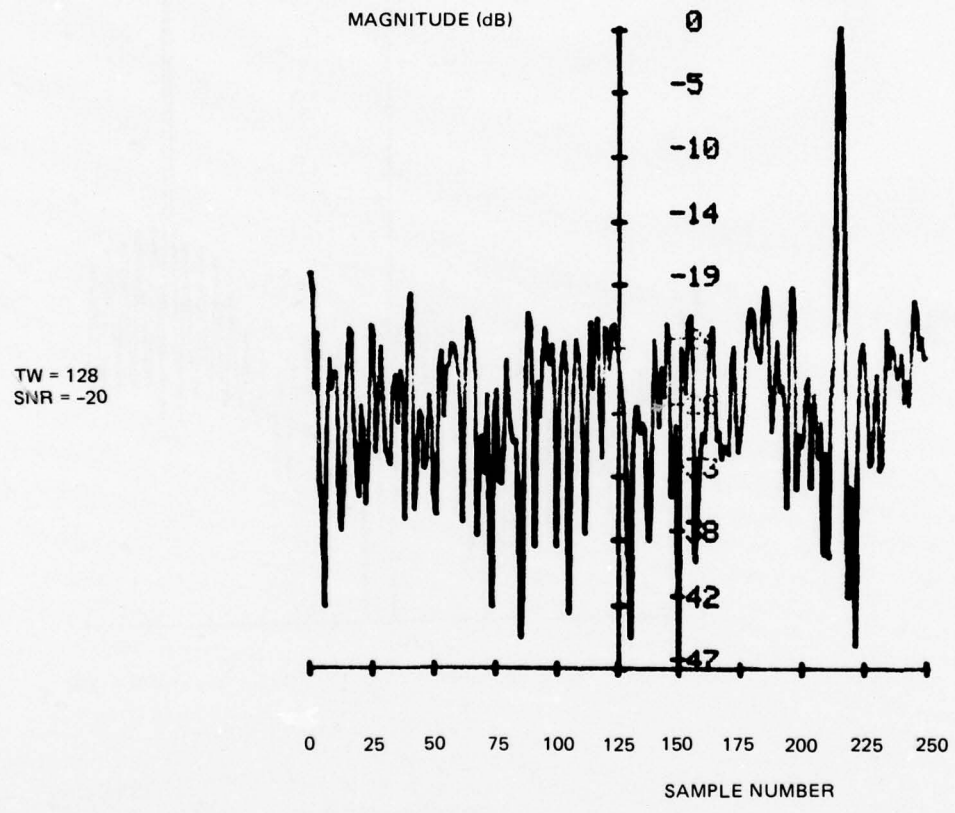

Figure 50. Continued.

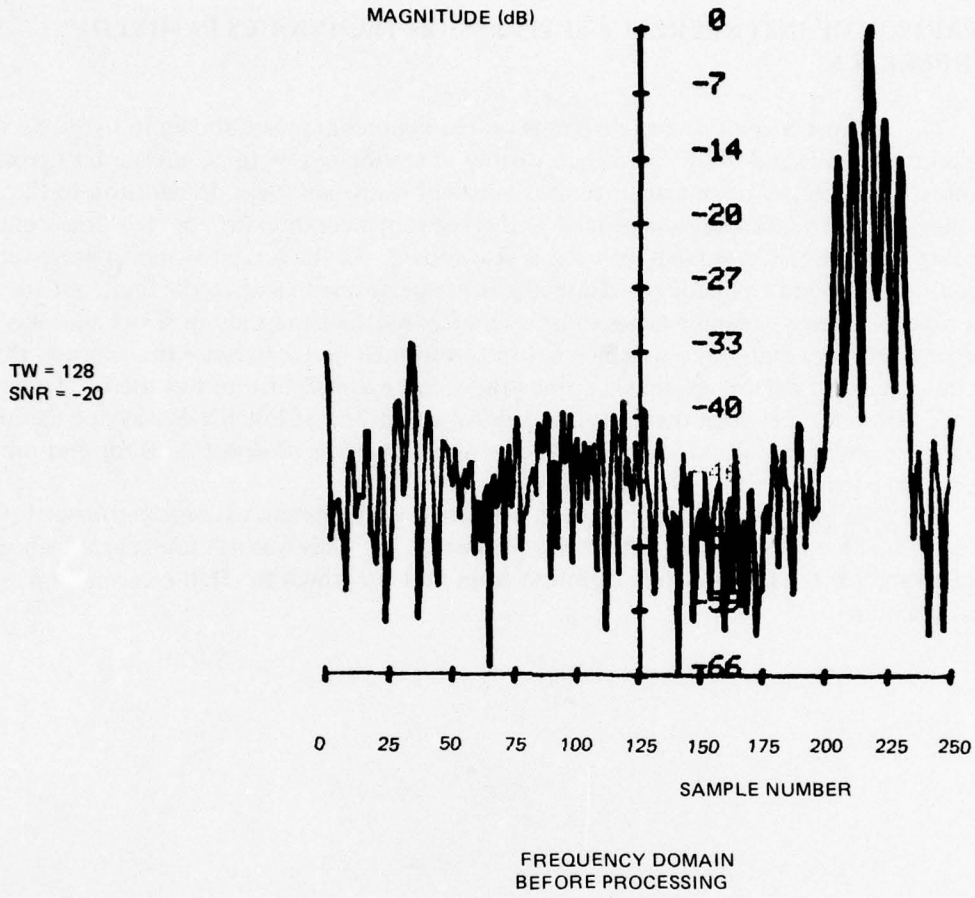

Figure 51. Frequency spectrum after smooth time excision.

TABLE 5. TIME-CLIPPING/FREQUENCY-EXCISION PERFORMANCE RESULTS.

Clipping Level	Percent Time Domain Clipped	P_ϵ After Frequency Excision
4	52	0.382
6	15	0.219
8	8	0.200

Burst Noise INR = 15 dB

CW Noise INR = 11 dB

SNR = -12 dB

COMPARISON OF INTERFERENCE-SUPPRESSION TECHNIQUES IN MIXED INTERFERENCE

The performance of several different processing techniques is shown in figure 52 for a mixed interference and noise channel consisting of stationary, white, Gaussian background noise plus slow sweep-tone interference plus bursts of Gaussian noise. In addition to the processing alternatives already mentioned in this section, a combination of Hall time-domain processing and frequency-domain excision is also shown. At the lowest signal-to-noise ratios, the modified time and frequency excision algorithm performed close to the limits set for excision performance in simple types of interference (narrowband only or wideband only). At higher SNRs, the grid-processing alternatives performed better because the excision threshold could be more reliably established since the single point algorithm was used. The performance difference between the grid and excision algorithms at low SNRs was due mainly to the difference in resolution, amounting to an additional loss of about 2 dB for grid processing in this particular case.

The combination of Hall processing with frequency-domain excision performed poorly on this channel for both values of the noise parameter, m. This was not unexpected since the noise used for the test was very different from that for which the Hall-receiver configuration is optimum.

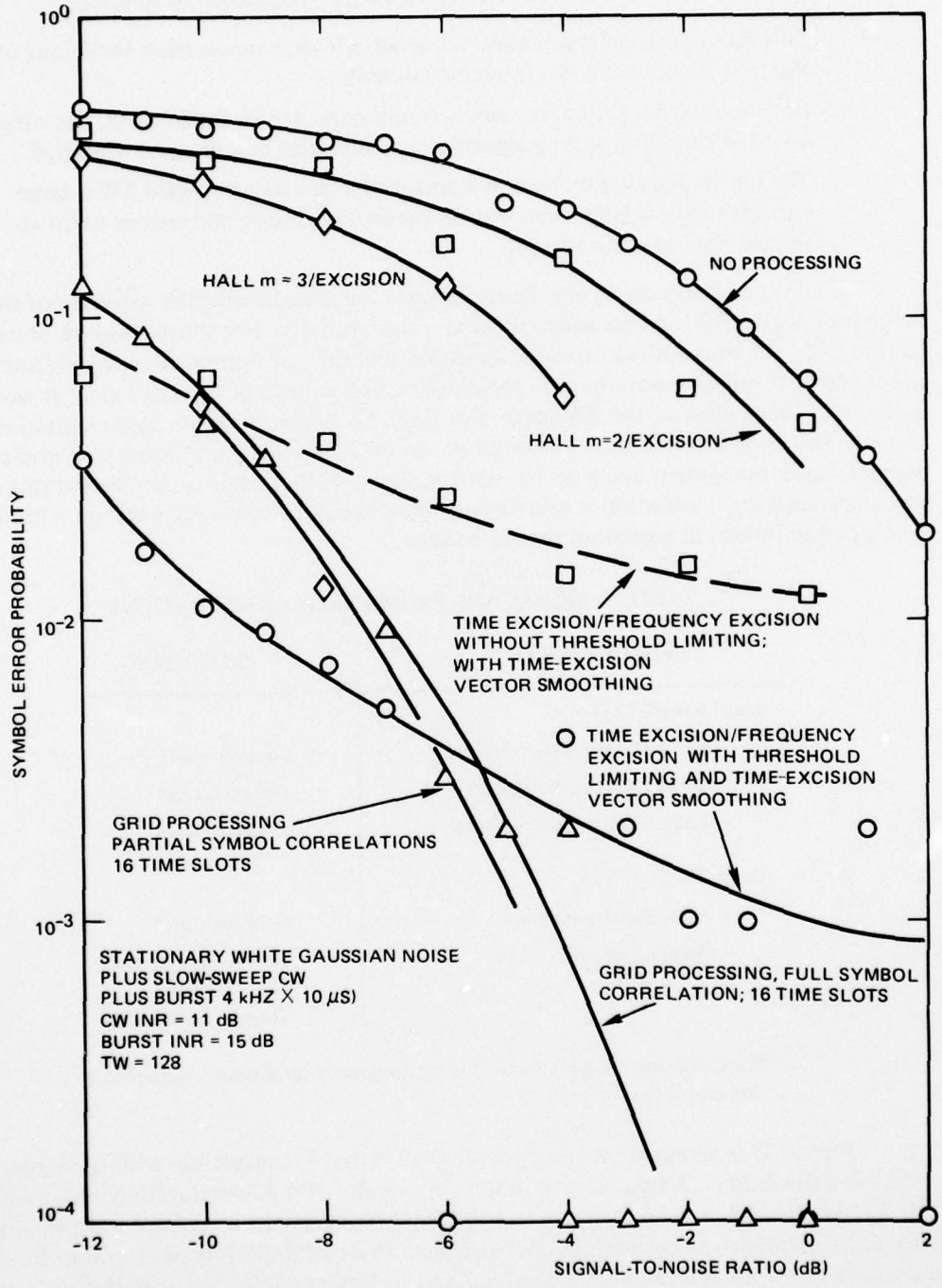

Figure 52. Interference-suppression algorithm performance on the mixed-interference channel.

IMPLEMENTATION CHOICES

The following conclusions can be reached from the algorithm simulations:

1. Threshold excision is generally the most effective suppression technique in the time domain and the frequency domain.
2. For the mixed-interference environment expected in the hf band, the simple quantile threshold setting algorithm is ineffective and must be modified.
3. The grid-processing technique works well when the processed TW is large enough to allow good time and frequency resolution and/or few narrowband interfering tones are present.

The type of processing also depends upon the time-bandwidth structure of the signal being processed. Table 6 lists some of these considerations. For short-duration or narrowband signals, the unmodified quantile algorithm and time or frequency excision (not both) can be used. If mixed interference is present, excision cannot be effective since it would require eliminating most of the TW space. For large TW-product signals, grid excision is effective when enough time-frequency resolution can be achieved. The efficiency of grid processing depends upon the system being nearly synchronized, so that prior to synchronization, or when the time/frequency resolution is insufficient, time excision/frequency excision with the modified quantile threshold algorithm should be used.

TABLE 6. SIGNAL AND PROCESSING CONSIDERATIONS.

TYPE OF SIGNAL	PROCESSING
Small TW (≤ 128)	
– Short Duration Narrowband	No Processing
– Short Duration Wideband	Freq Excision
– Long Duration Narrowband	Time Excision
Large TW (> 128)	
– After Synchronization	Grid Excision*
– Before Synchronization	Time/Freq Excision Using Modified Threshold Algorithm

*Grid excision can only be used if the frequency resolution requirements are met; equation (17)

Figure 53 is an example of a signal structure that is compatible with the signal-processing flexibility. A basic chip is defined as a pulse of 0.32-ms duration and 3.125 kHz bandwidth, TW = 1. A high-rate, narrowband transmission would use a string of the pulses, differentially phase modulated, to achieve a rate of 3125 bits per second. By increasing the clock rate, sub-chips can be derived. For example, doubling the clock rate produces the second subchip (0.16 ms X 6.25 kHz) and increasing the clock rate by a factor of 32 produces the thirty-second subchip (0.01 ms X 100 kHz). Any combination of

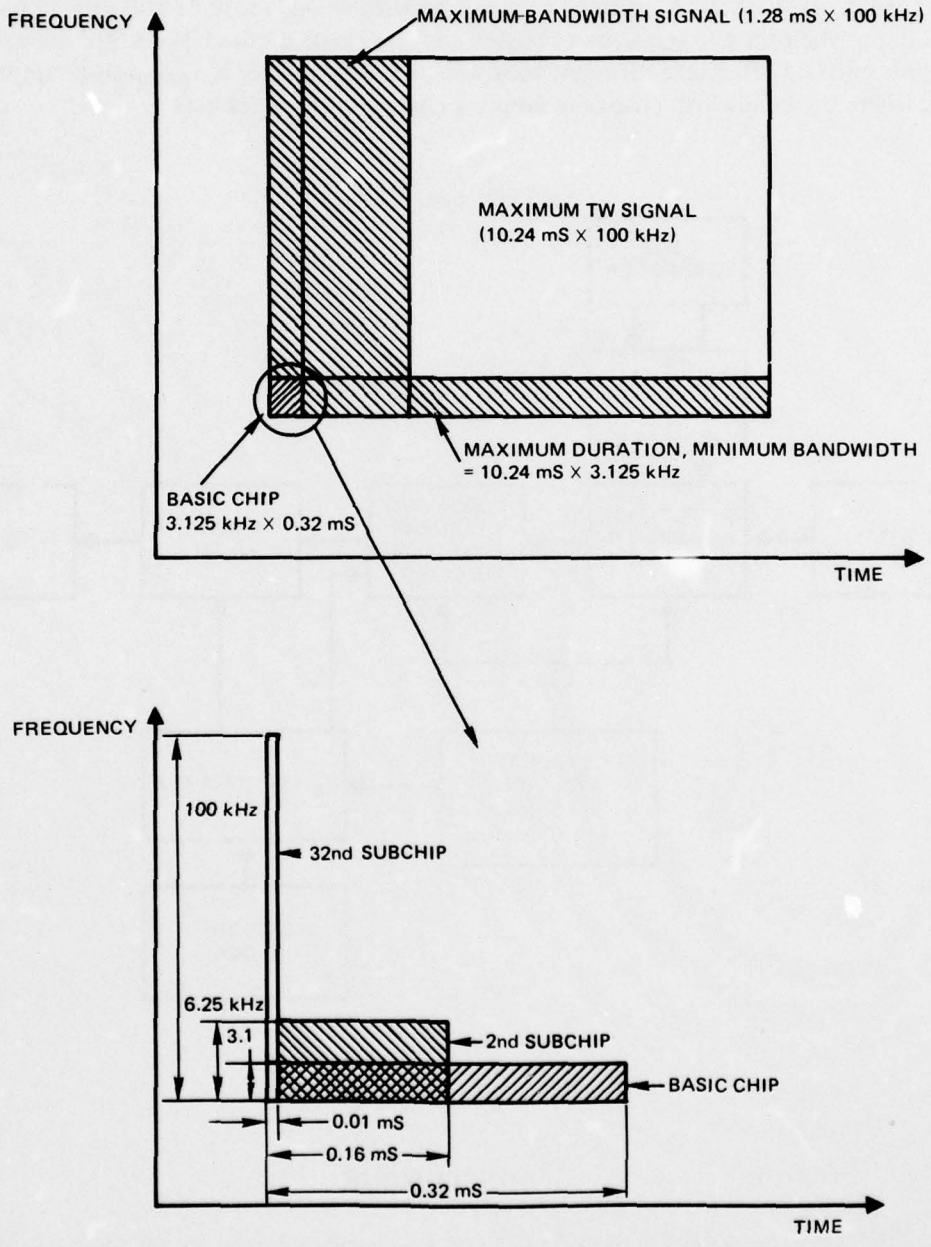

Figure 53. Variable TW symbol structure.

symbol bandwidth (k X 3.125 kHz) and duration (n X 0.32 ms) can be selected by specifying the clock-rate multiplication factor, k, and total number of pulses, n X k. The only limitation is that fine enough frequency resolution be maintained by limiting n to values of 4 or more; and that the product n X k be a power of 2 (or close to it) for convenient fast Fourier transformations. A simple flow diagram for such a signal generator is shown in figure 54. In the figure, an alphabet size of 2 is assumed, and the code information is stored in 2 buffers. If symbol "A" is to be transmitted with a bandwidth of 100 kHz and a duration of 1.28 ms, the first 128 elements of buffer "A" are clocked out at 100 kHz. Since the symbols must be filtered to different bandwidths, a digital filter is a convenient implementation, where the bandwidth change is simply a change in the clock rate.

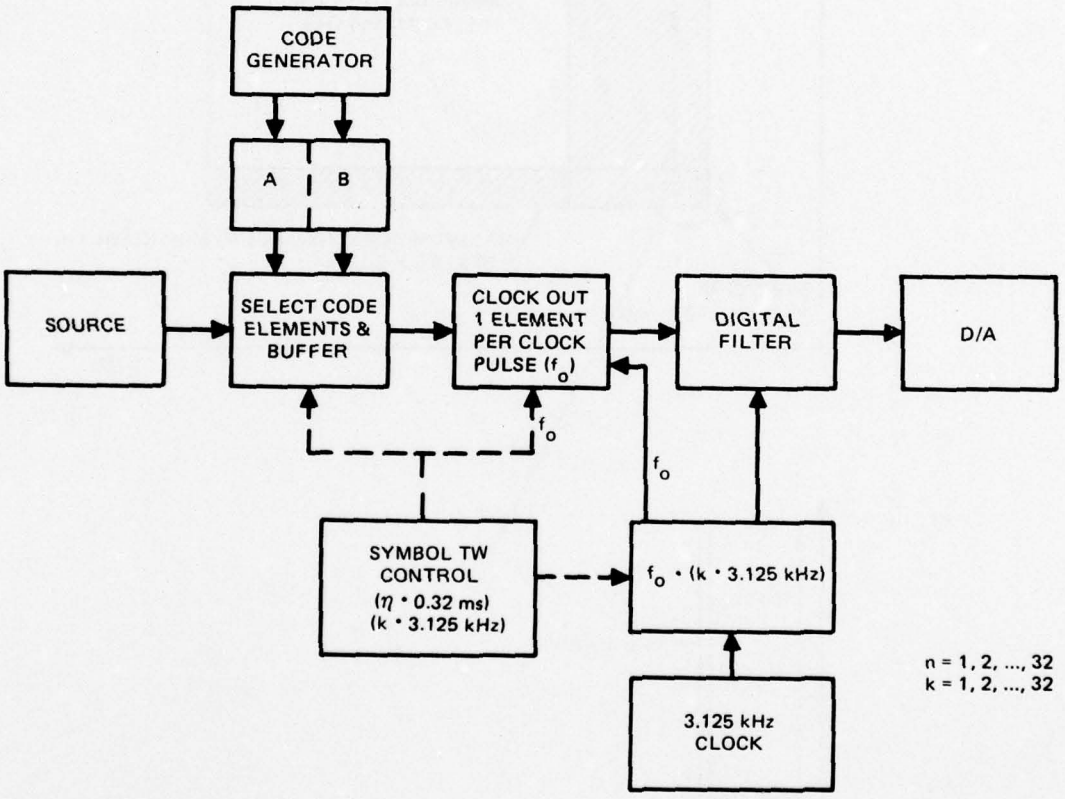

Figure 54. Digital-symbol generator.

CONCLUSIONS

1. For simple types of noise (SWGN + narrowband only, or SWGN + broadband only) threshold excision based on a simple quantile algorithm works well in both the time domain and the frequency domain for a variety of interference conditions.

2. Several other techniques, including threshold clipping (time domain), Hall receiver (time domain), and threshold whitening (frequency domain) performed about equally as well as threshold excision.

3. The quantile threshold algorithm worked well down to a TW product of about 128. If fewer than this number of samples are to be processed, a moment algorithm setting the threshold based on the first and/or second moments of the input samples must be used.

4. In a simple noise environment, the excision algorithm effectively suppressed all except about 2 dB of the interfering power, for interference that remained within the dynamic range of the receiving system. The performance losses are summarized in table 7.

5. In a mixed-interference environment, where both narrowband and broadband burst noises were present, the simple quantile threshold and excision techniques were ineffective. The primary problem was that the quantile algorithm set the threshold too high and interference was not detected. A secondary problem occurred when the time-domain excision caused spreading of any narrowband interference present.

6. A modified quantile algorithm performed well when good statistical estimates of the noise could be made (large processed TW) or when symbol error rates greater than about 10^{-3} were acceptable.

TABLE 7. PROCESSING LOSSES ON A SIMPLE NOISE CHANNEL.

Process (TW = 128)	Loss
Input Windowing	0.5 dB
Non-Orthogonality Quantization, Transform Noise, Non-White Signal	1.5 dB
Time Domain Excision*	0.3 dB
Orthogonality Loss Due to Excision	0.2 dB
Unsuppressed Interference (Time Excision)	1-2 dB
Unsuppressed Interference (Time Clipping)	2-3 dB
Hall Processing*	1.5 dB
Unsuppressed Interference (Hall)	1 dB
Unsuppressed Interference (Freq Excision)	0-2 dB (1-5 tones)
Unsuppressed Interference (Freq Whitening)	0-1.5 dB (1-5 tones)
*Loss on stationary white Gaussian noise channel	

7. Grid Processing worked well when a small number of interfering tones were present, even for a TW size as small as 128. Grid processing was also simple to implement when a small synchronization ambiguity was present.

8. The loss due to tone spreading could be minimized by smoothing of the excision vector.

9. The best interference-suppression technique depended upon the type of interference present, the TW over which the processing took place, and the SNR at the receiver. Two techniques were most satisfactory in general: (1) threshold excision in the time and frequency domains where the time domain threshold was set using a quantile algorithm based upon two points of the exceedance function; and (2) grid processing, where the TW space was divided into a grid and the grid elements were threshold excised.

The processing losses for mixed interference are summarized in table 8.

TABLE 8. PROCESSING LOSSES ON A MIXED-NOISE CHANNEL.

Process (TW = 128)	Loss
Unmodified Time/Frequency Excision	Large
Modified Time/Frequency Excision	<1 dB for SNR <-12 dB Increasing for Larger SNRs.
Grid	Loss depends on number of narrowband tones and resolution
Excision Spreading – No Excision-Vector Smoothing (Single Tone)	~ 2 dB
Excision Spreading – Excision-Vector Smoothing (Single Tone)	~ 0.5 dB

APPENDIX A: THE SIMULATION TEST FACILITY

The Simulation Test Facility (STF) performs the functions of noise, interference, and signal generation, noise and interference suppression, and spread spectrum demodulation. For each of these functions, several options are available as outlined in table A-1. The STF is implemented as a combination of analog and digital equipments. The waveforms representing noise and interference are generated at an rf frequency, are received, down-converted to baseband, and sampled in quadrature at the Nyquist rate with a 10-bit bipolar analog-to-digital converter. This provides the PDP-11/20 computer with a baseband double sideband representation[5] of the noise and interference. A similar representation of a random-phase coded, constant-envelope signal is generated numerically by the computer and is added at the required level to give the desired signal-power-to-noise-power ratio (SNR). The STF is presently set up with a 100-kHz bandwidth (±50 kHz at baseband), a sample rate of 100 kHz (complex samples) and processes signal time-bandwidth products of from 2 to 128. For any given TW product, the results can be scaled to any desired duration and bandwidth that equals TW as long as the interference is similarly scaled. A functional flow diagram of the signal and noise generation process for the STF is given in figure A-1. The STF simulations used two random-phase coded signals and the correlation processing took place in the frequency domain as shown in figure A-2. The Fourier transform of one TW = 128 signal is shown in figure A-3 (note the folded frequency scale), followed by its autocorrelation and cross-correlation functions. Note the rounded form of the correlation functions caused by time-domain application of a window function.

TABLE A-1. STF FUNCTIONS AND OPTIONS.

FUNCTION	OPTIONS
Noise and Interference Generation	1. Stationary White Gaussian (SWG) 2. Pulsed Gaussian 3. Fixed Tone 4. Swept Tone 5. Multiple Fixed Tones 6. SWG + Tone(s) 7. SWG + Burst 8. SWG + Tone(s) + Burst
Signal Generation	1. Constant Envelope, Random Phase Code, Alphabet = 2 2. TW = 2 to 128 (powers of 2)
Broadband Noise Suppression (Time Domain Processing)	1. Threshold Clipping 2. Threshold Excision 3. Log Weighting (Hall)

TABLE A-1. (CONTINUED)

FUNCTION	OPTIONS
Narrowband Noise Suppression (Frequency-Domain Processing)	1. Threshold Whitening 2. Threshold Excision
Broadband/Narrowband Combination	1. Any Combination of Two Above 2. Time/Frequency Grid Processing
Other	1. Variable Quantization After Noise Suppression

To obtain the maximum possible speed on the STF, the signal-processing and data-manipulation functions were performed using a set of Assembly Language programmed-array processing routines that were called by, and controlled from, a BASIC language program. This technique proved most useful, allowing complicated signal-processing programs to be written easily and quickly at little sacrifice in processing speed relative to pure assembly language programs. The fast-array processing routines placed some limitations on the STF. All processing was limited to 16-bit block floating-point arithmetic and the input dynamic range was limited to about 45 dB. The arithmetic limitation was not considered a problem since the resultant processing loss is negligible; however, the dynamic range did limit the maximum allowable interference to noise ratios (INR).

Operator interaction with the STF was through a keyboard for input of test parameters, and a graphics display and printer for output. The procedure followed for a typical simulation run is outlined in figure A-4. Throughout the processing flow, the operator has the option of examining the intermediate data via the graphics display terminal. Any or all of the plots could be displayed, according to switches set by the operator. Note that the simulation procedure differentiates between "background" noise and interference. Ordinarily, the background noise is stationary white Gaussian noise (SWGN) and the interference is a wideband pulse, narrowband tone, or combination of the two. The signal-processing performance is a function of both the signal-to-background noise ratio (SNR) and the interference-to-noise ratio (INR). Each symbol was always assumed to contain one bit of information, regardless of the symbol TW product. A larger TW product would provide more processing gain, but would not change the information rate per symbol.

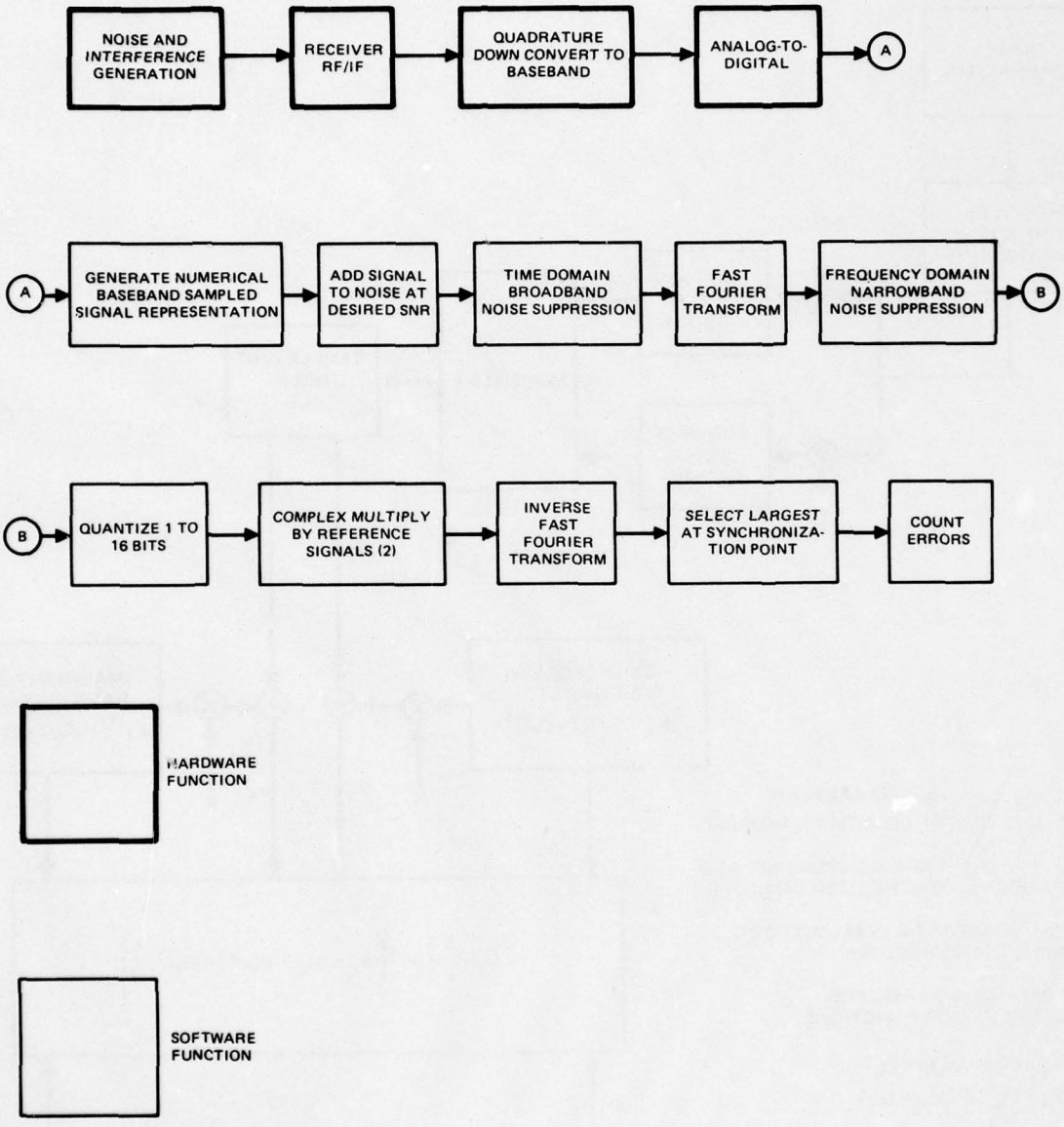

Figure A-1. Functional flow diagram for Simulation Test Facility.

AD-A049 138 NAVAL OCEAN SYSTEMS CENTER SAN DIEGO CALIF F/G 17/2.1
HIGH-FREQUENCY INTERFERENCE SUPPRESSION. INTERFERENCE IS IDENTI--ETC(U)
AUG 77 G J BROWN
UNCLASSIFIED NOSC/TR-155 NL

2 OF 2
ADA049138

END
DATE FILMED
2-78
DDC

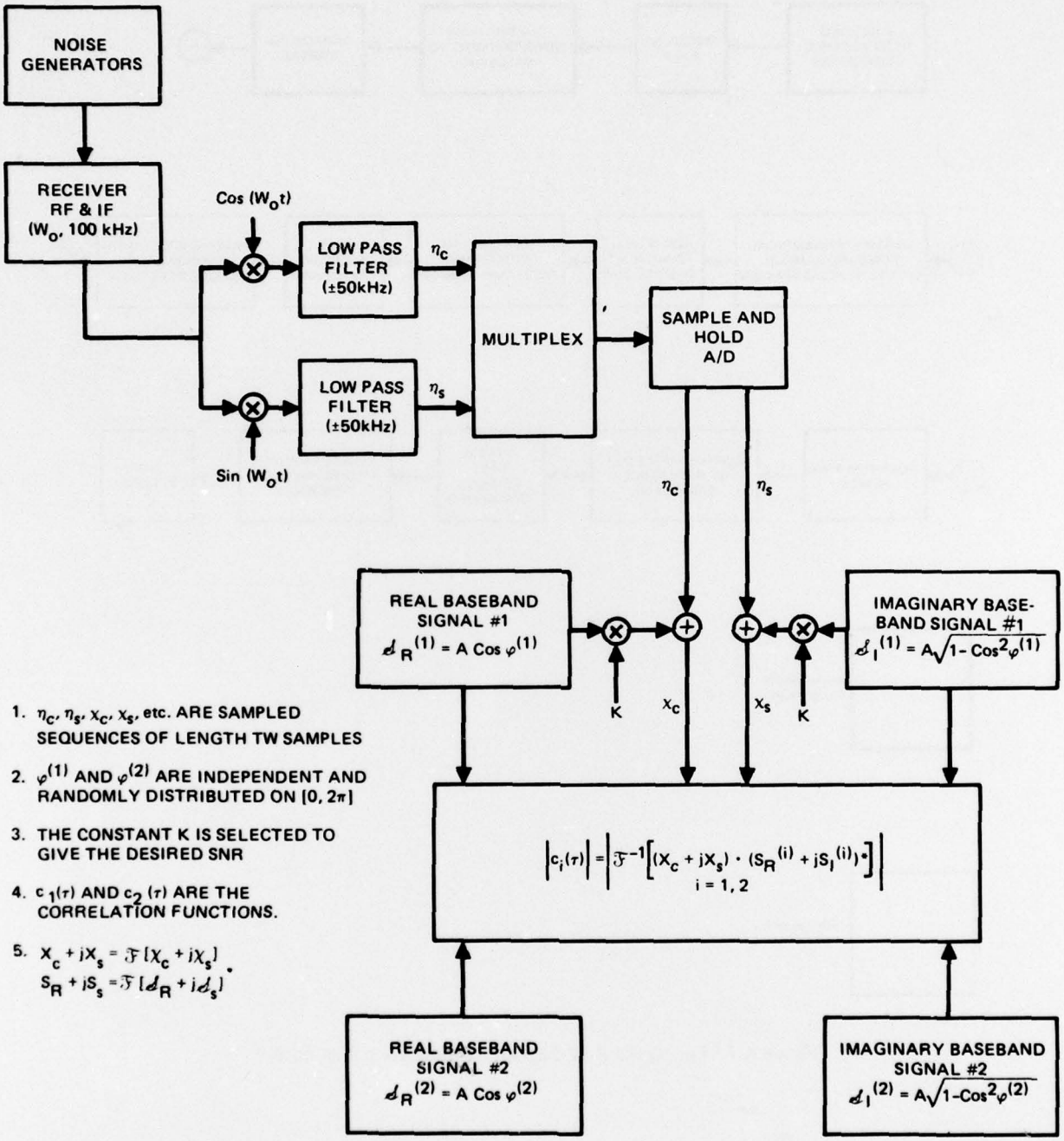

1. η_c, η_s, x_c, x_s, etc. ARE SAMPLED SEQUENCES OF LENGTH TW SAMPLES
2. $\varphi^{(1)}$ AND $\varphi^{(2)}$ ARE INDEPENDENT AND RANDOMLY DISTRIBUTED ON $[0, 2\pi]$
3. THE CONSTANT K IS SELECTED TO GIVE THE DESIRED SNR
4. $c_1(\tau)$ AND $c_2(\tau)$ ARE THE CORRELATION FUNCTIONS.
5. $X_c + jX_s = \mathcal{F}[\chi_c + j\chi_s]$
   $S_R + jS_s = \mathcal{F}[\mathcal{A}_R + j\mathcal{A}_s]$

Figure A-2. STF signal generation and basic processing.

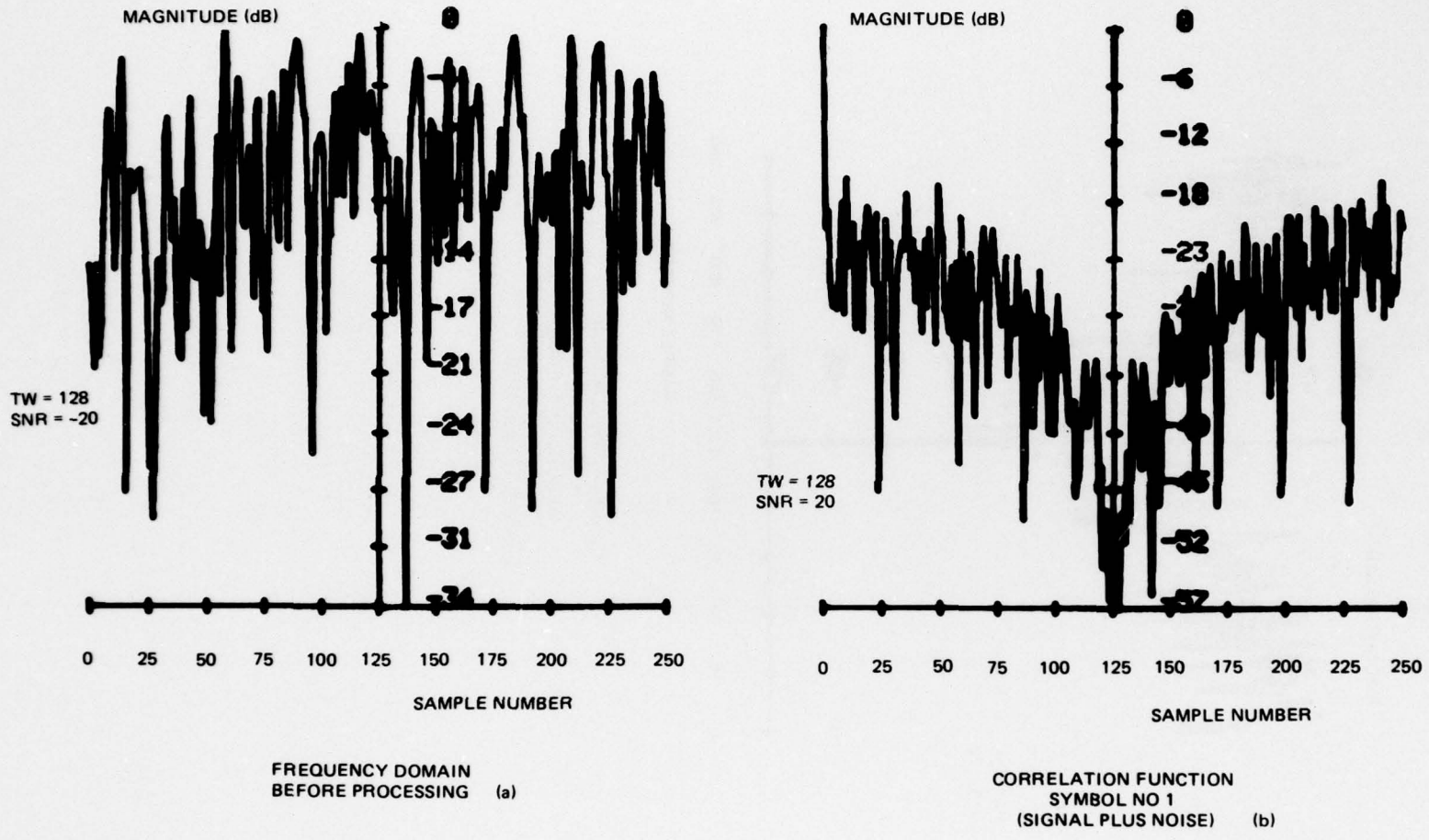

Figure A-3. Frequency spectrum of signal + noise taken from STF.

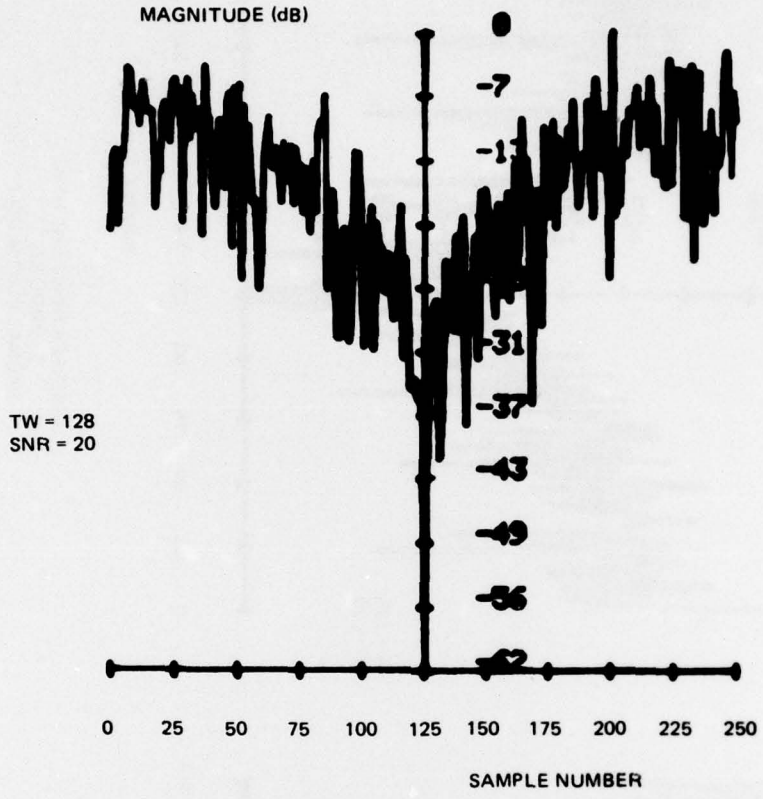

CORRELATION FUNCTION
SYMBOL NO 2
(SIGNAL PLUS NOISE) (c)

Figure A-3. Continued.

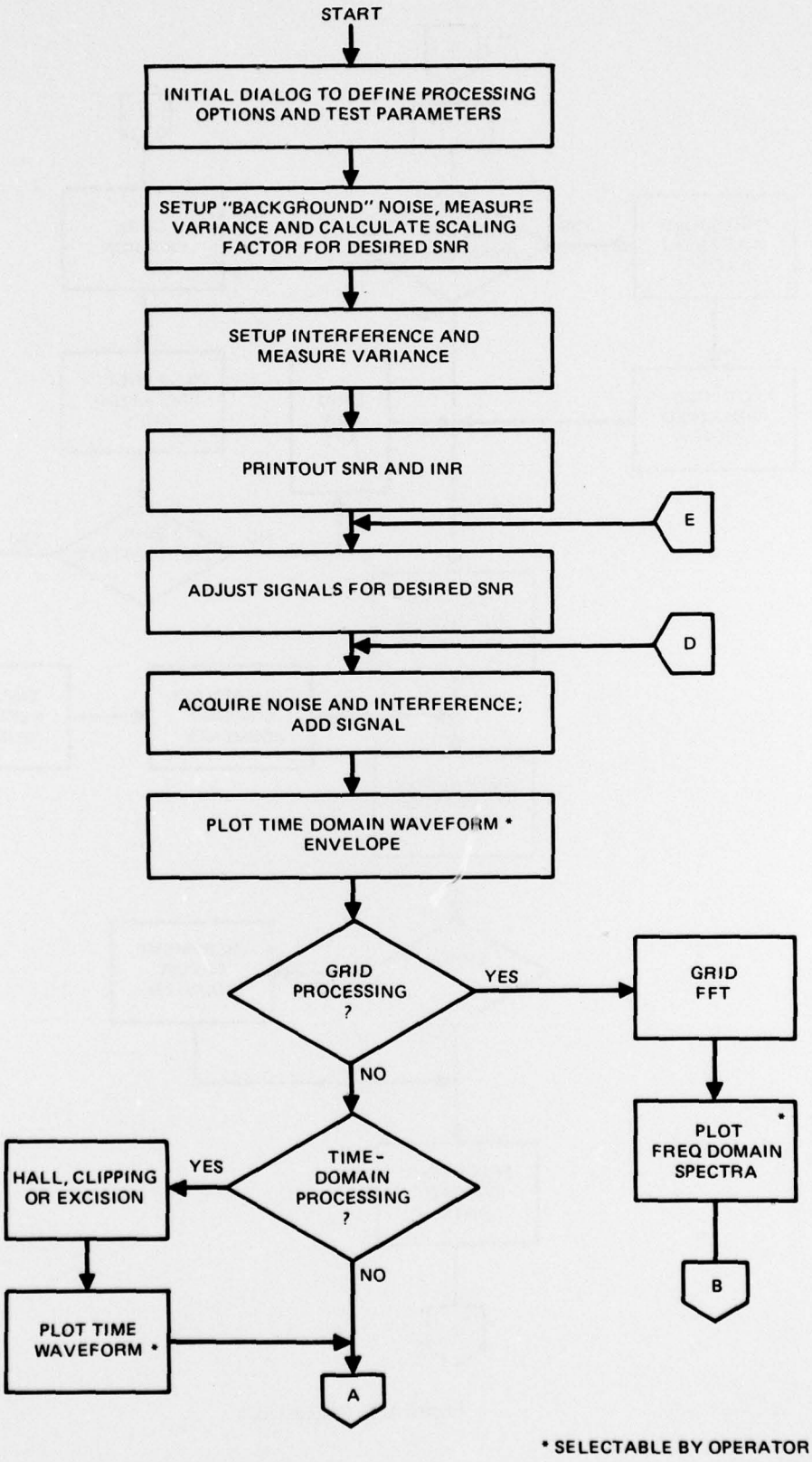

Figure A-4. STF flow diagram.

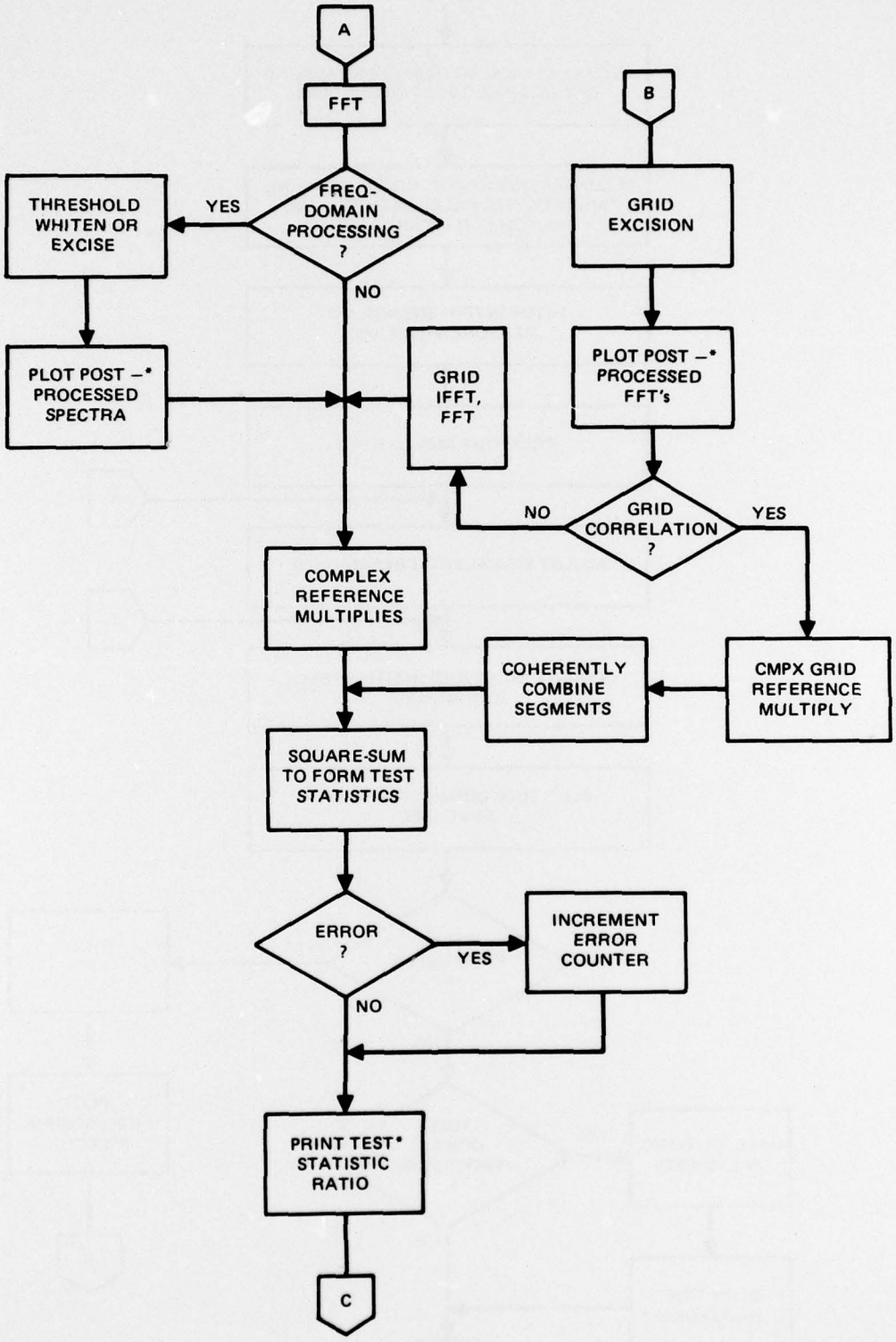

Figure A-4. Continued.

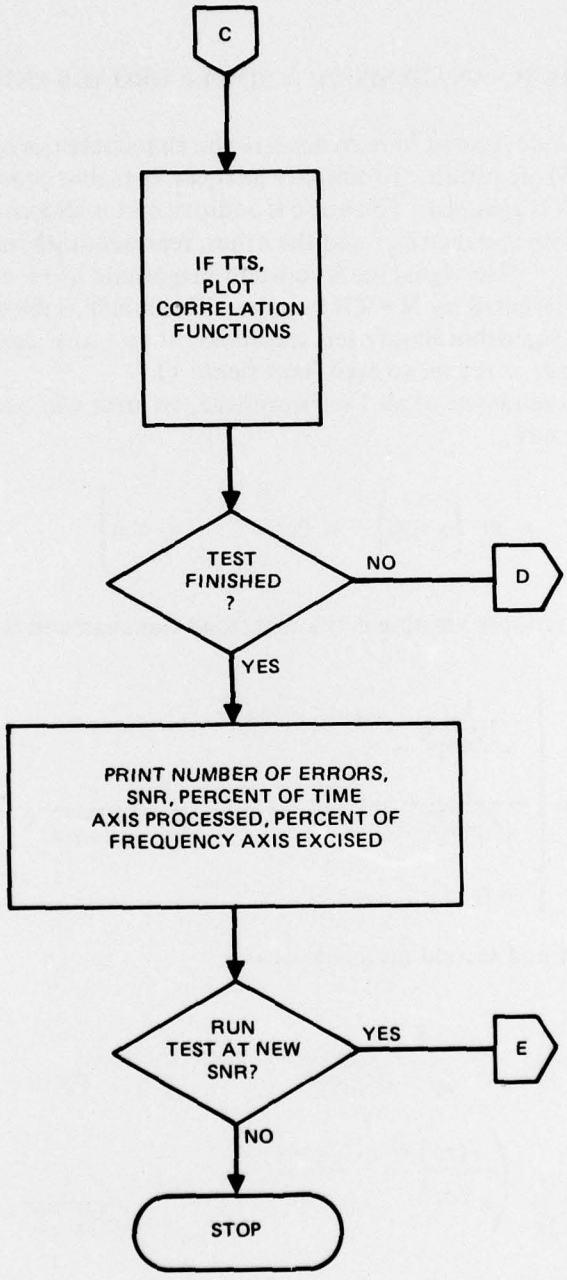

Figure A-4. Continued.

APPENDIX B: ANALYSIS OF A SIMPLE BROADBAND NOISE MODEL

A simple model is used here to analyze the characteristics of the broadband noise-suppression (BBNS) algorithm. To simplify analysis, coherent processing of binary antipodal phase-coded signals is assumed. The noise is additive and is chosen from one of two sample populations; one with variance σ_o^2 and the other, representing broadband interference, with variance $\sigma_1^2 >> \sigma_o^2$. The signal has a constant magnitude of +1 or −1 and a time bandwidth product of TW represented by N = TW samples. This model is illustrated in text figure 1.

The BBNS algorithm simply sets thresholds at ±z. Any signal-plus-noise values exceeding z or less than −z are set to zero (text figure 1).

Assuming a sequence of all 1's transmitted, an error will occur if the match filter output is less than zero,

$$\Pr\left\{\text{error}\right\} = \Pr\left\{z < 0\right\} = \Pr\left\{\sum_{i=1}^{N} y_i < 0\right\} \tag{B1}$$

The pdf for the y_i random variable is the truncated Gaussian and is a function of the noise variance present:

$$p_y(y;\sigma_i)_{i=0,1} = \begin{cases} \dfrac{1}{\sqrt{2\pi\sigma_i^2}}\, e^{-(y-1)^2/2\sigma_i^2} & ; -z<y<z \\ & y \neq 0 \\ \dfrac{1}{\sqrt{2\pi\sigma_i^2}}\, e^{-1/2\sigma_i^2} + 1 - \displaystyle\int_{-z}^{z} \frac{1}{\sqrt{2\pi\sigma_i^2}} e^{-(y-1)^2/2\sigma_i^2}\, dy & ; y = 0 \\ = 0 \; ; \; |y| > z & \end{cases} \tag{B2}$$

Solving for the first and second moments of y:

$$\mu_1(\sigma_i) = E\left\{|y|\right\} = \int_{-z}^{z} \frac{y}{\sqrt{2\pi\sigma_i^2}}\, e^{-(y-1)^2/2\sigma_i^2}\, dy$$

$$\mu_1(\sigma_i) = \frac{\sigma_i}{\sqrt{2\pi}}\left(e^{\frac{-(z+1)^2}{2\sigma_i^2}} - e^{\frac{-(z-1)^2}{2\sigma_i^2}}\right) + \int_{-z}^{z} \frac{1}{\sqrt{2\pi\sigma_i^2}}\, e^{-(y-1)^2/2\sigma_i^2}\, dy \tag{B3}$$

$$\mu_2(\sigma_i) = E\left\{y^2\right\} = \int_{-z}^{z} \frac{y^2}{\sqrt{2\pi\sigma_i^2}}\, e^{-(y-1)^2/2\sigma_i^2}\, dy$$

$$\mu_2(\sigma_i) = \frac{\sigma_i}{\sqrt{2\pi}}\left(ze^{\frac{-(z+1)^2}{2\sigma_i^2}} - ze^{\frac{-(z-1)^2}{2\sigma_i^2}}\right) + \sigma_i^2 \int_{-z}^{z} \frac{1}{\sqrt{2\pi\sigma_i^2}}\, e^{-(y-1)^2/2\sigma_i^2}\, dy + \mu(\sigma_i) \tag{B4}$$

and the variance of y is,

$$\sigma_y^2(\sigma_i) = \mu_2(\sigma_i) - \mu_1^2(\sigma_i) \tag{B5}$$

Under certain conditions (which probably apply here) the Central Limit Theorem may be used to approximate the pdf of

$$g = \sum_i y_i$$

as Normal with mean and variance,

$$\mu_g = \left[(1-p)\, N \int_{-z}^{z} p_y(y,\sigma_0)dy \right] \mu_1(\sigma_0) + \left[pN \int_{-z}^{z} p_y(y,\sigma_1)dy \right] \mu_1(\sigma_1) \tag{B6}$$

$$\sigma_g^2 = \left[(1-p)\, N \int_{-z}^{z} p_y(y,\sigma_0)dy \right] \sigma_y^2(\sigma_0) + \left[pN \int_{-z}^{z} p_y(y,\sigma_1)dy \right] \sigma_y^2(\sigma_1)$$

where $1 - p = \Pr\left\{\text{Noise Variance} = \sigma_0^2\right\}$

$p = \Pr\left\{\text{Noise Variance} = \sigma_1^2\right\}$.

In this case,

$$\Pr\left\{\text{error}\right\} = \int_{-\infty}^{0} \frac{1}{\sqrt{2\pi\sigma_g^2}} e^{-(z-\mu_g)^2/2\sigma_g^2}\, dz \tag{B7}$$

The BASIC program shown in figure B-1 was used to compute equation B7).

```
10    DIM D[2], H[2], M[2], G[2]
20    PRINT "INPUT THE SAMPLE SIZE"
30    INPUT N
40    PRINT "INPUT THE INR START, STOP, AND INCREMENT"
50    INPUT I0, I1, I2
60    PRINT "INPUT THE SNR START, STOP, AND INCREMENT"
70    INPUT R0, R1, R2
80    PRINT "INPUT THE THRESHOLD START, STOP, AND INCREMENT"
90    INPUT Z0, Z1, Z2
100   FOR K = 14 TO 14
110   P = 0, 05 * K
120   FOR I = I0 TO I1 STEP I2
130   I3 = 10↑ (R/10)
140   FOR Z = Z0 TO Z1 STEP Z2
150   PRINT "TW = "N
160   PRINT "INR = "I" DB", "THRESHOLD = "Z," INTER. PROB = "P
170   PRINT "  "
180   PRINT "SNR (DB)", "ERROR PROB."
190   FOR R = R0 TO R1 STEP 2
200   R3 = 10↑ (R/10)
210   D[2] = 1/R3
220   D[1] = 13*D[2]
230   U = 0
240   S = 0
250   FOR J = 1 TO 2
251   E1 = 0
252   E2 = 0
253   A = -(Z+1)*(Z+1)/(2*D[J])
254   IF A < -99 THEN 256
255   E1 = EXP (A)
256   B = -(Z-1)*(Z-1)/(2*D[J])
257   IF B < -99 THEN 280
258   E2 = EXP (B)
280   A = (-Z-1)/SQR (D[J])
290   B = (Z-1)/SQR(D[J])
300   X = B
310   GOSUB 2000
320   B = F
330   X = A
340   GOSUB 2000
350   G[J] = B - F
360   H[J] = SQR (D[J]/6.2831853)*(E1-E2) + G[J]
370   M[J] = SQR (D[J]/6.2831853)*(E1-E2)*Z+D[J]*G[J]+H[J]-H[J]*H[J]
380   NEXT J
390   U=P*N*H[1]*G[1]+(1-P)*N*H[2]*G[2]
400   S=P*N*M[1]*G[1]+(1-P)*N*M[2]*G[2]
410   X=-U/SQR(S)
420   GOSUB 2000
430   PRINT R, F
440   NEXT R
450   NEXT Z
460   NEXT I
470   NEXT K
480   STOP
2000  Y=X
2010  IF X>0
2020  Y=-X
2030  T=1/(1+0.2316419*Y)
2031  F=1
2032  IF Y*Y/2>99 THEN 2080
```

Figure B-1. BASIC program for calculation of equation (B7).

```
2040  G=0.39894228*EXP (-Y*Y/2)
2050  F=0.31938153*T-0.356563782*T*T+1.781477937*T*T*T
2060  F=F-1.821255978*T*T*T*T+1.330274429*(T↑5)
2070  F=1-G*F
2080  IF X>0 THEN 2100
2090  F=1-F
2100  RETURN
```

Figure B-1. Continued.

INITIAL DISTRIBUTION

NAVAL RESEARCH LABORATORY
CODE 5420 (J LINNEHAN)

NAVAL ELECTRONIC SYSTEMS COMMAND
NELEX-310 (D SWEET) (2)

STANFORD RESEARCH INSTITUTE
333 RAVENSWOOD AVE
MENLO PARK, CA 94025
J SCHLOBAHM

PROBE SYSTEMS INC
655 N PASTORIA AVE
SUNNYVALE, CA 94086
K SNOW

COOLEY ELECTRONICS LABORATORY
UNIVERSITY RESEARCH SECURITY OFFICE
PO BOX 622
ANN ARBOR, MI 48106
M RISTENBATT

STEIN ASSOCIATES, INC
280 BEAR HILL ROAD
WALTHAM, MA 02154
R REED

GAC MAGNAVOX
1200 MERMAID LANE
PHILADELPHIA, PA 19118
DR M GOUTMANN

DEFENSE DOCUMENTATION CENTER (12)